Universitat Autònoma de Barcelona

Mechanistic and genetic regulation of plant responses to vegetation proximity: the roles of DRACULA2 and HFR1

Sandi Paulišić

ADVERTIMENT. L'accés als continguts d'aquesta tesi doctoral i la seva utilització ha de respectar els drets de la persona autora. Pot ser utilitzada per a consulta o estudi personal, així com en activitats o materials d'investigació i docència en els termes establerts a l'art. 32 del Text Refós de la Llei de Propietat Intel·lectual (RDL 1/1996). Per altres utilitzacions es requereix l'autorització prèvia i expressa de la persona autora. En qualsevol cas, en la utilització dels seus continguts caldrà indicar de forma clara el nom i cognoms de la persona autora i el títol de la tesi doctoral. No s'autoritza la seva reproducció o altres formes d'explotació efectuades amb finalitats de lucre ni la seva comunicació pública des d'un lloc aliè al servei TDX. Tampoc s'autoritza la presentació del seu contingut en una finestra o marc aliè a TDX (framing). Aquesta reserva de drets afecta tant als continguts de la tesi com als seus resums i índexs.

ADVERTENCIA. El acceso a los contenidos de esta tesis doctoral y su utilización debe respetar los derechos de la persona autora. Puede ser utilizada para consulta o estudio personal, así como en actividades o materiales de investigación y docencia en los términos establecidos en el art. 32 del Texto Refundido de la Ley de Propiedad Intelectual (RDL 1/1996). Para otros usos se requiere la autorización previa y expresa de la persona autora. En cualquier caso, en la utilización de sus contenidos se deberá indicar de forma clara el nombre y apellidos de la persona autora y el título de la tesis doctoral. No se autoriza su reproducción u otras formas de explotación efectuadas con fines lucrativos ni su comunicación pública desde un sitio ajeno al servicio TDR. Tampoco se autoriza la presentación de su contenido en una ventana o marco ajeno a TDR (framing). Esta reserva de derechos afecta tanto al contenido de la tesis como a sus resúmenes e índices.

WARNING. The access to the contents of this doctoral thesis and its use must respect the rights of the author. It can be used for reference or private study, as well as research and learning activities or materials in the terms established by the 32nd article of the Spanish Consolidated Copyright Act (RDL 1/1996). Express and previous authorization of the author is required for any other uses. In any case, when using its content, full name of the author and title of the thesis must be clearly indicated. Reproduction or other forms of for profit use or public communication from outside TDX service is not allowed. Presentation of its content in a window or frame external to TDX (framing) is not authorized either. These rights affect both the content of the thesis and its abstracts and indexes.

UNIVERSITAT AUTONOMA DE BARCELONA
FACULTAT DE BIOCIENCIES

Mechanistic and genetic regulation of plant responses to vegetation proximity: the roles of DRACULA2 and HFR1

Sandi Paulišić

2018

UNIVERSITAT AUTONOMA DE BARCELONA
FACULTAT DE BIOCIENCIES
Doctoral program of Plant Biology and Biotechnology

PhD thesis

Mechanistic and genetic regulation of plant responses to vegetation proximity: the roles of DRACULA2 and HFR1

Dissertation presented by Sandi Paulišić for the degree of Doctor of Plant Biology and Biotechnology at Autonomous University Barcelona. This work was performed in the Centre for Research in Agricultural Genomics.

Thesis director	Thesis tutor	PhD candidate
Dr. Jaime F. Martínez-García	Dra. Carlota Poshenrieder Wiens	Sandi Paulišić

Barcelona, June 2018

Acknowledgements

These four amazing years seem to have passed in a blink, and I am grateful to so many of you. Being on the minimalist side, I'll keep this short.

First, I want to thank Jaume Martínez-García for giving me this amazing opportunity to participate in the projects of his lab as a PhD student. For all the encouragement and enthusiasm. I've learned a lot in these four years, grew, and wouldn't change this experience for anything.

Also, I greatly appreciate the work of all the people that have contributed to these two projects, our collaborators and the AGAUR for providing me the fellowship. A very special gratitude also goes to all the CRAG service members, for helping me when needed.

To all the members of the lab 205, the current ones and the ones that are no longer in this lab. You are the best, and you know this also goes for tolerating my sarcasm and for sharing all the laughs, fiestas, coffees and some of the most memorable moments. It was great being part of this lab and being with you all these years.

Thanks to all my friends from CRAG, the new ones, the old ones, the ones who were always here to support me and share lots of love. For the amazing moments we spent together, I will not forget this.

And to all my amazing friends back home, for their "long distance support" and being there for me when needed.

Finally, to my family who always stood by me, and supported me in any circumstance and any occasion, I don't thank you enough.

Summary

Light provides essential energy for plant photosynthesis and information about the surrounding environment. Light challenging conditions, such as vegetation proximity and shade, require fast response and a fine-tuned signalling network to properly adapt plant development. Several transcriptional regulators are at the core of plant responses to vegetation proximity, including the positively-acting PHYTOCHROME INTERACTING FACTORs (PIFs) and the antagonistic HFR1. Nonetheless, knowledge about the regulation of shade responses improves continuously. DRACULA2 (DRA2) is a newly identified *Arabidopsis thaliana* shade avoidance regulator, part of the nuclear pore complex (NPC), which affects several aspects of plant development (e.g., shade-induced hypocotyl elongation) through transport-dependent and -independent activities. Besides its pleiotropic phenotype shared with other nucleoporin (NUP)-deficient mutants, DRA2 is specifically involved in the regulation of shade-induced gene expression. We found that DRA2 is a dynamic NUP, i.e., not exclusively NPC located, which could allow it to act independently of the NPC. Moreover, transport-dependent functions of the NPC might be part of a broader mechanism of shade regulation. While shade avoidance is better studied, we are beginning to understand the regulation of an alternative plant strategy to vegetation proximity, tolerance to shade, by using *Cardamine hirsuta*, a close relative of *A. thaliana*. We demonstrated that *C. hirsuta HFR1* inhibits hypocotyl elongation in shade by constraining the expression profile of shade induced genes. HFR1 accumulates in shade and directly interacts with various PIFs, such as the major shade avoidance promoting PIF7 in *A. thaliana*. We show that a higher stability in shade coupled with higher expression levels can lead to a higher biological activity of HFR1 in *C. hirsuta* resulting in the shade tolerance habit of *C. hirsuta*.

Resumen

La luz proporciona energía para la fotosíntesis e información sobre el medio ambiente circundante. La información lumínica avisa de situaciones desafiantes, como la proximidad de la vegetación y la sombra, que requiere de la planta una red de señalización que proporcione respuestas rápidas y ajustadas para adaptar el desarrollo, respuestas que conjuntamente conforman el síndrome de huida de la sombra. Varios reguladores transcripcionales controlan estas respuestas, incluidos los PHYTOCHROME INTERACTING FACTORs (PIF), de acción positiva, y HFR1 con un papel antagonista. No obstante, el conocimiento sobre la regulación de las respuestas a sombra se amplía continuamente. DRACULA2 (DRA2) es una nucleoporina (NUP) de *Arabidopsis thaliana* que forma parte del complejo del poro nuclear (NPC), que regula el alargamiento del hipocotilo inducido por la sombra a través de actividades dependientes e independientes de su papel en el transporte de macromoléculas. Además de su fenotipo pleiotrópico compartido con otros mutantes deficientes en NUPs, DRA2 está específicamente involucrado en la regulación de la expresión génica inducida por la sombra. Encontramos que DRA2 es una NUP dinámica, es decir, que no está ubicada exclusivamente en NPC, lo que podría permitirle actuar independientemente del NPC. Además, las funciones del NPC dependientes del transporte podrían ser parte de un mecanismo más amplio de regulación de la sombra. Mediante el uso de *Cardamine hirsuta* (una planta emparentad con *A. thaliana*) hemos empezado a comprender la regulación de la tolerancia a la proximidad vegetal, una estrategia vegetal alternativa a la huida de la sombra. Hemos demostrado que la proteína HFR1 de *C. hirsuta* inhibe la elongación del hipocotilo a la sombra al restringir el perfil de expresión génica. HFR1 se acumula en respuesta a la sombra e interactúa directamente con varios PIF a los que inhibe, como PIF7. Mostramos que una mayor estabilidad de ChHFR1 junto con la inducción de sus niveles de expresión en sombra puede conducir a una mayor actividad biológica de HFR1 en *C. hirsuta*, que contribuiría al establecimiento de la tolerancia a la sombra de esta especie.

ABREVIATIONS

Abbreviations

5-FU	5-fluorouracil
AD	Activation domain
ADH1	*ALCOHOL DEHYDROGENASE 1*
At WT	*A. thaliana* wild type (Col-0)
ATI	Polar auxin transport inhibitor
AUX	Auxin
AXR1	AUXIN RESISTANT 1
BBX	B-BOX DOMAIN PROTEIN
BD	Binding domain
bHLH	Basic helix-loop-helix
CAB	*CHLOROPHYLL A/B-BINDING*
CFP	Cyano-fluorescent protein
Ch WT	*C. hirsuta* wild type (Ox)
chfr1	*C. hirsuta* mutant in *ChHFR1*
ChHFR1	*C.hirsuta HFR1*
ChIP	Chromatin immunoprecipitation
CHX	Cycloheximide
CKII	Casein kinase II
CO	CONSTANS
Col-0	Columbia-0 ecotype of *A. thaliana*
COP1	CONSTITUTIVE PHOTOMORPHOGENIC 1
cry1/2	Cryptochrome 1/2
DIS	Dark-Induced Senescence
dra2	*A. thaliana* mutant in *DRACULA2* (*DRA2*)
DRAL	DRA2-LIKE
EF1α	*ELONGATION FACTOR 1α*
ELYS	EMBRYONIC LARGE MOLECULE DERIVED FROM YOLK SAC
EOD-FR	End-of-day far-red
EXP	EXPANSIN
FG	Phenylalanine-glycine repeats
FHL	FHY1-LIKE

FHY1	FAR-RED ELONGATED HYPOCOTYL 1
FKF1	FLAVIN-BINDING, KELCH REPEAT, F-BOX
FLC	*FLOWERING LOCUS C*
FR	Far-red light
GA	Gibberellin
GA20ox	*GA 20-OXIDASE*
GA3ox	*GA 3-OXIDASE*
G-box	CACGTG sequence motif
GFP	Green fluorescence protein
GID1	GA INSENSITIVE DWARF1
GM-	Plant growth medium without sucrose
GUS	β-glucuronidase
HA	Influenza hemagglutinin
HAC1/12	HISTONE ACETYLTRANSFERASE 1/12
HD-Zip	Homeodomain zip
HFR1	LONG HYPOCOTYL IN FAR-RED 1
hfr1	*A. thaliana* mutant in *AtHFR1*
HLH	Helix-loop-helix
HL$_{W}$	Hypocotyl length in W
HL$_{W+FR}$	Hypocotyl length in W+FR
HMR	HEMERA
HOS1	HIGH EXPRESSION OF OSMOTICALLY RESPONSIVE GENES1
HY5	ELONGATED HYPOCOTYL 5
IAA	Indol-3 acetic acid
IAA17/19/29	INDOLE-3-ACETIC ACID INDUCIBLE 17/19/29
IPA	Indol-3-pyruvic acid
LKP2	LOV KELCH PROTEIN2
LMI1	*LATE MERISTEM IDENTITY 1*
LOV	Light Oxygen Voltage
LUC	*LUCIFERASE*
mCherry	Variant of red fluorescent protein
MDa	Mega Daltons
NB	Nuclear body

NE	Nuclear envelope
NLS	Nuclear localization signal
NPA	N-1-naphthylphthalamic acid
NPC	Nuclear pore complex
NUA	NUCLEAR PORE ANCHOR
NUP	Nucleoporin
ORF	Open reading frame
Ox	*C. hirsuta* Oxford ecotype
p53	TUMOR PROTEIN P53
PAR	Photosynthetically active radiation
PAR1/2	PHYTOCHROME RAPIDLY REGULATED 1/2
pAtHFR1	Promoter of *A. thaliana HFR1*
PBA	2-(1-pyrenoyl) benzoic acid
PBL	pPHYB:LUC line in Ws-2
pChHFR1	Promoter of *C. hirsuta HFR1*
Pfr	Active far-red-absorbing phytochrome form
phyA/B/C/D/E	Phytochrome A/B/C/D/E
PIF	PHYTOCHROME INTERACTING FACTOR
PIFQ	PIF QUARTET: PIF1, PIF3, PIF4 and PIF5
pifq	*A. thaliana PIFQ* quadruple mutant
PIL1	PIF3-LIKE 1
PPT	Phosphinothricin
Pr	Inactive red-absorbing phytochrome form
pU6	*U6* promoter
PVDF	Polyvinylidene fluoride
qPCR	Real time quantitative PCR
R	Red light
RAE1	*RNA EXPORT FACTOR 1*
RCO	*REDUCED COMPLEXITY*
RAN1	*RAS-RELATED NUCLEAR PROTEIN-1*
RNAi-DRA2	RNA interference against *DRA2*
RUB	RELATED TO UBIQUITIN
SAR1/3	SUPRESSOR OF AUXIN RESISTANT 1/3
SAS	Shade avoidance syndrome

SAV3	SHADE AVOIDANCE 3, also known as TAA1
SCF	Skp1-Cul1/Cdc53-F-box
SD	Synthetic defined medium
SDS-PAGE	Sodium dodecyl sulfate - polyacrylamide gel electrophoresis
SE	Standard error
sis1	*C. hirsuta* mutant *slender in shade 1*
SPA1	SUPPRESSOR OF PHYA-105 1
SV40	SIMIAN VACUOLATING VIRUS 40
TAA1	TRYPTOPHAN AMINOTRANSFERASE OF ARABIDOPSIS 1, also known as SAV3
TCU1	TRANSCURVATA1
TIBA	2,3,5-triiodobenzoic acid
TRP	TRANSLOCATED PROMOTER REGION
UBQ10	*UBIQUITIN 10*
W	Continuous white light
W+FR	White light supplemented with far-red
Ws-2	Wassilewskija-2 ecotype of *A. thaliana*
XPO1B	*NUCLEAR EXPORTIN 1B*
XTH	XYLOGLUCAN ENDOTRANSGLUCOSYLASE / HYDROLASE
XTH15/XTR7	*XYLOGLUCAN ENDOTRANSGLYCOSYLASE 7*
Y2H	Yeast two-hybrid assay
YUC	YUCCA
ZTL	ZEITLUPE

TABLE OF CONTENTS

Table of Contents

INTRODUCTION

1. Importance of light conditions in nature: types of light signals........................1
2. Adaptations of plants to vegetation proximity..3
   2.1 The shade avoidance syndrome (SAS) in *Arabidopsis thaliana* 3
3. Light perception in plants...5
   3.1 Perception of UV-B light...5
   3.2 Perception of UV-A/blue light 6
   3.3 Perception of shade through R and FR..7
4. Shade signalling: from perception to transcription..8
   4.1 Phytochrome – PIF light signalling hub 8
   4.2 Additional mechanism of shade signalling: Nuclear Pore Complex (NPC) 11
      4.2.1 Structure and function of NPC 11
      4.2.2 Association of NPC with light (shade) signalling..................................... 12
      4.2.3 Chromatin regulation by NPC.. 13
5. Alternative strategies of response to shade..14
   5.1 Shade tolerance 14
   5.2 *Cardamine hirsuta* as a model for comparative studies 16

OBJECTIVES..19

CHAPTER I

1. Introduction 21
   1.1 *DRA2* encodes nucleoporin NUP98a. 22
   1.2 Nucleoporin mutants share general physiological defects, impairment in nuclear function and response to shade 23
   1.3 Attenuated shade response of *PAR* genes is characteristic of *dra2-1* but not other NUP mutants...25
2. Results...28
   2.1 RNAi-DRA2 lines behave as the strong *dra2-1* mutant..........................28
   2.2 NtDRA2 acts as a dominant negative form...28

2.3 DRA2 is a dynamic nucleoporin 31
2.4 Expression of *PAR* genes promoted by DRA2 in shade does not involve PIF-DRA2 interaction 31
2.5 TIBA application simulates defective NPC 33
2.6 Intranuclear phyB-GFP movement is affected by TIBA 35
3. Discussion 37
4. Materials and methods 41
4.1 Plant material and growth conditions 41
4.2 Generation of transgenic lines 42
4.3 Measurement of hypocotyl length 42
4.4 Gene expression analyses 42
4.5 Agroinfiltration of tobacco leaves and confocal microscopy 42
4.6 Chromatin immunoprecipitation (ChIP) 43
4.7 TIBA and NPA treatments 43
5. Supplementary 44
5.1 Generation of RNAi-DRA2 plants in *A. thaliana* Ws-2 background 44
5.2 Generation of *A. thaliana* Col-0 transgenic line expressing *GFP-DRA2-GFP* under the control of the 35S promoter 44
5.3 Generation of *NtDRA2-GFP* and *GFP-CtDRA2-GFP* fusion constructs for confocal microscopy 44
5.4 Tables: 45
6. References 47

CHAPTER II

1. Introduction 53
2. Results 55
2.1 *HFR1* is required for *C. hirsuta* shade tolerance habit 55
2.2 Expression of *HFR1* gene is constitutively higher in *C. hirsuta* compared to *A. thaliana* 57
2.3 ChHFR1 has higher biological activity than AtHFR1 58
2.4 Stability of HFR1 determines its activity in shade 60

2.5 HFR1 modulates the elongation response to shade through interaction with PIF7 63

2.6 Different PIF regulated processes are affected by high HFR1 activity in *C. hirsuta* 65

3. Discussion........ 67

3.1 ChHFR1 has a role in shade signalling in *C. hirsuta* 67

3.2 ChFR1 has higher biological activity than AtHFR1 68

3.3 High ChHFR1 activity affects several PIF regulated processes in *C. hirsuta* 70

3.4 Final remarks 70

4. Materials and Methods 72

4.1 Plant material and growth conditions 72

4.2 Measurement of hypocotyl length 72

4.3 Generation of transgenic lines, mutants and crosses 72

4.4 Gene expression analyses 73

4.5 Protein extraction and immunoblotting analyses 73

4.6 Yeast 2 Hybrid (Y2H) assays 74

4.7 Photosynthetic pigments quantification 74

5. Acknowledgements 74

6. Supplementary information 75

6.1 Generation of RNAi-HFR1 plants of *C. hirsuta* 75

6.2 Isolation of *HFR1* mutants of *C. hirsuta* 75

6.3 Generation of *A. thaliana hfr1-5* transgenic lines expressing *AtHFR1* or *ChHFR1* under the control of different promoters 76

6.4 Generation of constructs for the Yeast 2 Hybrid (Y2H) assays 78

6.5 GUS lines 78

6.6 GUS staining 79

6.7 Photosynthetic pigments quantification 79

6.8 Tables: 80

7. References 90

GENERAL DISCUSSION 97

CONCLUSIONS 99

GENERAL REFERENCES 101

INTRODUCTION

1. Importance of light conditions in nature: types of light signals

Diverse light conditions in natural environments have major impact on plant life. Usually, direct solar radiation or sunlight that reaches the ground is rather constant in quantity and quality during the day (Smith 1982). The spectrum of sunlight used for photosynthesis, called the photosynthetically active radiation (PAR), corresponds to the spectrum visible to the human eye, from ~400 nm (blue light) to the ~700 nm (red light, R) (**Figure 1A**). The characteristics of PAR can change daily, seasonally and due to several external factors. On a daily basis, PAR can become enriched with blue and far-red light (FR) parts of the spectrum during the twilight (Hughes *et al.* 1984), and it can change its composition depending on the time of the year (Franklin and Whitelam 2007). External factors, such as clouds or the vegetation that casts shade to its neighbouring plants can reduce the intensity of PAR and affect light quality (**Figure 1A**) (Smith 1982). These diverse environmental light conditions can be grouped into three situations according to the presence of vegetation proximity or shade (**Figure 1B**):

A) Unshaded conditions are present in low density and sparse vegetation communities where plants do not directly shade each other, including early colonizing environments that were previously bare of plants. The sunlight that reaches the ground in these conditions is unaltered (high UV-B, blue and R) and maintains a high ratio between R and FR (R:FR<1.2-1.5) (Roig-Villanova and Martínez-García 2016) (**Figure 1B**).

B) In dense vegetation communities, vegetation proximity significantly changes light quality but not light quantity (high UV-B, blue and R). Mostly, this is a result of a selective absorption of parts of light spectrum by the photosynthetic tissues. Photosynthetic pigments chlorophylls and carotenoids absorb most of the PAR, with peaks of absorbance in blue (400-500 nm) and R (600-700 nm) (**Figure 1A**). Some green light gets transmitted through or reflected from the plant tissues, although this colour has little relevance as a cue announcing vegetation proximity. In addition, majority of the FR part of the spectrum (700-750 nm) is also reflected or transmitted through the green tissues of the plants (Martínez-García *et al.* 2010; Fiorucci and Fankhauser 2017). This leads to a local enrichment with the FR and lowers the R:FR ratio of horizontally propagated light (Ballare *et al.* 1987), while the overall light intensity may not be significantly changed (Casal 2013) (**Figure 1B**). This signal, known as **proximity shade**, is perceived by the photoreceptors as an indication of potential shading by the neighbouring vegetation and in many species induces a set of responses aimed at avoiding shade (shade avoidance syndrome – SAS).

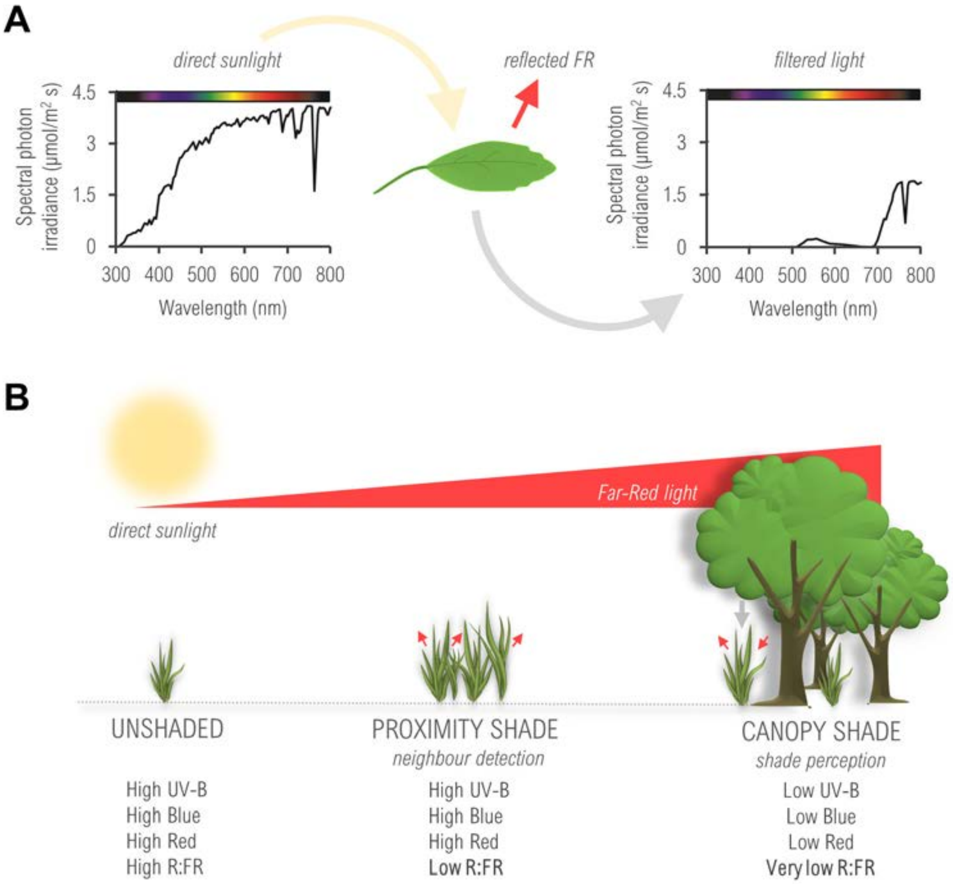
A
direct sunlight
Spectral photon irradiance (µmol/m² s)
4.5
3
1.5
0
300 400 500 600 700 800
Wavelength (nm)
reflected FR
filtered light
Spectral photon irradiance (µmol/m² s)
4.5
3
1.5
0
300 400 500 600 700 800
Wavelength (nm)
B
direct sunlight
Far-Red light
UNSHADED
High UV-B
High Blue
High Red
High R:FR
PROXIMITY SHADE
neighbour detection
High UV-B
High Blue
High Red
Low R:FR
CANOPY SHADE
shade perception
Low UV-B
Low Blue
Low Red
Very low R:FR

Figure 1. **(A)** Direct sunlight has high amounts of blue (~450-500 nm), green (~500-570 nm), red (R, ~620-700 nm) and far-red (FR, ~700-750 nm) parts of the spectrum. Photosynthetic pigments of green tissues selectively and strongly absorb most of the blue and R, whereas FR is reflected and even emitted from the leaves. **(B)** Different characteristics of the light properties encountered in unshaded and shaded conditions in nature. When growing in low vegetation density (unshaded), the direct sunlight that reaches an isolated plant contains high amounts of UV-B, blue and R, yet low amounts of FR, which results in a high R:FR. In dense vegetation environments, FR reflected from the neighbouring plants lowers the R:FR of sunlight and announces light competition and the potential formation of a vegetation canopy which we call proximity shade. Under a vegetation canopy, light conditions are characterized by low light intensity of UV-B, blue and R, due to light being filtered through the leaves, which results in a very low R:FR known as canopy shade. Shade avoider plants growing in dense vegetation (either proximity or canopy shade) sense their neighbours through a decreased R:FR ratio and induce a set of adaptive responses to avoid shade and outcompete their neighbours (e.g., promotion of elongation growth). By contrast, shade tolerant plants are adapted for life under low light intensity and amongst others, do not respond by elongating. Adapted from (Fiorucci & Fankhauser, 2017; Kami, Lorrain, Hornitschek, & Fankhauser, 2010).

C) Direct plant **canopy shade** significantly limits light availability. Because of strong and specific filtering by the leaves, below a vegetation canopy sunlight is depleted in UV-B and PAR (low UV-B, blue and R) but not so much in FR. In this condition, R:FR tends to be lower than in the proximity shade, and both light quality and quantity are affected (**Figure 1B**). On the example of a forest, a vertical stratification of a light gradient can be observed, where the top of a tree crown will receive the highest available light irradiation and be subsequently reduced by the time it reaches the ground. This has a major impact on the understory plants which must not only survive but efficiently use the available light energy and reproduce under these conditions. The adaptive strategy used by most of the naturally-growing understory plants is to tolerate shade.

Light availability in shaded canopy areas can also change during the time of the day or seasonally. Examples for this are sun flecks that can appear at a specific time of the day and locally increase the irradiation of light reaching the understory life (Sellaro *et al.* 2011). Seasonal loss of tree leaves in temperate deciduous forests during the winter or dry season dramatically increases the light availability for plants growing underneath them. Therefore, light available for understory plant species is highly heterogeneous and depends on location, presence of gaps, and time of the day or season, bringing complexity into the mechanistic regulation of responses to these cues.

2. Adaptations of plants to vegetation proximity

2.1 The shade avoidance syndrome (SAS) in *Arabidopsis thaliana*

Presence of neighbouring vegetation or canopy shade affects all stages of *A. thaliana* development (**Figure 2**). At the seed stage, presence of low R:FR inhibits germination and imposes secondary dormancy in *A. thaliana* (Shinomura *et al.* 1996; Smith and Whitelam 1997). The germination of seeds will most likely be delayed until the environmental conditions improve, i.e., light reaches higher R:FR, since the ability of newly germinated seedling with low energy resources to thrive in shaded areas are reduced. Past beyond the seed stage, emerging seedlings have adopted a suit of responses to have better chances in surviving in shaded conditions. The first and most obvious physiological response of seedlings to shade is the elongation of hypocotyls (**Figure 2**). This is a fast and well-studied response whose high predictability makes it a reliable indicator of SAS (Martínez-García *et al.* 2014). Cotyledons and primary leaves of seedlings expand longitudinally as a response to shade (Martínez-García *et al.* 2010), mostly due to elongation of their petioles (Djakovic-Petrovic *et al.* 2007;

Lorrain *et al.* 2008; Tao *et al.* 2008), but overall this response happens later than hypocotyl elongation. Additionally, the cotyledons and primary leaves bend upwards (become hyponastic). In both seedlings and adult plants, several metabolic changes occur, such as the reduction in pigment content, specifically chlorophylls and carotenoids (Roig-Villanova *et al.* 2007).

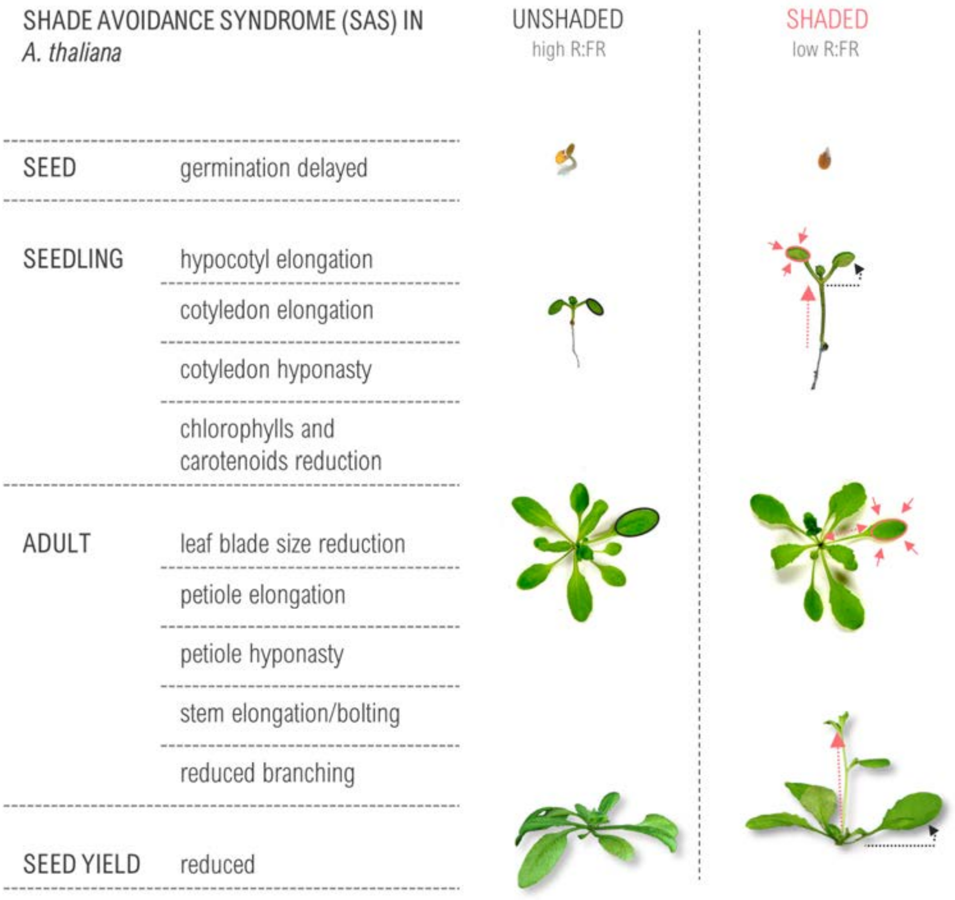
SHADE AVOIDANCE SYNDROME (SAS) IN
A. thaliana
UNSHADED
high R:FR
SHADED
low R:FR
SEED
germination delayed
SEEDLING
hypocotyl elongation
cotyledon elongation
cotyledon hyponasty
chlorophylls and
carotenoids reduction
ADULT
leaf blade size reduction
petiole elongation
petiole hyponasty
stem elongation/bolting
reduced branching
SEED YIELD
reduced

Figure 2. Shade avoidance syndrome (SAS) in A. thaliana is characterized by a set of distinctive adaptive responses. From seed to reproductive phase, vegetation proximity (low R:FR) affects all life stages of A. thaliana plant. It delays the germination of seeds, induces elongation of hypocotyls and affects size and position of cotyledons. In adult plants, shade promotes elongation of petioles, repositioning of leaves to better capture light, earlier flowering and reduced seed yield, among others.

Similar elongation responses are observed in adult plants, where the petiole length increases as a response to shade, while the leaf blade area reduces in size (Franklin 2008; Tao *et al.* 2008). Leaves also reorientate upwards due to faster growth on the lower side and become hyponastic (Vandenbussche *et al.* 2005; Franklin 2008; Millenaar *et al.* 2009). In a rosette plant, such as *A. thaliana*, shade promotes bolting (Halliday *et al.* 1994; Vandenbussche *et al.* 2005; Franklin 2008) characterized by the emergence of cauline stems that elongate more in shade than those of unshaded plants (Botto and Smith 2002). In addition, apical dominance increases, resulting in reduced branching (Smith and Whitelam 1997; Gonzalez-Grandio *et al.* 2013). Stem elongation together with the leaf hyponasty might help the plant to elevate above its competing neighbours and to better capture light (Ballaré 1999), while the accelerated flowering accompanied by a reduced seed set and truncated fruit development (Halliday *et al.* 1994; Smith and Whitelam 1997; Martínez-García *et al.* 2010) serves to enhance the production of viable offspring in unfavourable conditions.

3. Light perception in plants

Information about the dynamic changes of the spectral composition, light intensity, changes in light direction and duration are detected by several different photoreceptors in plants. These signals are then translated into appropriate developmental adaptations to improve plant fitness. In *A. thaliana* specifically, five classes of photoreceptor families have been identified: phytochromes, which absorb R and FR (Rockwell *et al.* 2006; Franklin and Quail 2010; Li *et al.* 2011), cryptochromes, phototropins and zeitlupes, specific for UV-A/blue light perception (Lin and Shalitin 2003; Chen *et al.* 2007; Kim *et al.* 2007; Demarsy and Fankhauser 2009; Christie *et al.* 2015) and UVR8, a UV-B photoreceptor (Jenkins 2014; Galvão and Fankhauser 2015). All photoreceptors, except UVR8, are chromoproteins structurally composed of an apoprotein and a covalently or noncovalently bound chromophore (Ahmad *et al.* 1995; Christie *et al.* 1998; Rockwell and Lagarias 2006; Christie *et al.* 2015). UVR8 instead uses a triad of tryptophan residues to perceive the light (Jenkins 2017). Special attention will be given to the phytochromes which perceive the changes in R:FR (Burgie and Vierstra 2014) with a brief overview of other photoreceptor families.

3.1 Perception of UV-B light

UVR8 is the only photoreceptor in *A. thaliana* found to mediate the UV-B light responses (Rizzini *et al.* 2011; Jenkins 2014). Upon perception of UV-B light, UVR8 homodimers dissociate to active monomers (Yang *et al.* 2015) and establish interactions with CONSTITUTIVE PHOTOMORPHOGENIC 1 (COP1) (Rizzini *et al.* 2011) to mediate several developmental and acclimation responses. Among those are inhibition of hypocotyl elongation, downward leaf curling (Fierro *et al.* 2015), accumulation of flavonols and anthocyanins (Favory *et al.* 2009; Morales *et al.* 2013; Huang *et al.* 2014) and entrainment of circadian clock (Fehér *et al.* 2011). UVR8 has been implicated in SAS responses as well (Mazza and Ballaré 2015; Hayes *et al.* 2017). It has been proposed that in canopy gaps, active UVR8 represses auxin biosynthesis and elongation growth to modulate SAS phenotypic plasticity (Mazza and Ballaré 2015).

3.2 Perception of UV-A/blue light

Cryptochromes are UV-A/blue light photoreceptors, structurally related to a family of DNA repair-involved photolyases (Mei and Dvornyk 2015). Two of them are found in *A. thaliana*, cry1 and cry2, with partially overlapping functions. In general, cry1 has been implicated in high temperature-promoted hypocotyl elongation and cry2 in the regulation of photoperiodic flowering (Liu *et al.* 2008; Liu *et al.* 2013). Cryptochromes are activated by blue light which leads to conformational modifications and enables interaction with signalling intermediates such as SUPPRESSOR OF PHYA-105 1 (SPA1) (Lian *et al.* 2011; Zuo *et al.* 2011; Yang *et al.* 2017). Recently, cryptochromes have been shown to interact with PHYTOCHROME INTERACTING FACTOR 4 (PIF4) and PIF5 (see below), possibly repressing PIFs activity (Ma *et al.* 2016; Pedmale *et al.* 2016). Moreover, it has been proposed that a reduction in blue light, as found in canopy shade, activates the cry1 response pathway and boosts the SAS response (Keller *et al.* 2011).

Another UV-A/blue light photoreceptors are the Zeitlupe family, comprised of ZEITLUPE (ZTL), FLAVIN-BINDING, KELCH REPEAT, F-BOX (FKF1) and LOV KELCH PROTEIN2 (LKP2) proteins (Suetsugu and Wada 2013), all containing a characteristic Light Oxygen Voltage (LOV) domain (Ito *et al.* 2012). Zeitlupes control floral transition and entrainment of circadian clock (Song *et al.* 2014; Christie *et al.* 2015) and are not directly involved in SAS responses.

Phototropins also perceive UV-A/blue light and are part of the AGC kinase family. Structurally similar to zeitlupes, they contain two LOV domains (Christie *et al.* 2015). *A. thaliana* has two phototropins, phot1 and phot2, which regulate phototropism, stomatal opening and leaf flattening (Sakai *et al.* 2001). Perception of blue light by phototropins causes a signalling cascade and an establishment of auxin gradient that directs growth towards the light (Fiorucci and Fankhauser 2017). In shaded conditions particularly, phototropins can enhance directional bending of plant towards higher amount of blue light (Fiorucci and Fankhauser 2017).

3.3 Perception of shade through R and FR

R and FR are perceived by a small family of photoreceptors known as phytochromes. Five of them are present in *A. thaliana* (phyA-phyE) (Rockwell *et al.* 2006; Franklin and Quail 2010). Structurally, phytochromes are dimers, consisting of two monomeric apoproteins with covalently bound tetrapyrrole chromophores called phytochromobilins (Li *et al.* 2011; Kreslavski *et al.* 2018). They exist in two photoconvertible forms, the inactive R-absorbing (Pr) and the active FR-absorbing (Pfr) form. They are synthesised in the cytoplasm in the inactive Pr form (λ_{max} of absorbance at 665 nm) where they also remain if the plant is in the dark. Upon perception of light, Pr form photoconverts into biologically active Pfr form (λ_{max} of absorbance at 730 nm) (Mancinelli 1994; Eichenberg *et al.* 2000). This photoconversion induces conformational changes and exposes nuclear localization signals (NLSs) which leads to a translocation into the nucleus (Nagatani 2004; Van Buskirk *et al.* 2012). Pfr form can be subsequently reconverted to Pr form either with exposure to FR or through a light-independent dark reversion (Mancinelli 1994; Legris *et al.* 2016). Since both Pr and Pfr forms have overlapping absorption spectra, light triggers simultaneous Pr>Pfr and Pfr>Pr photoconversion even with monochromatic R or FR light. However, the concentration of Pr and Pfr forms will ultimately depend on the relative amount of R and FR (i.e., the R:FR) present in the light perceived by the plant (Chen *et al.* 2004; Bae and Choi 2008; Franklin 2008), resulting in a dynamic equilibrium between these two forms of phytochrome.

Genetic analyses have established a role for phytochromes in seedling de-etiolation and SAS responses. First, it was determined that phyA is exclusively responsible for de-etiolation under continuous FR, while phyB has a major role in this process under continuous R (Chen *et al.* 2004; Bae and Choi 2008). Moreover, phyA, which was shown to be the most abundant phytochrome in dark-grown seedlings, is photolabile: upon perception of R or white light (W) with high R:FR, it becomes rapidly photoconverted into Pfr form which is then degraded by the 26S proteasome (Seo *et al.* 2004). By contrast, phyB is photostable and prevalent in W with high R:FR. This allows phyB to have a major role in controlling the photomorphogenesis (Bae and Choi 2008). In fact, active Pfr form of phyB represses SAS and hypocotyl elongation (Martínez-García *et al.* 2010). Upon the perception of low R:FR as in shade, a large pool of phyB photoconverts into the inactive form resulting in induction of SAS and hypocotyl elongation (Martínez-García *et al.* 2010). In addition, mutants deficient in phyB have long hypocotyls in W and an early flowering phenotype, resembling the response of wild-type plants to low R:FR (Devlin *et al.* 2003). Regarding other phytochromes, genetic analyses have shown that phyD and phyE act redundantly with phyB in controlling the SAS responses (Devlin *et al.* 1998; Devlin *et al.* 1999) and phyC is involved in the regulation of photoperiodic flowering (Sánchez-Lamas *et al.* 2016).

4. Shade signalling: from perception to transcription

4.1 Phytochrome – PIF light signalling hub

Phytochromes and cryptochromes directly regulate a group of transcription factors from the basic helix-loop-helix (bHLH) family of proteins known as the PHYTOCHROME INTERACTING FACTORS (PIFs) (Leivar *et al.* 2008; Leivar and Monte 2014). Seven different PIFs are described: PIF1 and PIF3-8. They form a central signalling hub for light regulated developmental and adaptive processes, including SAS. Active nuclear Pfr form of phytochromes directly interacts with PIFs through the phyA (only PIF1/3) and phyB interacting domains (Ni *et al.* 1998; Chen and Chory 2011; Leivar and Quail 2011). This interaction leads to phosphorylation and a subsequent ubiquitination (e.g., PIF4 and PIF5), and proteasome-mediated degradation (Lorrain *et al.* 2008; Leivar and Quail 2011; Zhang *et al.* 2013). While this has been confirmed for PIF1, PIF3, PIF4 and PIF5 (together known as the PIF quartet, or PIFQ), an exception to this rule is PIF7 that upon phosphorylation is not degraded although it is no longer able to regulate gene transcription (Li *et al.* 2012). It was shown that cryptochromes also physically interact with PIF4 and PIF5 (Ma *et al.* 2016; Pedmale *et al.* 2016), possibly repressing their transcriptional activity (Ma *et al.* 2016).

Phytochromes inactivated by low R:FR are unable to bind PIFs, which allows PIFs to accumulate and regulate the transcription of their target genes, preferentially binding to the promoter regions rich in E-box and G-box motifs (Leivar and Monte 2014). This results in a rapid induction of expression of the so-called *PHYTOCHROME RAPIDLY REGULATED* (*PAR*) genes, several of them shown to regulate SAS (Roig-villanova and Martínez-García 2016). Many of the *PAR* genes are transcriptional regulators with a role in hypocotyl elongation and can be grouped in partially redundant functional modules. They are comprised of several protein families, including members of the bHLH (e.g., HFR1, PAR1, PAR2, PIL1, BIM1, BEE1), HD-Zip (e.g., ATHB2, ATHB4, HAT1, HAT2 and HAT3) and BBX family members (BBX21, BBX22, BBX24, BBX25) (Salter *et al.* 2003; Sessa *et al.* 2005; Roig-Villanova *et al.* 2006; Roig-

Villanova *et al.* 2007; Bou-Torrent *et al.* 2008; Hornitschek *et al.* 2009; Sorin *et al.* 2009; Cifuentes-Esquivel *et al.* 2013; Gangappa *et al.* 2013). Their role in SAS regulation was determined through analyses of their mutants, establishing positive growth-promoting (BEEs, BIMs, BBX24, BBX25) or negative (HFR1, PAR1, PIL1) roles.

Among those with a negative role in SAS are the atypical bHLH LONG HYPOCOTYL IN FAR-RED 1 (HFR1), PHYTOCHROME RAPIDLY REGULATED 1 (PAR1) and PAR2 (Fairchild *et al.* 2000; Hornitschek *et al.* 2009; Galstyan *et al.* 2012; Hao *et al.* 2012; Zhou *et al.* 2014). These proteins lack the DNA-binding capability and are thought to prevent the excessive elongation by forming competitive dimers with PIFs (Hornitschek *et al.* 2009; Galstyan *et al.* 2011). This type of negative feedback loops exhibited by HFR1, PAR1 and PAR2 provide another level of mechanistic regulation of PIF activity required for controlled growth in shade (**Figure 3**). The bZIP protein ELONGATED HYPOCOTYL 5 (HY5) (Nawkar *et al.* 2017) inhibits hypocotyl elongation to promote photomorphogenesis through a transcriptional regulation of its target genes (Gangappa and Botto 2016). Furthermore, phytochromes, together with cryptochromes and UVR8 suppress the activity of COP1/SPA E3 ubiquitin ligase which mediates the ubiquitin-proteasome-dependent degradation of proteins. This leads to stabilization of several negative regulators such as the before mentioned HFR1, PAR1 and HY5 (Yang *et al.* 2005; Zhou *et al.* 2014; Nawkar *et al.* 2017) increasing their potential for inhibiting PIF activity (**Figure 3**).

Besides transcriptional regulators, PIFs promote the expression of a wide variety of genes, e.g., enzymes related to cellular expansion, cell-wall modification and hormone biosynthesis. Specifically, PIFs are known to control auxin biosynthesis and signalling (Roig-Villanova *et al.* 2007; Hornitschek *et al.* 2012). Indole acetic acid (IAA), the endogenous and bioactive auxin, is produced from the tryptophan (Trp) amino acid using the enzyme TRYPTOPHAN AMINOTRANSFERASE OF ARABIDOPSIS 1 (TAA1, also known as SHADE AVOIDANCE 3, SAV3) to convert Trp into indole-3-pyruvic acid (IPA); then YUCCA (YUC) enzymes, a group of flavin monooxygenases, convert it to IAA (Zhao 2012) (**Figure 3**). Several *YUC* genes are induced in low R:FR in a PIF-dependent manner, including *YUC2*, *YUC5*, *YUC8* and *YUC9* (Hornitschek *et al.* 2012; Li *et al.* 2012; Kohnen *et al.* 2016); in fact PIF7 was shown to bind to *YUC5*, *YUC8* and *YUC9* promoters (Hornitschek *et al.* 2012; Li *et al.* 2012). Evidence for supporting the role of *YUCs* in SAS is found in quadruple YUC mutant (*yuc2589*) due to the absence of responses to low R:FR (Kohnen *et al.* 2016; Müller-Moulé *et al.* 2016). In addition, hypocotyls in low R:FR have specifically elevated levels of auxins (D. H. Keuskamp *et al.* 2010), partially due to PIN-dependent polar auxin transport which directs auxin from cotyledons to hypocotyl where it is distributed to different cell layers and induces elongation (D. H. Keuskamp *et al.* 2010). Cell expansion is seen as the major driving force of shade-induced organ elongation, especially in seedlings. XYLOGLUCAN ENDOTRANSGLUCOSYLASE / HYDROLASE (XTH) are specific cell wall modifying enzymes which loosen cell walls by acting on xyloglucan-cellulose cross links and allow the cell to expand (Rose *et al.* 2002; Sasidharan *et al.* 2011). *XTHs* are, together with another cell-modifying enzymes called *EXPANSINs* (*EXP*), induced in low R:FR and PIFs were shown to directly regulate *XTH15*/*XTR7* in shade (Hornitschek *et al.* 2009).

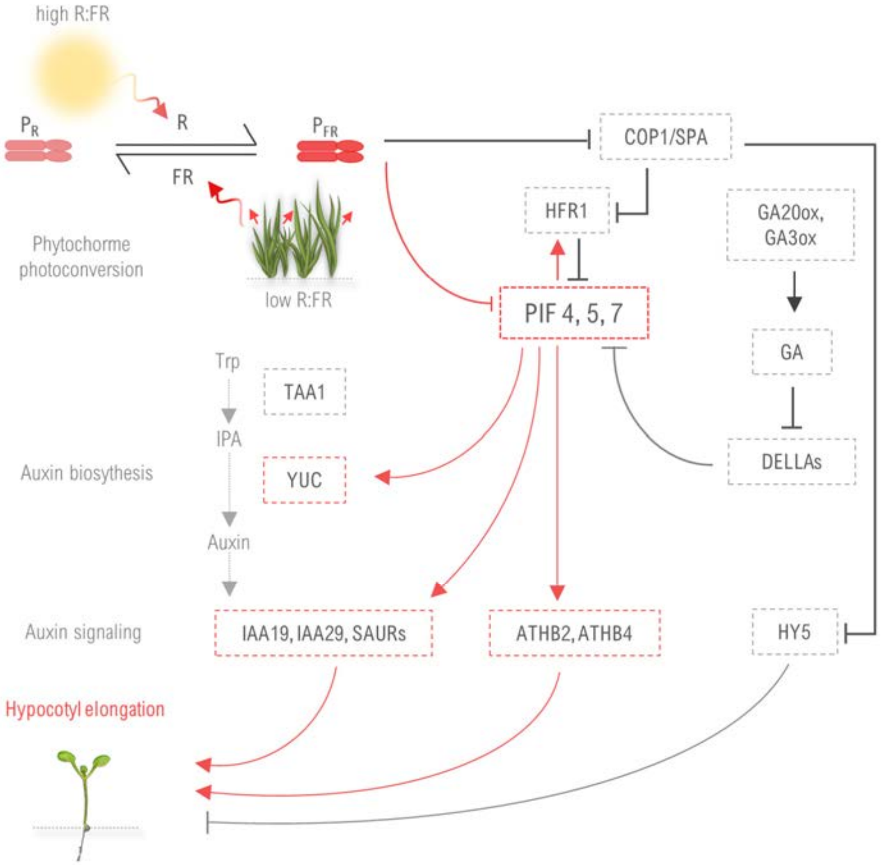
high R:FR
PR
R
FR
PFR
COP1/SPA
HFR1
GA20ox, GA3ox
Phytochorme photoconversion
low R:FR
PIF 4, 5, 7
GA
Trp
TAA1
IPA
Auxin biosynthesis
YUC
DELLAs
Auxin
Auxin signaling
IAA19, IAA29, SAURs
ATHB2, ATHB4
HY5
Hypocotyl elongation

Figure 3. Phytochromes and PIFs are central players of shade signalling pathway. Plants detect their neighbouring vegetation through the perception of low R:FR by phytochromes. Under direct sunlight (high R:FR), phytochromes are mostly in their active FR absorbing state (P_{FR}); in shade, low R:FR displaces most of phytochrome to its inactive R absorbing state (P_R). This allows PIFs to induce a signalling cascade to promote hypocotyl elongation. HFR1, DELLAs and HY5 act as negative modulators while auxin signalling positively contributes to this response. Adapted from (Pierik & Testerink, 2014; Sheerin & Hiltbrunner, 2017)

Low R:FR also promotes the biosynthesis of gibberellins (GA) known to stimulate growth (Bou-Torrent *et al.* 2014), and that is at least partially a result of the upregulation of GA biosynthetic enzymes *GA3ox* and *GA20ox* (Hisamatsu *et al.* 2005) and a reduction in GA 2-oxidase activity, which degrades bioactive GAs (Martinez-Garcia *et al.* 2000). Bioactive GAs through interaction with GID1 receptor, lead to polyubiquitination of DELLAs and their subsequent degradation by the proteasome (Djakovic-Petrovic *et al.* 2007; Schwechheimer 2008; Schwechheimer and Willige 2009; Leone *et al.* 2014). Since DELLAs were shown to bind PIFs (e.g., PIF4) (Feng *et al.* 2008; de Lucas *et al.* 2008), their degradation in low R:FR releases PIFs from DELLA-dependent repression and allows PIF-mediated transcriptional regulation (**Figure 3**).

4.2 Additional mechanism of shade signalling: Nuclear Pore Complex (NPC)

4.2.1 Structure and function of NPC

All the communication between the cytoplasm and the nucleoplasm depends on the transport through large protein structures called Nuclear Pore Complexes (NPCs) (Rout and Wente 1994; Marelli *et al.* 2001; Gasiorowski and Dean 2003). NPCs are established around the aqueous pores of the double membrane layer of nuclear envelope (NE), and resemble a doughnut shaped structures of around 40-60 MDa (Brohawn *et al.* 2009). They are composed of nucleoporins (NUPs) assembled into different subcomplexes (Rout *et al.* 2000; Cronshaw *et al.* 2002). So far, up to ~30 different plant NUPs have been identified, sharing a similar organization of their domains with vertebrate and yeast counterparts (Meier and Brkljacic 2009; Tamura *et al.* 2010; Tamura and Hara-Nishimura 2014). NUPs with transmembrane domains function as a scaffold for the NPC (Güttinger *et al.* 2009) upon which other NUPs assemble. Some NUPs contain Trp-Asp (WD) repeats and form a β-propeller structure that mediates the assembly of NPC scaffold subdomains (Smith *et al.* 1999; Rabut *et al.* 2004). A third of NPC mass is comprised of NUPs with hydrophobic Phe-Gly (FG) repeats, which form a selective barrier for nucleocytoplasmic transport. This barrier is in a form of a hydrogel that reseals when molecules pass through the NPC (Frey and Görlich 2009; Jovanovic-Talisman *et al.* 2009). FG-NUPs also prevent nonkaryophilic proteins larger than 40 kDa from entering or exiting the nucleus simply by diffusion (Patel *et al.* 2007). Nuclear import of proteins usually involves recognition of a certain peptide sequence motif such as the classical nuclear localization signal (NLS), by the import receptors. In *A. thaliana* 8 putative importin α and 17 importin β-like nuclear transport receptor genes have been identified (Kanneganti *et al.* 2007; Merkle 2011). Some of the importin β-like nuclear transport receptors might function in the protein export as well.

4.2.2 Association of NPC with light (shade) signalling

Many aspects of shade signalling involve a critical nucleocytoplasmic translocation step. For instance, in etiolated seedlings, phyB was shown to be mostly cytoplasmic while in light-grown seedlings, it prevails in the nucleus (Yamaguchi *et al.* 1999; Patricia *et al.* 2000). R induces phyB nuclear import and FR reverses this process and inactivates phyB (Kircher *et al.* 1999). The nuclear import of phyB is a process which requires recognition of some sort of an NLS present on the C-terminal domain of phyB and its subsequent translocation through the NPC. Even though this process is not completely understood yet, since the NLS has not been identified, it is possible that the phyB import is NLS-independent (Kevei *et al.* 2007). Contrary to phyB, the mechanism of phyA nuclear import requires direct interaction of the active form of phyA with FAR-RED ELONGATED HYPOCOTYL 1 (FHY1) and partially redundant FHY1-LIKE (FHL) (Hiltbrunner *et al.* 2005; Hiltbrunner *et al.* 2006). When in the nucleus, FHY1/FHL-phyA complex dissociates and frees inactive phyA, while the FHY1/FHL recycles back to the cytoplasm.

The auxin signalling pathway is also partitioned between the cytoplasm and nucleoplasm (Leyser 2018) and connected through the NPC. Several NUPs were reported to be involved in auxin signalling (**Figure 4**) and to partially suppress the *axr1* auxin resistance phenotype (Parry *et al.* 2006; Jacob *et al.* 2007; Ferrández-Ayela *et al.* 2013). Specifically, the *axr1* mutant accumulates Aux/IAA proteins which then repress auxin regulated transcription (Lincoln 1990). This is due to the fact that AXR1 is a subunit of the RUB-activating enzyme which modifies cullin and enables proper formation of Skp1-Cul1/Cdc53-F-box (SCF) complex (del Pozo *et al.* 2002). SCF complex then mediates the auxin dependent degradation of AUX/IAA repressors (del Pozo *et al.* 2002). NUPs such as NUP160/SAR1 (Parry *et al.* 2006), NUP96/SAR3 (Jacob *et al.* 2007), NUP58 (Ferrández-Ayela *et al.* 2013), NUA/Tpr (Jacob *et al.* 2007) and NUP62 (Boeglin *et al.* 2016) all seem to have a role in auxin signalling. For instance, SAR1 and SAR3 retain the AUX/IAA17 transcriptional regulator inside the nucleus; it was proposed that NUP62 might act as a negative regulator of auxin responses in a similar way (Boeglin *et al.* 2016). Therefore, SAR1 and SAR3 are required for Aux/IAA nuclear transport in response to auxin signalling (Robles *et al.* 2012).

Early flowering is a common phenotype of various NUP mutants (**Figure 4**). It has been reported for *nup58* (Ferrández-Ayela *et al.* 2013), *nup62* (Zhao and Meier 2011), *nup136/nup1* (Lu *et al.* 2010; Tamura *et al.* 2010), *nup160/sar1* (Dong *et al.* 2006; Parry *et al.* 2006), *hos1/elys* (Ishitani *et al.* 1998; Lazaro *et al.* 2012; MacGregor *et al.* 2013) and *trp/nua* (Jacob *et al.* 2007; Xu *et al.* 2007). In the *trp/nua* mutant, the expression of flowering-related genes was found to be significantly affected (Xu *et al.*

2007) which led to the identification of TRP/NUA as a suppressor of *FLC* expression (Jacob *et al.* 2007). Another well studied example is the one of HOS1/ELYS, which regulates flowering time independently of FLC (Lazaro *et al.* 2012; Lee *et al.* 2012). It is suggested that HOS1/ELYS is implicated in a proteasome-dependent degradation of CONSTANS (CO) at the NPC (Lazaro *et al.* 2012; Seo *et al.* 2013) since it physically interacts with CO and regulates its abundance (Lazaro *et al.* 2012).

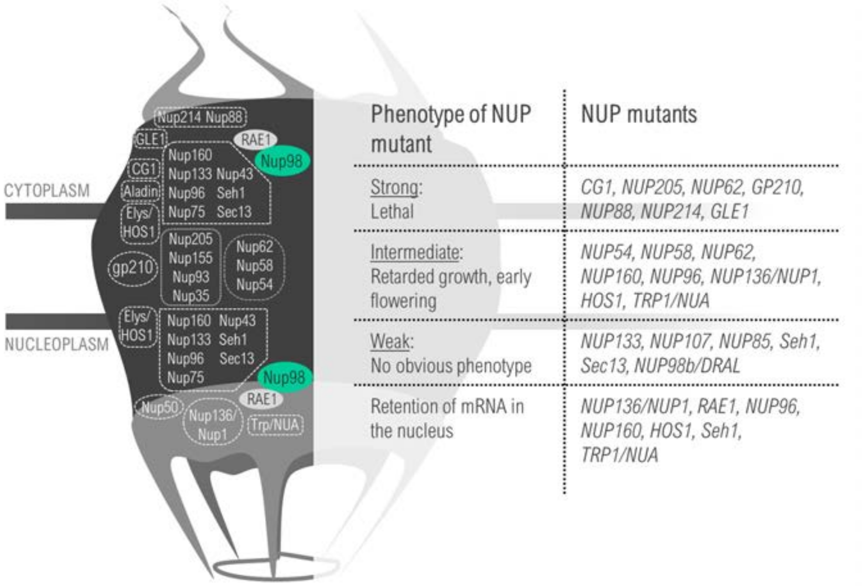
CYTOPLASM
NUCLEOPLASM
Nup214 Nup88
GLE1
RAE1
Nup98
CG1
Aladin
Elys/ HOS1
Nup160
Nup133 Nup43
Nup96 Seh1
Nup75 Sec13
gp210
Nup205
Nup155
Nup93
Nup35
Nup62
Nup58
Nup54
Elys/ HOS1
Nup160 Nup43
Nup133 Seh1
Nup96 Sec13
Nup75
Nup98
RAE1
Nup50
Nup136/ Nup1
Trp/NUA

Phenotype of NUP mutant	NUP mutants
Strong: Lethal	*CG1, NUP205, NUP62, GP210, NUP88, NUP214, GLE1*
Intermediate: Retarded growth, early flowering	*NUP54, NUP58, NUP62, NUP160, NUP96, NUP136/NUP1, HOS1, TRP1/NUA*
Weak: No obvious phenotype	*NUP133, NUP107, NUP85, Seh1, Sec13, NUP98b/DRAL*
Retention of mRNA in the nucleus	*NUP136/NUP1, RAE1, NUP96, NUP160, HOS1, Seh1, TRP1/NUA*

Figure 4. Nucleoporins (NUPs) are basic structural units of the Nuclear Pore Complex (NPC) with specific and general roles in plant development. The NPC is a multiprotein complex formed by around 30 distinct NUPs, arranged in an eightfold symmetry. It mediates the transport of mRNAs and big proteins (larger than 40 kDa). NUP deficient mutants are classified by the strength of their phenotype; strong phenotype is lethal, intermediate is characterized with slower vegetative growth and early flowering, and weak has no obvious developmental effects. Among general characteristics of NUP mutants is the retention of mRNA inside the nucleus. Adapted from (Tamura, Fukao, Iwamoto, Haraguchi, & Hara-Nishimura, 2010; Xu et al., 2007; Zhao & Meier, 2011).

4.2.3 Chromatin regulation by NPC

So far, increasing evidence has shown that NPCs do not function only as regulators of nucleocytoplasmic transport but in addition they participate in the regulation of multiple cellular processes in a transport-independent manner (Raices and D'Angelo 2012). First evidence for a role of NPC in gene expression regulation comes from yeast *Saccharomyces cerevisiae*. The Nup84 scaffold subcomplex of yeast NPC was shown to be a transcriptional activator (Menon *et al.* 2005), and several other NUPs were shown to be associated with transcriptionally active genes (Casolari *et al.* 2004; Schmid *et al.* 2006). Moreover, several yeast genes are targeted to the nuclear periphery; specific sequences in their promoters are recognized by transcription factors which ultimately mediate the relocation of genes (Randise-Hinchliff *et al.* 2016; Randise-Hinchliff and Brickner 2016). Association of these genes with the NPC is not necessary for their activation but increases their efficiency (Brickner and Walter 2004; Taddei *et al.* 2006; Texari *et al.* 2013), and in some cases transcription factors only mediate the relocation and not the gene activation (Brickner *et al.* 2012; Randise-Hinchliff and Brickner 2016). This type of NPC-tethering also suggests that gene repositioning is a separate process from its transcriptional regulation (Raices and D'Angelo 2017).

In *A. thaliana*, a similar gene repositioning process has been discovered with the light inducible *CHLOROPHYLL A/B-BINDING* (*CAB*) gene locus (Feng *et al.* 2014). From the nuclear interior, *CAB* locus relocates to the nuclear periphery before its full transcriptional activity. It is not known whether *CAB* repositioning induced by light is actually required for its activity, but it could be triggered by the degradation of PIF3 by phytochromes (Leivar and Quail 2011; Feng *et al.* 2014). This example does not imply all light-inducible genes are relocated to the nuclear periphery upon light induction, but nonetheless it does demonstrate that a similar mechanism is conserved across fungal, animal and plant kingdoms.

5. Alternative strategies of response to shade

5.1 Shade tolerance

Light competition in shaded areas is an important factor influencing plant performance and fitness. From an ecological point of view, shade tolerance refers to the capacity of a plant to tolerate low light levels (Valladares and Niinemets 2008) and it can also be defined as the minimum amount of light required for plant survival (Graves *et al.* 1911; Shugart and West 1980; Bonan and Shugart 1989; Valladares *et al.* 2016). But even though shade is usually treated as an environmental condition of low light, it involves an array of heterogeneous conditions capable of inducing shade adaptive responses in plants, from vegetation proximity to direct canopy shade (**Figure 1**). Tolerance to shade can be achieved by a variety of different trait suits in different species and involves changes in the morphology of the whole plant or only of particular organs (Valladares and Niinemets 2008). Two hypotheses have been developed to describe which suit of traits are responsible for shade tolerance: 1) maximization of the net carbon gain, and 2) maximization of the tolerance to stress

(Givnish 1988; Kitajima 1994; Valladares and Niinemets 2008). Carbon gain hypothesis describes any trait that improves the efficiency of light use, to improve the carbon gain, as beneficial for shade tolerance (Givnish 1988), including higher photosynthetic capacity and light harvesting efficiency (Niinemets and Tenhunen 1997; Niinemets *et al.* 1998). Contrary, stress tolerance hypothesis suggests that plant resistance to biotic and abiotic stresses is more relevant to survival in shade (Kitajima 1994). Different forms of plant growth may also be favoured in different habitats, with erect form preferred in low-light and rosette growth form in high-light habitats (Bonser and Geber 2005). Some authors have proposed that long-lived herbaceous plants under competition will invest their energy in uptake of resources and delay the reproduction, while short-lived plants will preferentially accelerate reproduction (Turkington *et al.* 1993; Grime 2007), as seen in *A. thaliana* under shade (Roig-villanova and Martínez-García 2016). This is known as the strategy theory (Grime 2007). On a seedling level, hypocotyl elongation is an indicator of shade avoidance strategy in many herbaceous plants including *A. thaliana* (Robson *et al.* 1993; Franklin and Whitelam 2005; Diederik H. Keuskamp *et al.* 2010), and the absence of it can indicate a shade tolerant strategy. It is still not known how common are these differences between shade avoidant and tolerant species, and how common is for the plants to alter the response strategies during their lifetime, e.g., from juvenile to adult stage (Smith 1994; Henry and Aarssen 1997).

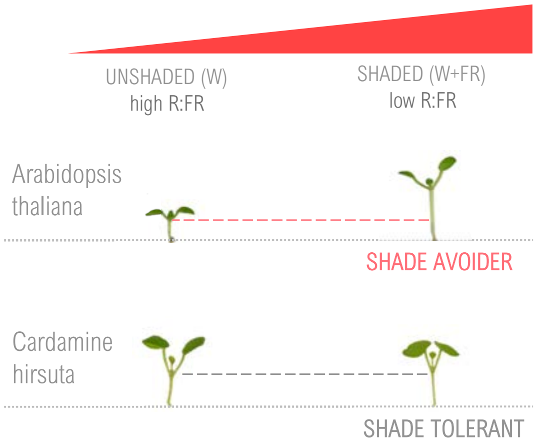

Figure 5. Hypocotyls of C. hirsuta seedlings are unresponsive to shade. Comparison of A. thaliana (shade avoider) and C. hirsuta (shade tolerant) 7-day old seedlings grown in continuous W simulating unshaded conditions (high R:FR) and in W supplemented with FR (W+FR) which simulates shaded conditions (low R:FR). A. thaliana hypocotyls elongate in response to shade while those of C. hirsuta do not.

5.2 *Cardamine hirsuta* as a model for comparative studies

In our laboratory, we decided to employ an herbaceous plant *C. hirsuta*, a close relative of *A. thaliana* (Hay *et al.* 2014) that is known to be shade tolerant in seedling stage, i.e., having hypocotyls unresponsive to shade (**Figure 5**) (Hay *et al.* 2014). *C. hirsuta* is a widespread, ruderal species of weed similar to *A. thaliana* (**Figure 6A**), native to Europe and commonly found growing in gardens, nurseries and disturbed ground (Rich 1991; Lihova *et al.* 2006; Hay *et al.* 2014). It is a diploid, self-compatible annual plant (usually winter annual) with a short reproductive cycle of around 8 weeks, and a small rosette (**Figure 6A**). *C. hirsuta* can be transformed easily with floral dipping method using *Agrobacterium tumefaciens*, allowing genetic and molecular studies and having a potential to be a good model system alongside *A. thaliana*.

From an evolutionary point of view, *C. hirsuta* and *A. thaliana* lineages have separated sometime between 13 and 43 million years ago (Beilstein *et al.* 2008; Couvreur *et al.* 2010), leaving its mark on the genome of both species and causing a divergence of developmental and physiological characteristics, such as leaf shape (**Figure 6B**), flower characteristics and seed dispersal mechanism among others (Hay and Tsiantis 2006; Barkoulas *et al.* 2008; Blein *et al.* 2008). *C. hirsuta* counts with 198 Mbp sized genome, organized into 8 chromosomes, compared to 135 Mbp genome and 5 chromosomes of *A. thaliana* (**Figure 6C**) (The Arabidopsis Genome Initiative 2000; Gan *et al.* 2016; Cheng *et al.* 2016 Apr 5). The genome of *C. hirsuta* is largely syntenic to the genomes of *A. thaliana* (**Figure 6C**) and related *A. lyrata*, although *C. hirsuta* retains more ancestral features, such as karyotype and genome size, than *A. thaliana* (Hay *et al.* 2014; Gan *et al.* 2016).

Comparative genetic analyses between *C. hirsuta* and *A. thaliana* have helped to understand the differences in morphological traits between both species. For instance, a gene duplication event led to the emergence of *REDUCED COMPLEXITY* (*RCO*) type genes from *LATE MERISTEM IDENTITY 1* (*LMI1*) within the *Brassicaceae*, before the common ancestor of *Brassica* and *Arabidopsis* (Hay and Tsiantis 2006; Barkoulas *et al.* 2008; Vlad *et al.* 2014). *RCO* has a distinct expression pattern in the leaf base which leads to a development of pinnately compound leaves with leaflets on both sides of the rachis in *C. hirsuta* (**Figure 6B**) (Vlad *et al.* 2014). Secondary loss of *RCO* in *A. thaliana* left only *LMI1* type and simple leaf shape. Other divergent morphological traits between these two species include structure of trichomes, which are unbranched in *C. hirsuta* and only present on leaves, unlike in *A. thaliana* (Hay *et al.* 2014).

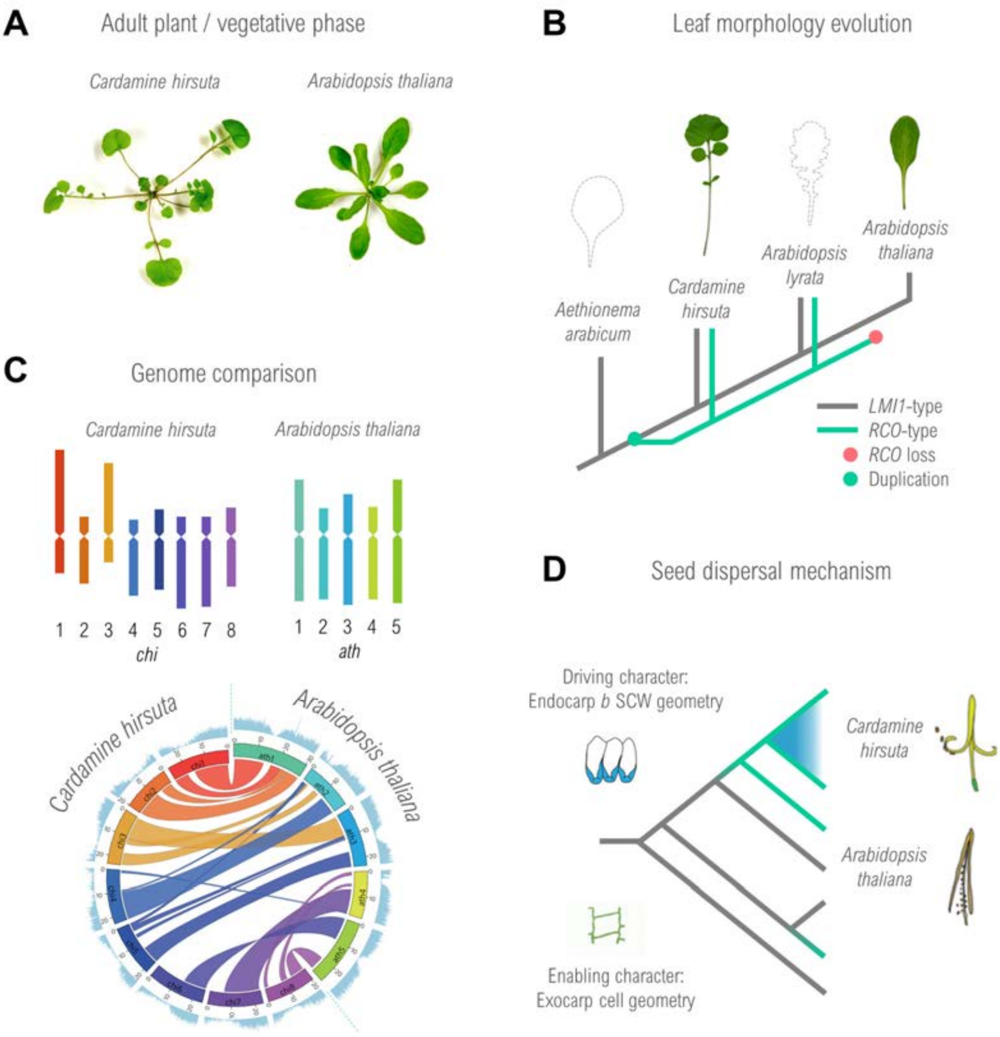
A
Adult plant / vegetative phase
Cardamine hirsuta
Arabidopsis thaliana
B
Leaf morphology evolution
Aethionema arabicum
Cardamine hirsuta
Arabidopsis lyrata
Arabidopsis thaliana
LMI1-type
RCO-type
RCO loss
Duplication
C
Genome comparison
Cardamine hirsuta
Arabidopsis thaliana
1 2 3 4 5 6 7 8
chi
1 2 3 4 5
ath
Cardamine hirsuta
Arabidopsis thaliana
chi1
chi2
chi3
chi4
chi5
chi6
chi7
chi8
ath1
ath2
ath3
ath4
ath5
D
Seed dispersal mechanism
Driving character: Endocarp b SCW geometry
Cardamine hirsuta
Arabidopsis thaliana
Enabling character: Exocarp cell geometry

Figure 6. Comparison of morphological, genomic and evolutionary characteristics between A. thaliana and C. hirsuta. (A) Aspect of 3-week-old A. thaliana and C. hirsuta plants. (B) Evolution of leaf morphology. Complex dissected leaf shape in C. hirsuta is a result of an RCO-type gene emergence from an early LMI1-type gene duplication. In A. thaliana RCO-type gene was lost after this species diverged from A. lyrata, leading to a simple leaf shape. (C) C. hirsuta has 8 and A. thaliana 5 chromosomes (upper). Circos plots (lower) are displaying synteny between the genomes of C. hirsuta and A. thaliana. Outer circle represents gene density distribution with a window size of 100 kbp. (D) Explosive seed dispersal mechanism in C. hirsuta was driven by an innovative character trait of endocarp b secondary cell walls (SCW) geometry while exocarp cell geometry was the enabling character trait for this innovation. Adapted from (Gan et al., 2016; Hay et al., 2014; Hofhuis & Hay, 2017)

C. hirsuta plants are also more branched than *A. thaliana* and develop morphologically distinguishable flowers compared to *A. thaliana*, with altered stamen number and more spoon-shaped petals with reduced petal number (0-4) (Hay *et al.* 2014). *C. hirsuta* produces five time larger seeds than *A. thaliana*, which are longitudinally flattened to form a disc shape (Hay *et al.* 2014). The seed dispersal strategy of *C. hirsuta* is also radically different from that of *A. thaliana* (**Figure 6D**). *C. hirsuta* uses an explosive seed dispersal mechanism (Vaughn *et al.* 2011; Hofhuis and Hay 2017), during which the two valves of the fruit pod rapidly coil and become explosive, dispersing seeds away. Two cellular innovations allowed this trait: 1) the emergence of squared cells in the fruit exocarp, and 2) the asymmetric secondary cell wall (SCW) geometry in endocarp *b* cells (**Figure 6D**) (Gan *et al.* 2016; Hofhuis *et al.* 2016; Hofhuis and Hay 2017). This trait probably contributed to its success as an invasive and colonizing species. The same mechanism could also allow *C. hirsuta* to project seeds far from or into the shaded areas, potentially improving survival rate of its offspring. Seeds of *C. hirsuta* retain good germination in laboratory conditions and develop larger seedlings with longer hypocotyls that also have adventitious roots and a thicker primary root (Hay *et al.* 2014).

In summary, *C. hirsuta* can be a good model species for comparative studies of divergent morphological and physiological traits, such as seedling responses to shade in *Brassicaceae*, as it can provide insight into evolutionary, genetic and molecular basis for differences that established shade tolerant trait in this species.

OBJECTIVES

Objectives

The general objective of this work is to expand the current understanding of the mechanistic and genetic regulation of plant responses to vegetation proximity. For this purpose, we have focused on two specific objectives:

1. Molecular characterization of the newly identified SAS regulator DRA2 and its implication in shade signalling. Using *Arabidopsis thaliana*, we want to focus on the specific mechanism of action of DRA2 within the shade signalling, as well as to explore the general implications of nuclear pore complex (NPC) function in SAS regulation.

2. Comparative genetic and molecular analyses of *A. thaliana* and *Cardamine hirsuta*, two related species with divergent elongation responses to shade. We aim to search for common regulators of these divergent responses with differential mechanism of action within shade signalling. Specifically, we will compare HFR1 function and activity in these two related species.

CHAPTER I

Part of Chapter I has been published in the research article:

DRACULA2 is a dynamic nucleoporin with a role in regulating the shade avoidance syndrome in Arabidopsis.

Marçal Gallemí, Anahit Galstyan, Sandi Paulišić, Christiane Then, Almudena Ferrández-Ayela, Laura Lorenzo-Orts, Irma Roig-Villanova, Xuewen Wang, Jose Luis Micol, Maria Rosa Ponce, Paul F. Devlin, Jaime F. Martínez-García (2016). *Development* 143: 1623-1631; doi: 10.1242/dev.130211

1. Introduction

Response of plants to vegetation proximity and canopy shade (named shade avoidance response - SAS) has been a popular topic of interest for many years, and while many aspects of these regulatory mechanisms have been described, we are still far from fully deciphering SAS. Towards this goal, a new genetic screening was established to isolate novel regulators of shade signalling. This screening employed an EMS mutagenized shade-inducible transgenic line of *A. thaliana*, PBL, which expresses the *LUCIFERASE* (*LUC*) gene under the *PHYTOCHROME B* (*PHYB*) promoter in a Ws-2 background (Bognár *et al.*, 1999). The high throughput screening was based on the detection of altered luciferase activity in shade, that resulted in the isolation of a single allele of the *dracula2* (*dra2-1*) mutant, shown to be recessive and monogenic. Besides a significantly attenuated luciferase activity in shade, *dra2-1* mutant has longer hypocotyls in W and an attenuated hypocotyl response to W+FR (**Figure 1A-B**).

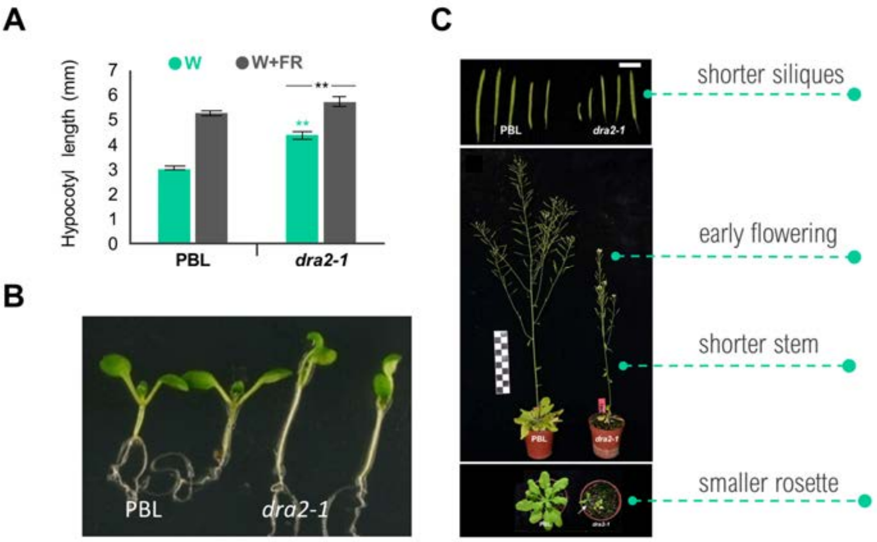

Figure 1. dra2-1 mutant seedlings have an attenuated response to shade, while adult plants have a constitutive SAS phenotype. **(A)** Hypocotyl length of 7-day old PBL and dra2-1 seedlings in W and W+FR. Seedlings were grown for 7 days in continuous W or for 2 days in W and then for additional 5 days in W+FR. Hypocotyl length is the mean ± SE of at least 20 seedlings per genotype and treatment. Green asterisks indicate significant differences (Student's t-test, ** $p<0.01$) relative to PBL grown in the same light conditions. Black asterisks indicate significant differences (two-way ANOVA, ** $p<0.01$) in the shade response between dra2-1 and PBL. **(B)** Aspect of 7-day old W-grown PBL and dra2-1 seedlings. **(C)** Phenotypes of adult PBL and dra2-1 plants, displaying aspect of siliques, flowering stems and rosettes. Adapted from (Gallemí et al., 2016).

Moreover, *dra2-1* seedlings present strongly hyponastic cotyledons (**Figure 1B**). Adult *dra2-1* plants display a constitutive SAS phenotype in long-day conditions, with smaller rosettes, shorter stems and siliques, as well as early flowering (**Figure 1C**). Overall, the aspect of the plant is weak and resembles the phenotype of a plant grown in shade, suggestive of the impairment in shade signalling mechanisms.

1.1 *DRA2* encodes nucleoporin NUP98a.

Positional cloning aimed to discover the gene responsible for *dra2-1* phenotype pointed to a candidate region in chromosome 1, more precisely, gene *At1g10390* encoding a nucleoporin (NUP) with similarity to mammalian Nup98 (mNup98). Sequencing of *At1g10390* in *dra2-1* and the control PBL lines revealed a nonsense mutation at Trp780, due to a G to A transition, introducing a premature STOP codon (**Figure 2**). It was concluded that DRA2 is NUP98a, which is a structural part of the nuclear pore complex (NPC) (**Figure 2**).

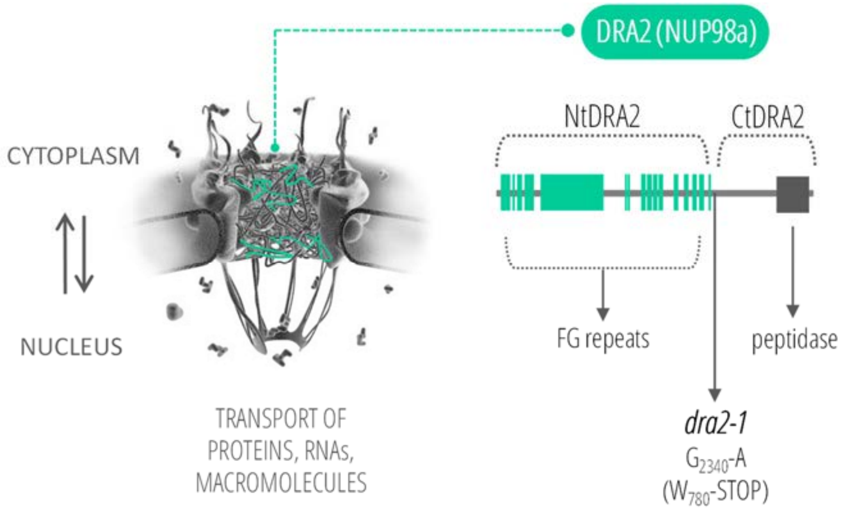

Figure 2. DRA2 is a nucleoporin, part of the NPC. Cartoon depicting DRA2 (NUP98a) as a structural part of the NPC, which is involved in nuclear trafficking (left). Schematic representation of DRA2 protein structure with phenylalanine-glycine (FG) repeats on the N-terminal part (Nt) and a putative autopeptidase domain on the C-terminal part (Ct) of the protein (right). The mutation of the dra2-1 allele is located between Nt and Ct and leads to a premature STOP codon. Adapted from (Gallemí et al., 2016; Patel, Belmont, Sante, & Rexach, 2007).

Moreover, the recessive *dra2-1* mutation can be complemented with *DRA2-GFP* overexpression, resulting in transgenic lines that display a wild-type phenotype. Several other T-DNA insertional mutants of *DRA2* in Col-0 background are known (*dra2-2* to *dra2-5*), all having an insertion within the ORF of the *DRA2* gene, except *dra2-2* (Alonso *et al.*, 2003). However, all these mutants have slightly longer hypocotyls than Col-0 in W but a WT response to shade. Overall, their phenotype can be considered as mild compared to *dra2-1*, a possible consequence of a Col-0 genomic background as suggested by the reduction of the strong *dra2-1* phenotype, specifically cotyledon hyponasty, when backcrossing this allele several times with Col-0. Therefore, the discrepancy between the strong *dra2-1* phenotype in Ws-2 background and mild phenotypes of other *DRA2* mutants in Col-0 background raised doubts about the molecular identity of DRA2 and prompted to further establish whether *dra2-1* phenotype is truly caused by the nonsense mutation within the *At1g10390* gene.

NUP98a/DRA2 is a 1041 amino acids long protein, of ~105 kDa molecular weight. Structurally, it belongs to a group of proteins with hydrophobic phenylalanine-glycine (FG) repeats (**Figure 2**) named FG NUPs (Xu and Meier, 2008). DRA2 shows high sequence similarity with NUP98b (which we named DRA2-LIKE, DRAL) (Xu and Meier, 2008; Tamura *et al.*, 2010), a possible consequence of a gene duplication during evolution. In mammals, DRA2 homolog mNup98 is better characterized, with defined functions for its Nt and Ct regions (Radu, Moore and Blobel, 1995; Hodel *et al.*, 2002). The Nt region of mNup98 is involved in forming a permeable NPC barrier regulating trafficking, while the Ct region is responsible for docking mNup98 into NPC (Hodel *et al.*, 2002). Since virtually no information was available about the function of DRA2 in plants, we aimed to determine the function of DRA2 in SAS regulation and within the NPC. In that respect, (i) can the knowledge about mNup98 be useful for understanding the function of DRA2 due to their structural similarities and cross-species conservation, and (ii) does DRA2 behave dynamically as it was shown for mNup98 (Griffis, 2002)?

1.2 Nucleoporin mutants share general physiological defects, impairment in nuclear function and response to shade

Different NUP mutants generally have longer hypocotyls in W compared to WT, but diverge in the strength of the altered response to W+FR (Gallemí *et al.*, 2016). In fact, the phenotype of a range of NUP mutants can be classified in two groups: strong (*sar1-4*, *sar3-1*, *tcu1-1*, *nup62-1* and *nup62-2*) with significant attenuation of response to shade as *dra2-1*, or weak (*sar3-3*, *nup54-1*, *nup54-2*, *tcu1-2*, *tcu1-4*, *dra2-*

2 to *dra2-5*), responding as WT (Gallemí *et al.*, 2016). Therefore, a general defect in the regulation of hypocotyl length in W and W+FR might be a consequence of an impaired NPC, e.g., affecting some aspects of seedlings development such as auxin regulation. Early flowering is another characteristic shared by several NUP mutants, such as strong *sar1*, *sar3* (Dong *et al.*, 2006; Parry *et al.*, 2006), *nup62* (Zhao and Meier, 2011), *nup136* (Tamura and Hara-Nishimura, 2011), *transcurvata 1* (*tcu1*)/*nup58* (Ferrández-Ayela *et al.*, 2013), *nuclear pore anchor* (*nua*) (Jacob *et al.*, 2007; Xu *et al.*, 2007; Jacob and Michaels, 2008) and *dra2*. In addition to the developmental consequences of NUP absence, whole-mount in situ hybridization of poly(A)$^+$ RNA revealed that SAR1 and SAR3 are involved in the nuclear transport of mRNA to the cytoplasm (Dong *et al.*, 2006; Parry *et al.*, 2006). The same effect was observed in other NUP mutants, such as *nup136* (Lu *et al.*, 2010; Tamura *et al.*, 2010), *hos1* (MacGregor *et al.*, 2013), *seh1* (Wiermer *et al.*, 2012), *nua* (Jacob *et al.*, 2007; Xu *et al.*, 2007) and in the *dra2-1* mutant (Gallemí *et al.*, 2016), placing DRA2 among them. Besides physiological defects, NUP-deficient mutants also share altered molecular responses, e.g., misregulated gene expression (Parry, 2014). It was unknown whether DRA2 shares this aspect of transport-dependent function with other NUPs. Yet, further evidence supporting this idea is a specific upregulation of genes related to nuclear trafficking in *dra2-1* seedlings, such as *DRAL* (**Figure 3**), *RNA EXPORT FACTOR* (*RAE1*) and *NUCLEAR EXPORTIN 1B* (*XPO1B*), all three reported to be upregulated in two NUP-deficient mutants, *nup62* and *nup160* (Parry, 2014).

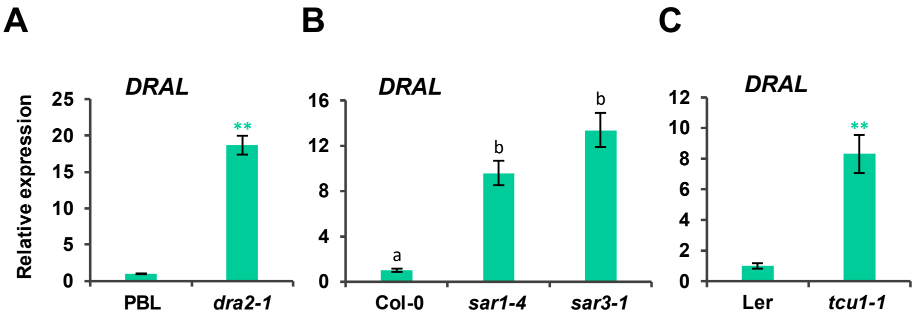

Figure 3. Several NUP deficient mutants have upregulated DRAL expression. Relative expression of DRAL in 7-day old W-grown seedlings of PBL and dra2-1 (A), Col-0, sar1-4 and sar3-1 (B) and Ler and 35S:TCU1-GFP (C), normalized to UBQ10. Expression values are the mean ± SE of three independent biological replicates relative to the data of 7-day old PBL (A), Col-0 (B) or Ler (C). Asterisks indicate significant differences (Student's t-test, ** $p<0.01$) relative to PBL (A) or Ler (C). Lowercase letters indicate significant differences (one-way ANOVA with Tukey test, $p<0.05$) among means (B). Adapted from (Gallemí et al., 2016).

The misexpression of *DRAL* seems to be related to the strength of the NUP mutant phenotype, with higher upregulation in the case of strong alleles (e.g., *dra2-1*, *sar3-1*) and a lesser one in weaker alleles (e.g., *tcu1-2, sar3-3*) (Gallemí *et al.*, 2016). Based on this molecular phenotype among different NUP mutants, *DRAL* expression can be considered a good marker of defective NPC function (Gallemí *et al.*, 2016). Altogether, the pleiotropy of the observed phenotypes in NUP-deficient mutants suggested that the main cause of these physiological abnormalities could be due to the general impairment of the NPC and the regulation of nuclear transport, i.e., they are transport dependent.

1.3 Attenuated shade response of *PAR* genes is characteristic of *dra2-1* but not other NUP mutants

PAR genes can be considered faithful markers of an early shade response (Roig-Villanova *et al.*, 2007; Bou-Torrent *et al.*, 2008). It was observed that shade-induced expression of several *PAR* genes, such as *PHYB*, *PIL1* and *HFR1*, was attenuated in *dra2-1* compared to the control PBL seedlings (**Figure 4A-B**). While *sar1-4* and *sar3-1* seedlings did share with *dra2-1* an attenuation of the shade-induced *PHYB* expression, *PIL1* and *HFR1* expression was clearly divergent, i.e., they were even more induced by shade than in the corresponding WT (**Figure 4A, C**). *TCU1* mutant seedlings (Ferrández-Ayela *et al.*, 2013), specifically *tcu1-1*, is another example of a NUP mutant with a pleiotropic phenotype. TCU1 is a nucleoporin exclusively located within the NPC (**Figure 5A**) (Tamura *et al.*, 2010), and the strong *tcu1-1* also results in upregulated *DRAL* expression (**Figure 3C**) but with no effect on the shade-induced *PAR* gene expression compared to its WT (**Figure 5B**). Therefore, DRA2 appears to be specifically involved in promoting shade-induced expression of *PIL1* and *HFR1*, and SAR1 and SAR3 together with DRA2 seem to regulate the expression of *PHYB*, while TCU1 does not affect any of the before mentioned genes. These results demonstrate that some NUPs have specific functions in regulating cellular processes (e.g., regulation of gene expression) that extend beyond their transport-dependent roles within the NPC. The dynamic behaviour of some plant NUPs, such as NUP136, shown to be highly mobile and to dynamically interact with the NPC (Tamura *et al.*, 2010), suggests that the transport-independent functions of plant NUPs are possible and common as observed with several other animal NUPs (Griffis, 2002; Labade, Karmodiya and Sengupta, 2016). In that sense, it was of our interest to explore if DRA2 is dynamic and if it might also act independently of its transport role within the NPC.

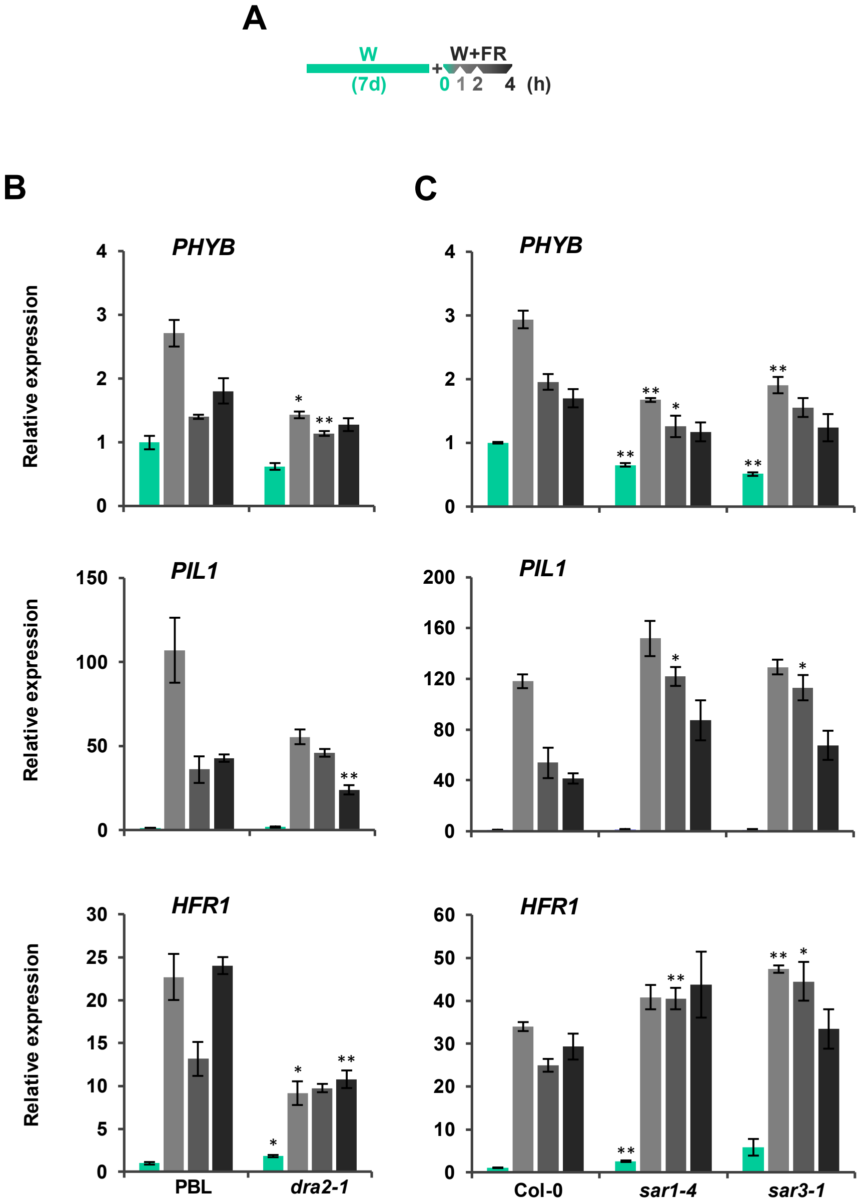

Figure 4. Shade-induced expression of several PAR genes is attenuated in dra2-1 but not in other nucleoporin mutants. (A) 7-day old W-grown seedlings were treated with W+FR for 0, 1, 2 or 4h. Relative expression of PHYB, PIL1 and HFR1 in 7-day old seedlings of PBL and dra2-1 (B), and Col-0, sar1-4 and sar3-1 (C), normalized to UBQ10. Expression values are the mean ± SE of three independent biological replicates relative to the data of PBL (B) or Col-0 (C) at time point 0h. Asterisks indicate significant differences (Student's t-test, * p<0.05, ** p<0.01) relative to PBL (left) or Col-0 (right) for each time point. Adapted from (Gallemí et al., 2016).

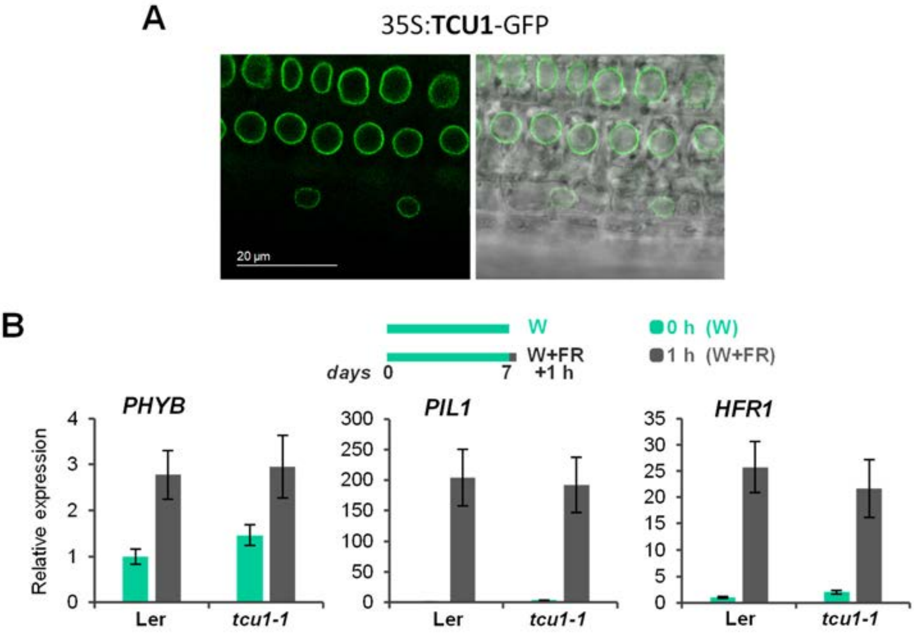

Figure 5. TCU1 is a nucleoporin not involved in the regulation of shade-induced PAR gene expression. (A) Fluorescent confocal images of a seedling root of 35S:TCU1-GFP A. thaliana transgenic line. Left image shows green fluorescence and right one the overlay of green fluorescence and brightfield images. Seedlings were grown for 7 days in continuous W. (B) Relative expression of PHYB, PIL1 and HFR1 in 7-day old seedlings of Ler and tcu1-1 normalized to UBQ10. Seedlings were grown for 7 days in continuous W and either kept in W or treated with 1 h of W+FR, as indicated at the top of the section. Expression values are the mean ± SE of three independent biological replicates relative to the data of Ler at time point 0h. There are no significant differences (Student's t-test) relative to Ler at the same time point. Adapted from (Gallemí et al., 2016).

We identified a NUP, DRA2, as a novel SAS regulator shown to affect several aspects of SAS that might be caused by transport-dependent and -independent activities. Structurally, DRA2 is similar to mammalian mNup98, with whom it shares several characteristics, such as the dominant negative effect that its overexpressed Nt region has in *A. thaliana*. In this chapter we explore whether DRA2 shares additional characteristics with mNup98, including subcellular localization, dynamic behaviour and the possible direct regulation of gene expression that might sustain its transport-independent activity. We further explored the use of a chemical treatment targeted to impair NPC function to study molecular aspects of SAS that might be related to the transport-dependent activity of DRA2.

2. Results

2.1 RNAi-DRA2 lines behave as the strong *dra2-1* mutant

To confirm that the strong *dra2-1* phenotype was truly caused by the nonsense mutation within the *DRA2* gene, we generated lines overexpressing RNAi construct against *DRA2* (35S:RNAi-DRA2) in Ws-2 background, to silence the levels of endogenous *DRA2* (**Figure 6A**). Several independent RNAi-DRA2 lines were selected and brought to homozygosis. Two representative RNAi-DRA2 lines displayed slightly longer hypocotyls in W but shorter hypocotyls in W+FR compared to Ws-2 (**Figure 6B, C**), indicative of attenuation of shade response. The phenotype of RNAi-DRA2 seedlings (**Figure 6C**) mildly resembled the *dra2-1* phenotype with slightly hyponastic cotyledons in W, even though we have observed strongly hyponastic cotyledons in a few severely developmentally affected lines which did not survive. Moreover, these lines had significantly reduced levels of *DRA2* (**Figure 6D**), as well as significantly upregulated levels of *DRAL* compared to Ws-2 (**Figure 6E**), as observed in *dra2-1* mutant compared to PBL (**Figure 3A**) (Gallemí *et al.*, 2016). These results indicated that the mutation of the *DRA2* gene in a Ws-2 background was indeed responsible for the characteristic and strong *dra2-1* phenotype.

2.2 NtDRA2 acts as a dominant negative form

The overexpression of the Nt region of the mammalian homologue mNup98 in neuronal progenitor cells was reported to have a dominant negative phenotype (Liang *et al.*, 2013). Because animal (mNup98) and plant NUP98a (DRA2) are conserved, we hypothesized that overexpression of the *NtDRA2* might also result in a dominant negative phenotype in *A. thaliana*. To test this possibility, the first 779 bp encoding the Nt region of *DRA2* fused to GFP was overexpressed in Col-0 plants and several independent lines were selected, brought to homozygosis and characterized. The two selected NtDRA2-GFP lines displayed an attenuated hypocotyl response to shade compared to Col-0 (**Figure 7A, B**) as observed in *dra2-1* mutant and RNAi-DRA2 lines. As expected, the selected NtDRA2-GFP line was significantly overexpressing *DRA2* compared to Col-0 (**Figure 7C**). In addition, the levels of *DRAL* were significantly upregulated in comparison to Col-0 (**Figure 7C**), resembling the molecular response of *dra2-1* and RNAi-DRA2 lines. Furthermore, NtDRA2-GFP was strongly suppressing the expression of several shade marker genes, such as *PIL1*, *HFR1* and *IAA19* (**Figure 7D**), indicating that *NtDRA2-GFP* overexpression emulated the effect of DRA2 absence and/or defective NPC. Altogether, these experiments supported that

NtDRA2 could have been interfering with the action of endogenous DRA2 and that it displays a dominant negative effect.

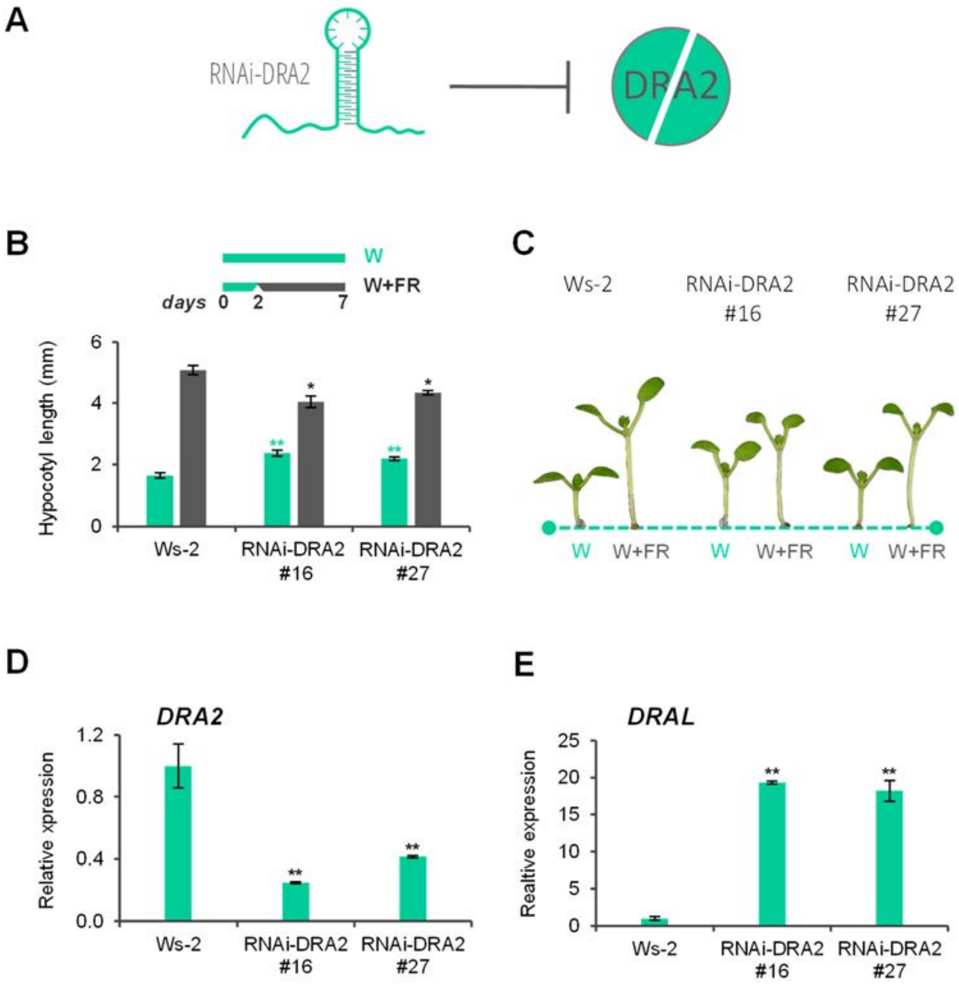

Figure 6. RNAi-DRA2 lines behave as dra2-1 mutant. **(A)** Cartoon depicting RNAi-DRA2 lines with reduced levels of DRA2. **(B)** Hypocotyl length of Ws-2 and two independent RNAi-DRA2 lines in W and W+FR. Seedlings were grown for 7 days in continuous W, or for 2 days in W then transferred to W+FR for additional 5 days, as represented at the top. **(C)** Aspect of representative seedlings grown as in (B) (roots are removed from the image). Relative expression of **(D)** DRA2 and **(E)** DRAL normalized to UBQ10 in 7-day old W-grown seedlings. Expression values are the mean ± SE of three independent biological replicates relative to data of Ws-2. Asterisks mark significant differences (Student t-test: ** p-value <0.01) relative to Ws-2 values.

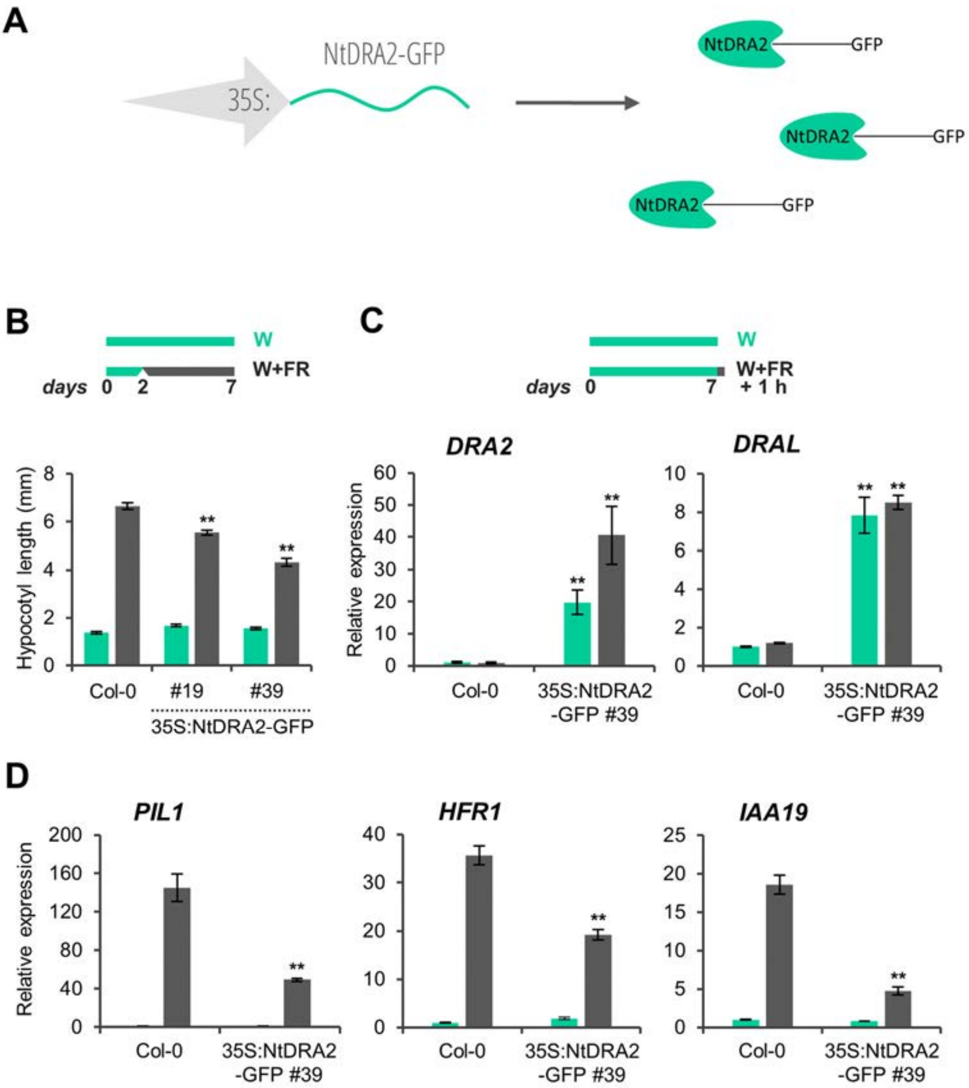

Figure 7. NtDRA2 acts as a dominant negative form. (A) Cartoon depicting the 35S:NtDRA2-GFP construct used. (B) Hypocotyl length of Col-0 and two independent 35S:NtDRA2-GFP lines (#19 and #39) in W and W+FR. Seedlings were grown for 7 days in continuous W, or for 2 days in W then transferred to W+FR for additional 5 days, as represented at the top. (C) Relative expression of DRA2 and DRAL in Col-0 and 35S:NtDRA2-GFP (line #39) seedlings in W and W+FR. 7-day old W-grown seedlings were transferred to W+FR for 1 h or maintained in W, as represented at the top. (D) Relative expression of PIL1, HFR1 and IAA19 in Col-0 and 35S:NtDRA2-GFP (line #39) seedlings in W and W+FR grown as in (C). Transcript abundance is normalized to UBQ10 levels. Expression values are the mean ± SE of three independent biological replicates relative to those of Col-0 in W. Asterisks mark significant differences (Student t-test: ** p-value <0.01) relative to Col-0 value of the same treatment.

2.3 DRA2 is a dynamic nucleoporin

The fusion protein DRA2-GFP was not detected when transiently overexpressed in tobacco (*Nicotina benthamiana*) leaves nor in transgenic *A. thaliana* seedlings, even though the *35S:DRA2-GFP* transgene complemented the *dra2-1* phenotype (Gallemí *et al.*, 2016). In addition to this, 35S:CtDRA2-GFP could not have been detected either (Gallemí Rovira, 2013). We speculated that the culprit might have been the conserved peptide motif located at the end of the Ct-part of DRA2 which in vertebrate NUP98 has autoproteolytic activity (Parry *et al.*, 2006). If this autopeptidase would indeed cleave the GFP fused to the Ct-part of DRA2, then the GFP signal might be lost due to subsequent degradation. For this reason, we generated triple fused constructs GFP-DRA2-GFP and GFP-CtDRA2-GFP to be expressed under the 35S promoter.

Tobacco leaves agroinfiltrated with the control 35S:DRA2-GFP construct (Gallemí *et al.*, 2016) did not show any GFP activity (**Figure 8A**) while the 35S:NtDRA2-GFP had fluorescent activity in speckles dispersed throughout the cell, including the nucleus and cytoplasm, but not in the nuclear envelope (**Figure 8B, E**). Overexpression of the triple fusion *GFP-DRA2-GFP* showed GFP signal inside the nucleus, in the nuclear rim (envelope) and the cytoplasm (**Figure 8C, E**). While the GFP-DRA2-GFP formed speckles throughout the cell as NtDRA2-GFP, it also displayed a dispersed signal within the nucleus and perinuclear region. By contrast, overexpression of *GFP-CtDRA2-GFP* showed GFP activity exclusively inside the nucleus (**Figure 8D, E**), meaning that the CtDRA2 was mainly responsible for nuclear localization. These results support the idea that DRA2, as its mammalian homologue mNup98, is a dynamic nucleoporin, i.e., it is not exclusively located within the NPC, and is able to shuffle between the NPC, nucleoplasm and the cytoplasm (**Figure 8E**).

2.4 Expression of *PAR* genes promoted by DRA2 in shade does not involve PIF-DRA2 interaction

Based on the specific effect that DRA2 has in the shade regulation of several *PAR* genes (*PIL1*, *HFR1*, *IAA19*) (**Figure 4B**), we hypothesized that DRA2 might directly regulate their expression by accessing their genomic regulatory regions through interaction with PIFs. Following this hypothesis, we wanted to test if we would be able to immunoprecipitate the chromatin of a 35S:GFP-DRA2-GFP line with anti-GFP antibodies and observe the enrichment around the specific PIF binding DNA regions (**Figure 9A**). It was reported previously that G-boxes (CACGTG) are the preferential DNA binding motif of PIFs (Martínez-García, Huq and Quail, 2000; Al-Sady *et al.*, 2008). Several G-boxes were identified and selected within the promoters of *PIL1*, *HFR1* and *IAA19* for ChIP-qPCR analyses (**Figure 9A**).

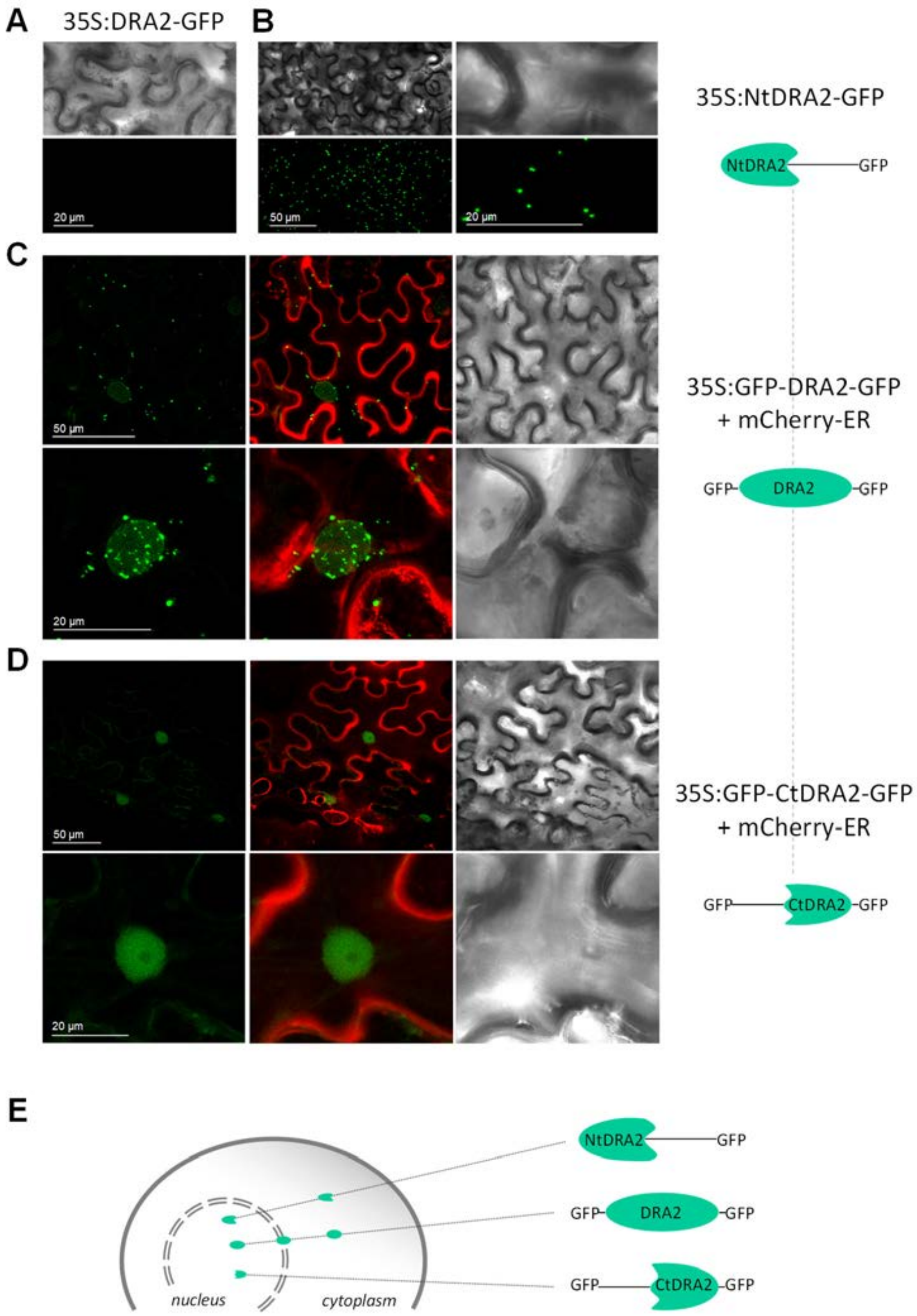
A
35S:DRA2-GFP
B
20 µm
50 µm
20 µm
35S:NtDRA2-GFP
NtDRA2
GFP
C
50 µm
20 µm
35S:GFP-DRA2-GFP
+ mCherry-ER
GFP
DRA2
GFP
D
50 µm
20 µm
35S:GFP-CtDRA2-GFP
+ mCherry-ER
GFP
CtDRA2
GFP
E
nucleus
cytoplasm
NtDRA2
GFP
GFP
DRA2
GFP
GFP
CtDRA2
GFP

Figure 8. DRA2 is located in the nuclear envelope, nucleus and cytoplasm. Fluorescent confocal images of tobacco leaf cells agroinfiltrated with **(A)** 35S:DRA2-GFP and **(B)** 35S:NtDRA2-GFP, as illustrated on the left. Upper row images show brightfield and lower row show green fluorescence. Fluorescent confocal images of tobacco leaf cells co-agroinfiltrated with mCherry-ER and **(C)** 35S:GFP-DRA2-GFP or **(D)** 35S:GFP-CtDRA2-GFP. DRA2-derived fusion constructs transiently expressed in tobacco are illustrated on the right. Series of images show green fluorescence (left), an overlay of green and red fluorescence (center) and brightfield (right). In (A) to (D), images are in the same scale in each series at the magnification indicated at the bottom of the green fluorescence images. **(E)** Schematic representation of cellular location of full length DRA2, NtDRA2 and CtDRA2.

For *PIL1* and *HFR1*, control regions were selected within the gene ORF itself (**Figure 9A**). As a control line, we used 35S:TCU1-GFP seedlings, since TCU1 does not affect the expression of any of the *PAR* genes tested previously and it was strictly NPC located (**Figure 5A**) (Ferrández-Ayela *et al.*, 2013), i.e., it is not a dynamic NUP. However, we did not observe any significant differences in the fold enrichment between the 35S:GFP-DRA2-GFP line and the control line 35S:TCU1-GFP for any of the G-box regions within the promoters of *PIL1*, *HFR1* and *IAA19*, neither in W nor in W+FR (**Figure 9B, C**). The control regions of *PIL1* and *HFR1* (P2, H2) did not differentiate between the 35S:GFP-DRA2-GFP and the control line 35S:TCU1-GFP (**Figure 9C**). These results suggested that DRA2 either does not bind to PIFs to promote the expression of specific *PAR* genes or such regulation is not easily detectable using ChIP assay.

2.5 TIBA application simulates defective NPC

The majority of pleiotropic responses of NUP-deficient mutants are thought to be caused by the disruption of the NPC regulated nucleocytoplasmic transport, i.e., are transport dependent. Some chemical treatments are also known to disrupt the function of the NPC, specifically 5-fluorouracil (5-FU) (Higby *et al.*, 2017) and the clathrin inhibitor Pitstop-2 (Liashkovich *et al.*, 2015). In mammalian cells, 5-FU increases NPC permeability in a calcium dependent manner, before completely disrupting the NPC (Higby *et al.*, 2017), while Pitstop-2 breaks the NPC permeability barrier without dissociation of the NUPs from NPC (Liashkovich *et al.*, 2015). In plants, some polar auxin transport inhibitors (ATIs), such as 2,3,5-triiodobenzoic acid (TIBA), 2-(1-pyrenoyl) benzoic acid (PBA) or N-1-naphthylphthalamic acid (NPA), have been shown to affect the trafficking of vesicles and proteins within the cell (Geldner *et al.*, 2001; Kleine-Vehn *et al.*, 2006). These experiments led to suggest that some compounds originally identified as ATIs may actually be inhibitors of membrane trafficking (Geldner *et al.*, 2001; Kleine-Vehn *et al.*, 2006) and that the inhibition of polar auxin transport is a consequence of impairment of the intracellular movement of auxin related proteins, such as PIN1.

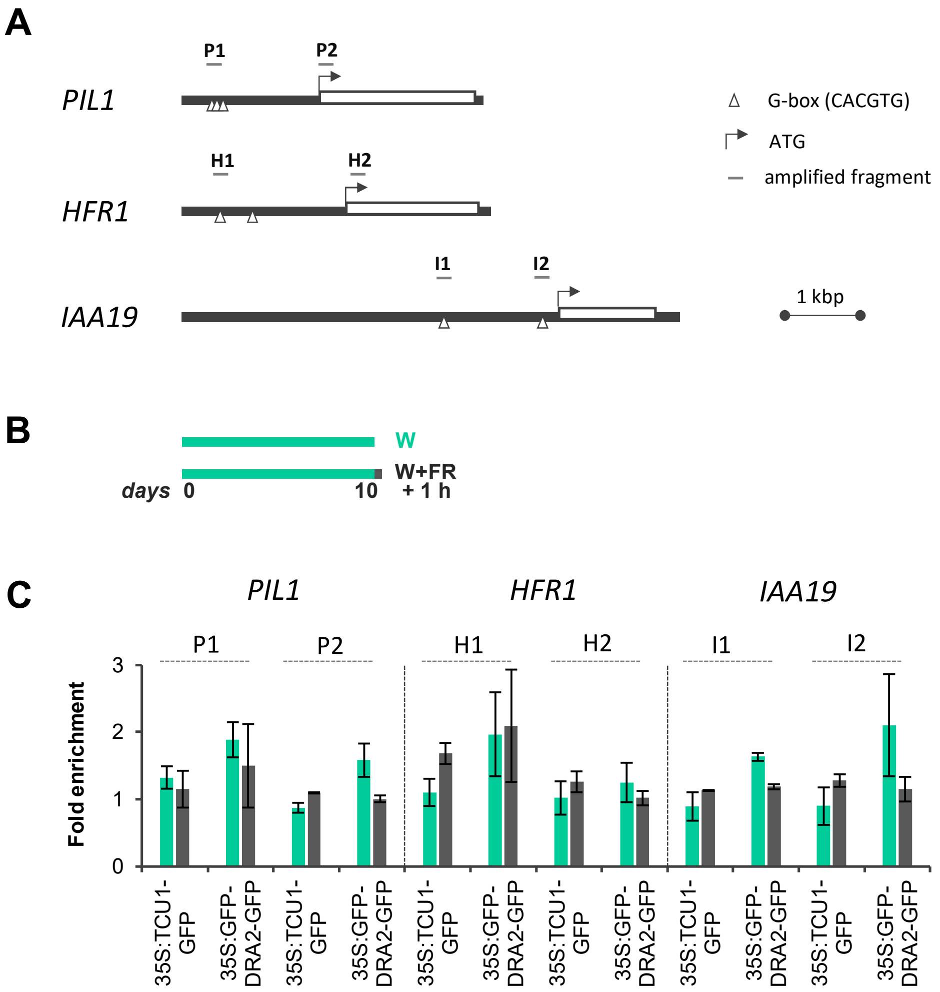

Figure 9. Chromatin immunoprecipitation (ChIP) assay of different regions of three PIF regulated genes in 35S:GFP-DRA2-GFP seedlings. **(A)** Schematic representation of the genomic region of PIL1, HFR1 and IAA19 genes and their promoters. Location of G-box (CACGTG) elements and qPCR amplified regions (P1, P2, H1, H2, I1 and I2) are marked with grey triangles and grey lines, respectively. **(B)** Seedlings were grown for 10 days in W and kept in W or transferred to W+FR for 1 h. **(C)** ChIP assay was performed using 35S:GFP-DRA2-GFP and 35S:TCU1-GFP (control) lines and anti-GFP antibodies (+anti-GFP). The fold enrichment of qPCR amplified regions in +anti-GFP samples in comparison to the -anti-GFP samples is shown in relation to the total chromatin input. Error bars indicate mean ± SE of two biological replicates.

The disruption of normal vesicle trafficking can be related to ATIs effect on actin cytoskeleton. Indeed, both TIBA and NPA affect actin organization but differently: while TIBA causes bundling of filamentous actin, NPA causes actin depolymerisation (Rahman *et al.*, 2007). Although TIBA and NPA coincide in some aspects of their effect, it is considered that they differ in molecular mechanisms of their action. It is, therefore, conceivable that some ATIs (e.g., TIBA), but not others (e.g., NPA), might disrupt more efficiently the intracellular trafficking of vesicles and proteins, and in broader terms, possibly affect nucleocytoplasmic trafficking. In that respect, results from NASCArrays service (http://www.bar.utoronto.ca/NASCArrays/) showed that TIBA treatment, but not NPA, induces the expression of specific genes which are also upregulated in several NUP-deficient mutants, such as *dra2-1* (Gallemí *et al.*, 2016), *nup62* and *nup160* (Parry, 2014) (**Table S4**). Among upregulated genes are *DRAL*, *RAE1*, *XPO1B* and *RAS-RELATED NUCLEAR PROTEIN-1* (*RAN1*). These results indicated a similarity between general NPC impairment and TIBA application. With this in mind, we aimed to use TIBA for studying the implication of NPC in early shade signalling, i.e., to study whether NPC function alters specific aspect of shade signalling.

2.6 Intranuclear phyB-GFP movement is affected by TIBA

It was previously shown that phyB fused to the GFP (phyB-GFP) forms characteristic nuclear bodies (NBs) when grown in W (Van Buskirk, Decker and Chen, 2012) or R (Yamaguchi *et al.*, 1999), and these NBs disappeared in the dark or rapidly after end-of-day FR (EOD-FR) treatments (Van Buskirk *et al.*, 2014). Consistently, when using 7-day old 35S:PHYB-GFP *A. thaliana* seedlings, we have observed distinctive NBs in the nuclei of root cells of W-grown seedlings (**Figure 10A, B**) that disappeared or reduced their size when seedlings were incubated for 4 h in the dark (**Figure 10C**). When the W-grown seedlings were given an EOD-FR treatment before a 4 h incubation in the dark, the disappearance of NBs was enhanced within the nucleus, and NB were not observed (**Figure 10D**). When the W-grown seedlings were treated with 25 µM NPA and kept in W for 4 h, no significant effect on the aspect of NBs was observed, resembling those in W-grown seedlings (**Figure 10E**). In contrast, W-grown seedlings treated with 25 µM TIBA and kept in W for 4 h resulted in a size reduction and dispersal of NBs within the nucleus (**Figure 10F**) resembling that observed in dark-treated seedlings (**Figure 10C**). The results indicated that TIBA, but not NPA, has an effect on the movement and localization of phyB-GFP within the nucleus. The strong effect of TIBA on the appearance and localization of NBs suggests that this chemical affects phyB-GFP movement within the nucleus or the ability to maintain the NBs.

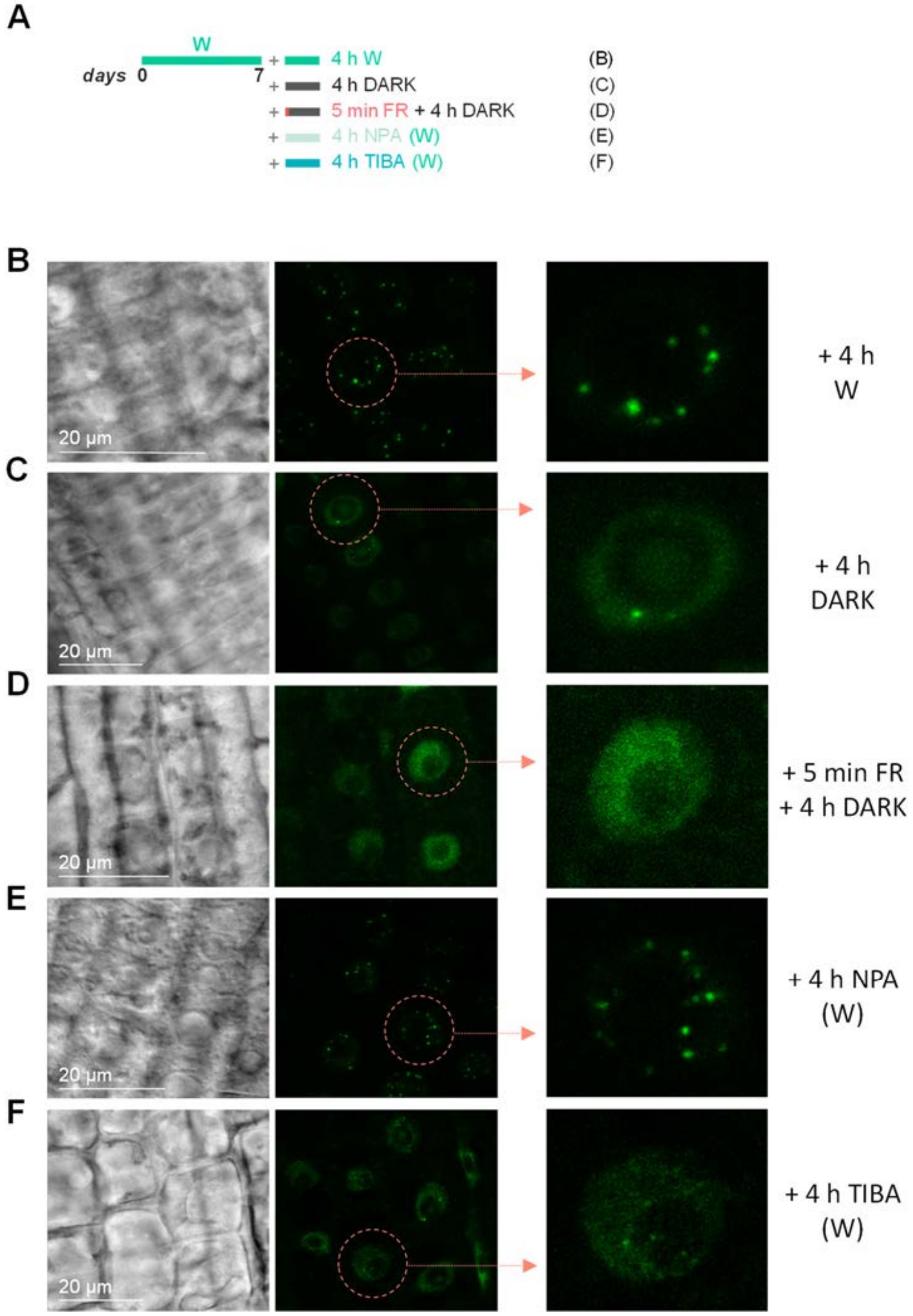
A
W
days 0
7
+ 4 h W (B)
+ 4 h DARK (C)
+ 5 min FR + 4 h DARK (D)
+ 4 h NPA (W) (E)
+ 4 h TIBA (W) (F)
B
20 µm
+ 4 h W
C
20 µm
+ 4 h DARK
D
20 µm
+ 5 min FR + 4 h DARK
E
20 µm
+ 4 h NPA (W)
F
20 µm
+ 4 h TIBA (W)

Figure 10. TIBA affects intranuclear phyB localization. (A) 7-day old seedlings were grown in continuous W and then either kept in W for 4 h, transferred to the dark for 4 h, treated for 5 min with FR and then incubated 4 h in the dark, or treated with 25 µM NPA or 25 µM TIBA and kept in W for 4 h, as indicated. Fluorescent confocal images of root cells

of 35S:PHYB-GFP A. thaliana transgenic seedlings incubated (B) 4 h in W, (C) 4 h in the dark, (D) treated for 5 min FR + 4 h dark, and kept 4 h in W treated with (E) 25 µM NPA and (F) 25 µM TIBA. Series of images shows brightfield (left), green fluorescence (center) and a magnified cell from second series (right). First and second series of images are in the same scale indicated at the bottom of the first images.

3. Discussion

The NPC is no longer seen exclusively as the regulator of nucleocytoplasmic trafficking. The diverse role of NPC components in the regulation of developmental processes has been shown on the examples of various isolated NUP mutants. In fact, many plant NUPs have been identified based on the comparisons with the vertebrate and yeast NUPs, which have been studied to a greater detail than the plant NUPs (Tamura *et al.*, 2010; Parry, 2014). In plants, the pleiotropic phenotype of NUP mutants can disguise and complicate the assessment of NUP specificity in regulatory processes; therefore, caution must be taken when studying NUPs to separate the effect of impaired NPC from additional specific NUP roles.

Previous research from our group resulted in the identification of a unique *dra2-1* mutant allele, displaying an attenuation in shade-induced hypocotyl and molecular responses in seedlings (**Figure 1A, C**) and a constitutive SAS phenotype in adult stage (**Figure 1B**). This mutation was affecting *DRA2*/*NUP98a* gene encoding for an FG-NUP (**Figure 2**), which we confirmed with RNAi-DRA2 lines in the same Ws-2 background in which *dra2-1* was found (**Figure 6A-D**). Despite the fact that several plant NUPs have been characterised in the past (Parry *et al.*, 2006; Jacob *et al.*, 2007; Parry, 2014), none of them was explicitly linked to SAS signalling as DRA2 seems to be.

Much of the information we have about the function of NUP98a (DRA2) in plants comes through comparison with the available information in animals, specifically with the mNup98 (Griffis, 2002). Both proteins are evolutionarily conserved on a structural level (Hodel *et al.*, 2002; Gallemí *et al.*, 2016) yet, the mNup98 is much better characterized and has been studied extensively due to is its implication with many forms of leukaemia (Taketani *et al.*, 2009; Struski *et al.*, 2017). In favour of the common functional similarities comes the fact that the Nt region of DRA2 behaves as a dominant negative form (Gallemí *et al.*, 2016) (**Figure 7**), as already observed with Nt region of mNup98 (Liang *et al.*, 2013). Thus, the observed dominant negative interference of NtDRA2 with the function of the native DRA2 indicates that this plant NUP has basic structural and functional similarities with mNup98, such as the possibility that DRA2 is also a dynamic NUP (see below).

Based on what we know about mNup98, the molecular action of DRA2 can also be assigned to two different processes: 1) to transport-dependent activity, as part of the

NPC, and 2) to transport-independent activity, specific to DRA2 (**Figure 11**). The pleiotropic effects that DRA2 shares with other NUPs (Dong *et al.*, 2006; Parry *et al.*, 2006; Wiermer *et al.*, 2012; Baluska *et al.*, 2013; Gallemí *et al.*, 2016) (**Figure 3**), suggest that these are the result of a general perturbation of transport-dependent activity of the NPC. By contrast, the specificity of DRA2 can be observed in the attenuated expression of shade marker genes *HFR1*, *PIL1* (**Figure 4A**) and *IAA19* (Gallemí Rovira, 2013), which might be regulated in a transport-independent way, i.e., this is the result of a specific activity of DRA2 not shared by other NUPs.

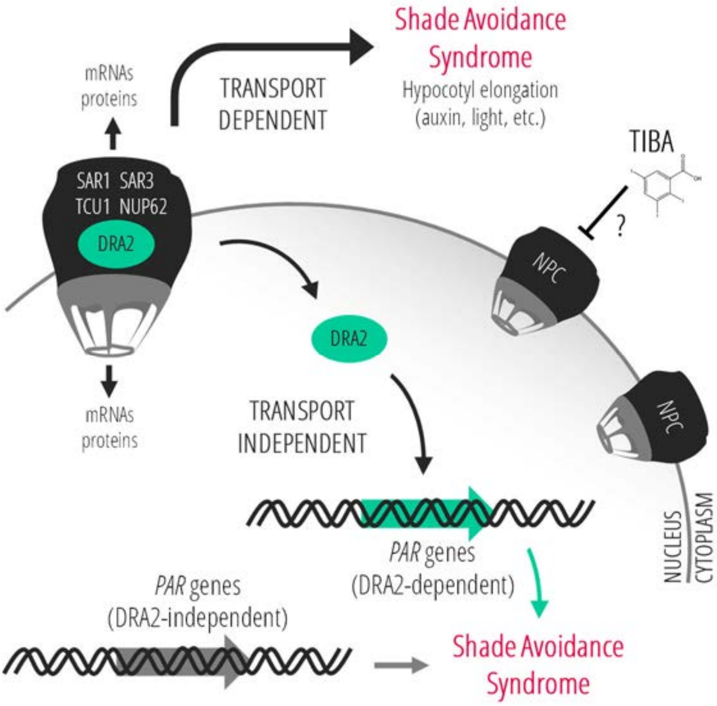
Shade Avoidance Syndrome
Hypocotyl elongation (auxin, light, etc.)
mRNAs proteins
TRANSPORT DEPENDENT
TIBA
?
SAR1 SAR3
TCU1 NUP62
DRA2
NPC
NPC
DRA2
mRNAs proteins
TRANSPORT INDEPENDENT
PAR genes (DRA2-dependent)
PAR genes (DRA2-independent)
NUCLEUS
CYTOPLASM
Shade Avoidance Syndrome

Figure 11. Working model of DRA2 and nucleoporin role in the SAS regulation in A. thaliana seedlings. Our working model (Gallemí et al., 2016) suggests a dual role for DRA2 in the regulation of SAS responses: a transport-dependent and a transport-independent. As part of the NPC, DRA2 and other nucleoporins (e.g., SAR1, SAR3, TCU1 and NUP62) affect hypocotyl elongation in W and shade through a transport-dependent mechanism, which might affect specific aspects of auxin or light. TIBA application might inhibit NPC function. Transport-independent function of DRA2 specifically affects expression of several shade-induced PAR genes (e.g. PIL1, HFR1, IAA19) and could be related to the dynamic nature of DRA2, which is shown to be located not only in the perinuclear region (i.e., as part of the NPC) but also in the nucleus and even the cytoplasm.

How DRA2 achieves specificity in SAS regulation independently of the NPC might be related to its potentially dynamic behaviour, which we proposed based on its similarity with the mammalian homologue mNup98 (Powers *et al.*, 1997; Fontoura, Blobel and Yaseen, 2000; Griffis, 2002). This dynamic behaviour primarily refers to its mobility, since mNup98 was found in the cytoplasm and nucleoplasm simultaneously (Powers *et al.*, 1997; Fontoura, Blobel and Yaseen, 2000; Griffis, 2002). Our confocal analyses have confirmed that GFP-DRA2-GFP can be detected in the cytoplasm, nucleoplasm and the nuclear envelope as part of the NPC (**Figure 8C-E**), similar as mNup98 (Griffis, 2002), supporting that DRA2 is a true dynamic NUP. Therefore, it is possible that the conserved structural similarities of DRA2 and mNup98 also impose their mobility. Apparently, full DRA2 protein is necessary for proper localization within NPC (**Figure 8C, E**). Functionally, Ct region of DRA2 determines DRA2 nucleoplasmic localization (**Figure 8D, E**), while Nt region does not seem to regulate that aspect. Nuclear localization of Nt region of DRA2 might be a consequence of either weak unidentified NLS or a misregulated NPC transport of FG rich NtDRA2. Moreover, the tendency of NtDRA2-GFP and GFP-DRA2-GFP to form speckles can probably be contributed to the specific properties of the FG repeats located on the Nt regions of DRA2 and mNup98. The propensity of hydrophobic FG repeats to spontaneously phase-separate into particle-like structures has been observed in human, yeast and *A. thaliana* Nup98 among others (Schmidt and Görlich, 2015).

Therefore, DRA2 is a dynamic and not an exclusively NPC located NUP. This dynamism could allow DRA2 to act independently of the NPC in the nucleus and specifically regulate gene expression, e.g., of *PAR* genes (**Figure 11**). It is also conceivable that such regulation might be dualistic, one acting from the NPC-bound DRA2 and other within the nucleus at the very genomic regulatory regions of the chromatin. Examples for such gene regulation by Nup98 are found in mammals and *Drosophila* (Capelson *et al.*, 2010; Kalverda *et al.*, 2010; Liang *et al.*, 2013), while in yeast, NUP-genome interactions are thought to occur only at the NPC (Ishii *et al.*, 2002; Casolari *et al.*, 2005). Direct interactions with the chromatin were also proposed for the metazoan Nup98 (Light *et al.*, 2013). Other aspect seemingly conserved across kingdoms is the preference of Nup98 for certain DNA motifs, such as GA-box motifs, bound by mNup98 in distinct genomic regions of different human cell types, and by *Drosophila* Nup98 (Liang *et al.*, 2013). The results also suggest that the association of Nup98 with the genome might require interacting partners capable of DNA binding, which in the case of *Drosophila* could be GAGA-binding transcription factors, or related Rap1 in yeast (Liang *et al.*, 2013). Since none of the known DNA binding domains were identified in DRA2, it was not likely that DRA2 would establish direct interactions with the DNA (Gallemí Rovira, 2013). Therefore, we assumed that, among several possibilities, DRA2 could be directly interacting with PIFs in shade to specifically promote the expression of PIF regulated genes *PIL1*, *HFR1* and *IAA19*. Our results, however, do not support that DRA2 physically associates with selected genomic regions of these genes (**Figure 9C**), at least not in the tested conditions we used. One of the possible explanations might be that the putative DRA2-PIF-chromatin associations are highly unstable; such weak interactions would require optimized ChIP protocol, e.g., double crosslinking (Liang *et al.*, 2013). However, we cannot discard the possibility that DRA2 forms some sort of transient complexes with transcription factors or chromatin modifiers to regulate the expression of specific *PAR* genes. In fact, some of the histone modifiers are predicted to interact with DRA2 (The Arabidopsis Interactions Viewer, http://bar.utoronto.ca/eplant), namely HISTONE ACETYLTRANSFERASE 1 (HAC1) and HAC12. HACs acetylate lysines in the Nt tail of histones, making chromosomal DNA more accessible to the transcriptional complex (Gorisch *et al.*, 2005). DRA2 might recruit such components to induce expression of its target *PAR* genes, which would work in pair with PIFs. It is still not clear how DRA2 would achieve such specificity in a light-regulated manner. Altogether, it seems reasonable to propose that DRA2 actively participates in the NPC-regulated gene gating (Blobel, 1985; Burns and Wente, 2014), which suggests that the NPCs interact with transcriptionally active portions of the genome and facilitate the formation of mature mRNA and their export. As a dynamic nucleoporin, DRA2 might easily access genomic regulatory regions of its target *PAR* genes and ultimately regulate the export of mRNAs through the NPC.

We have used TIBA to analyse the transport-dependent effects of NPC in controlling SAS signalling, i.e., those shared by DRA2 and other NUPs. It has been reported that the absence of particular NUP, or generally impaired NPC, might trigger a feedback mechanism to regulate the activity of the NPC, specifically upregulating the genes involved in NPC structure or nuclear transport (Parry, 2014). These molecular effects of impaired NPC could be mimicked with TIBA treatment (**Table S4**) through a yet unknown mechanism, possibly even affecting protein movements within the cell (Geldner *et al.*, 2001). In fact, we have observed that TIBA is capable of affecting phyB-GFP localization within the nucleus, resembling the effect of FR or dark on NBs (**Figure 10C, D**) (Van Buskirk *et al.*, 2014; Kaiserli *et al.*, 2015), which suggests that TIBA might also disturb this central aspect of shade signalling perception. Since NPA treatment does not result in the same effect as TIBA treatment (**Table S4**), we can discard the possibility that the gene upregulation shared with NUP mutants is linked to auxins, i.e., that it is a consequence of polar auxin transport inhibition in the case of TIBA or perturbations in auxin signalling in the case of NUP mutants. We cannot discard the possibility that TIBA indirectly impairs the function of the NPC resulting in similar gene expression output as in NUP-deficient mutants (**Figure 11**) which might be a consequence of altered downstream processes, such as protein synthesis. Retention of mRNA observed in various NUP-deficient mutants (Dong *et al.*, 2006; Parry *et al.*, 2006; Jacob *et al.*, 2007; Xu *et al.*, 2007; Lu *et al.*, 2010; Tamura *et al.*, 2010; Wiermer *et al.*, 2012; MacGregor *et al.*, 2013; Gallemí *et al.*, 2016) is likely to affect protein synthesis, which TIBA might also affect by disturbing actin cytoskeleton connected with ribosomal machinery (Stapulionis, Kolli and Deutscher, 1997; Gross and Kinzy, 2007; Chierchia *et al.*, 2015). Additionally, we can speculate that TIBA might also affect the nucleocytoplasmic transport of HEMERA (HMR) which was shown to be essential for phyB NBs formation (Chen *et al.*, 2010).

Therefore, TIBA could have multiple effects on various cellular processes, besides the inhibition of polar auxin transport, whose mechanism still needs to be clarified. Additional experiments will be needed to resolve if NPC-regulated transport in plants can directly target the shade-induced changes in phyB-GFP NBs. This can be addressed by studying the phyB-GFP NBs in a NUP-deficient mutant background. Such advances would allow us to establish if the transport-dependent activity of NUPs (including DRA2) also regulate a central aspect of shade signalling such as phyB activity.

4. Materials and methods

4.1 Plant material and growth conditions

Arabidopsis thaliana PBL and *dra2-1* lines, in Ws-2, and *sar1-4* and *sar3-1*, in Col-0 plants are described elsewhere (Parry *et al.*, 2006; Gallemí *et al.*, 2016). Plants were grown in the greenhouse to produce seeds, as described (Martínez-García *et al.*, 2014; Gallemí *et al.*, 2016, 2017). For hypocotyl assays, seeds were surface-sterilized and sown on solid growth medium without sucrose (0.5xGM-) (Murashige and Skoog, 1962; Paulišić *et al.*, 2017). For gene expression analyses and chromatin immunoprecipitation experiments seeds were sown on a sterilized nylon membrane placed on top of the solid 0.5xGM- medium. After stratification (dark at 4ºC) of 3-6 days, plates with seeds were incubated in plant chambers at 22ºC under continuous white light (W) for at least 2 h to break dormancy and synchronize germination (Paulišić *et al.*, 2017). W was emitted from vertical cool fluorescent tubes that provided ~20-25 µmol m^{-2} s^{-1} of photosynthetically active radiation (PAR) with a red:far-red light ratio (R:FR) >3.3. Simulated shade treatments were produced by supplementing W with FR (W+FR). FR was emitted from GreenPower LED module HF far-red (Philips), creating R:FR ratio from 0.02-0.09. Light fluence rates were measured with a Spectrosense2 meter (Skye Instruments Ltd) (Martínez-García *et al.*, 2014).

4.2 Generation of transgenic lines

Transgenic lines expressing *DRA2* and *NtDRA2* under the 35S promoter are described in (Gallemí *et al.*, 2016); a line expressing PHYB-GFP under the 35S promoter (Yamaguchi *et al.*, 1999), was generated in the Col-0 background and kindly provided to us (Ortiz Alcaide, 2017). Transgenic 35S:RNAi-DRA2 line is in *A. thaliana* Ws-2 background, and 35S:Nt-DRA2-GFP and 35S:GFP-DRA2-GFP lines in *A. thaliana* Col-0 background. Details of the constructs and primers used for the generation of transgenic lines are provided as Supplementary information (**Table S1**).

4.3 Measurement of hypocotyl length

Hypocotyl length was measured as described (Paulišić *et al.*, 2017). Experiments were repeated at least three times, and average values are shown.

4.4 Gene expression analyses

Total RNA was extracted from seedlings, using commercial kits (Maxwell® SimplyRNA and Maxwell® RSC Plant RNA Kits; www.promega.com). 2 µg of RNA was reverse-transcribed with Transcriptor First Strand cDNA synthesis Kit (Roche, www.roche.com). Biological triplicates were used for real-time qPCR analyses, as indicated elsewhere (Gallemí *et al.*, 2017). The *A. thaliana UBIQUITIN 10* (*UBQ10*) was used as a housekeeping gene for normalization. Primer sequences for qPCR analyses are provided as Supplementary information (**Table S2**).

4.5 Agroinfiltration of tobacco leaves and confocal microscopy

N. benthamiana leaves were co-agroinfiltrated with 35S:GFP-DRA2-GFP + mCherry-ER or 35S:GFP-CtDRA2-GFP + mCherry-ER as described elsewhere (Vilela *et al.*, 2013). 35S:DRA2-GFP and 35S:NtDRA2-GFP were used as controls. mCherry-ER construct localizes in the endoplasmic reticulum. Confocal microscopy was performed 3 days post agroinfiltration using either Leica TCS SP5 II or Olympus FV1000.2.4 microscope. Final images were projected as a stack of several optical sections of 1 µm slices.

4.6 Chromatin immunoprecipitation (ChIP)

For ChIP assay, 10-day old seedlings, treated as indicated, were harvested and processed as described in http://www.abcam.com/ps/pdf/protocols/chip_plant_arabidopsis.pdf. Chromatin was extracted in 100 µl of cold nuclei lysis buffer and sonicated for 10 min at 4°C with sonicator Bioruptor® (Diagenode) set to "HIGH" (30 s "ON cycle", 30 s "OFF cycle"). Chromatin was immunoprecipitated with 1 µg of anti-GFP (A-11122, Thermo Fisher Scientific, US). Primer sequences for qPCR analyses of *PIL1*, *HFR1* and *IAA19* genomic regions are provided as Supplementary information (**Table S3**).

4.7 TIBA and NPA treatments

TIBA (Sigma-Aldrich, http://www.sigmaaldrich.com) was dissolved in DMSO to a concentration of 50 mM. NPA (Duchefa, http://www.duchefa.com) was dissolved in ethanol (v/v) to a concentration of 50 mM. Stock solutions were kept at −20°C until use. Seedlings grown on top of nylon membrane were transferred to new plates containing 4 mL of 25 µM TIBA or 25 µM NPA solution in water and kept in W for 4 h. After treating the seedlings with these chemicals, confocal microscopy of seedling roots was performed using Olympus FV1000.2.4 microscope. Fluorescent confocal images were projected as a stack of several optical sections of 1 µm slices.

5. Supplementary information

5.1 Generation of RNAi-DRA2 plants in *A. thaliana* Ws-2 background

To generate an RNAi construct for silencing the *DRA2* in Ws-2 background, a 318 bp fragment was PCR amplified using the primers GO96+SPO1 (**Table S1**) from vector pCT9 (Gallemí *et al.*, 2016). Resulting PCR product was directionally subcloned into PCRII-TOPO (Invitrogen) to obtain pSP30 and was sequenced to confirm its identity. A *Xho*I-*Bam*HI fragment of pSP30 was subcloned into the same sites of pENTR3C vector (Invitrogen), flanked by the attL1 and attL2 sites, to give pSP31. The pSP31 was recombined with pHELLSGATE12 destination vector (Wesley et al., 2001), which contained attR1 and attR2 sites, using the Gateway LR Clonase II (Invitrogen), to generate pSP32 (35S:RNAi-DRA2), a binary plasmid conferring resistance to kanamycin in plants. *A. thaliana* Ws-2 plants were transformed with pSP32 via agrobacterium using the floral dip method (Clough and Bent, 1998). Resistant transgenic seedlings were selected on 0.5xGM- medium with kanamycin (50 µg/mL).

5.2 Generation of *A. thaliana* Col-0 transgenic line expressing *GFP-DRA2-GFP* under the control of the 35S promoter

To generate a triple fusion construct *GFP-DRA2-GFP* to be overexpressed under the 35S promoter, a *GFP* fragment was PCR amplified using the primers SPO40 + SPO41 (**Table S1**) from vector pCAMBIA1302. Obtained PCR product was flanked with introduced *Nco*I sites, subcloned into PCRII-TOPO which generated pSP76 and sequenced to confirm its identity. An *Nco*I fragment of pSP76 was subcloned into the same site of pCT9 which generated a binary vector pSP77 (35S:GFP-DRA2-GFP). pSP77 was used for transient expression of GPF-DRA2-GFP fusion protein in leaves of *N. benthamiana* via Agrobacterium and for transformation of *A. thaliana* Col-0 plants using the floral dip method. Resistant transgenic seedlings were selected on 0.5xGM- medium with kanamycin (50 µg/mL).

5.3 Generation of *NtDRA2-GFP* and *GFP-CtDRA2-GFP* fusion constructs for confocal microscopy

For generating the control construct 35S:NtDRA2-GFP to be transiently expressed in leaves of *N. benthamiana*, *NtDRA2* fragment was PCR amplified using the primers SPO4 + SPO5 (**Table S1**) from vector pMG56 (Gallemí *et al.*, 2016). The resulting PCR product was subcloned into PCRII-TOPO to obtain pSP36 and sequenced to confirm its identity. A *Bam*HI-*Bgl*II fragment of pSP36 was cloned into the *Bgl*II site of pMS51 to generate a binary vector pSP39 (35:NtDRA2-GFP).

To generate a triple fusion construct *GFP-CtDRA2-GFP* to be overexpressed under the 35S promoter, an *Nco*I fragment of pSP76 was subcloned into the same site of pMG55 (Gallemí *et al.*, 2016) which generated a binary vector pSP100 (35S:GFP-CtDRA2-GFP). pSP100 was used for transient expression of GPF-CtDRA2-GFP fusion protein in leaves of *N. benthamiana* via Agrobacterium.

5.4 Tables:

Table S1. Primers used for cloning

Gene	**Primer name**	**Sequence (5’ – 3’)**
DRA2 At1g10390 (RNAi-DRA2)	GO96	ATACGCCCAGTTCAACAGTGG
	SPO1	AAGAGCCTCGATATCTGCAC
DRA2 At1g10390 (NtDRA2)	SPO4	CCGGATCCATGGTTGGCTCATCTAATCC
	SPO5	GCAGATCTCCACTGTTGAACTGGGCGTA
GFP (mGFP5)	SPO40	GGCCATGGTAGATCTGACTAGTAA
	SPO41	GGCCATGGACACGTGGTGGTGGTGG

Table S2. Primers used for gene expression analyses

Gene	Primer name	Sequence (5’ – 3’)
HFR1 At1g02340	BO89	GATGCGTAAGCTACAGCAACTCGT
	BO90	AGAACCGAAACCTTGTCCGTCTTG
PIL1 At2g46970	BO87	GGAAGCAAAACCCTTAGCATCAT
	BO88	TCCATATAATCTTCATCTTTTAATTTTGGTTTA
PHYB At2g18790	MGO16	GCGACCATTGTCAACTGCTAGT
	MGO17	GAGCTGAGCTGAACGCAAAT
DRA2 At1g10390	SPO17	CACCAACTGTTGAGGCAGACA
	SPO18	GGCAGAAATAGATTCCAACTTTCC
DRAL At1g59660	MGO46	ACGGTGCAATTCGTGAAGCT
	MGO47	TTTTGTCGCCTCCGTGATTT
UBQ10 At4g05320	BO40	AAATCTCGTCTCTGTTATGCTTAAGAAG
	BO41	TTTTACATGAAACGAAACATTGAACTT
IAA19 At3g15540	NCO89	TGCTCTTGATAAGCTCTTCGGTT
	NCO90	TCTTTCAAGGCCACACCGAT

Table S3. Primers used for ChIP-qPCR analyses

Gene	**Primer name**	**Sequence (5' – 3')**
PIL1 region P1 At2g46970	SPO90	GAATCACGCGGCATTCAC
	SPO91	ACCTTCACGCCATTATTAAGAC
PIL1 region P2 At2g46970	SPO92	ATCTGAACCAAACATGATTTCTCC
	SPO93	AGCACCGACAGAACCATAAG
HFR1 region H1 At1g02340	SPO94	GTCGCTCGCTAAGACACCAAC
	SPO95	ACGTGATGCCCTCGTGATGGAC
HFR1 region H2 At1g02340	SPO96	TTGGCAGGTCGAATAATCAAGC
	SPO97	GCTCTTTCTGACATCATGCCCT
IAA19 region I1 At3g15540	SPO98	ACCACCGCATCCTCAGTTG
	SPO99	CGTTGGTCCACACGATAC
IAA19 region I2 At3g15540	SPO100	TGTCGTTTGGTAGCCTTTGG
	SPO101	CTTGTCTACCAACTTTGATCAATGG

Table S4. List of upregulated genes in *dra2-1*, *nup62*, *nup160*, TIBA and NPA treatment compared to WT or control treatment, respectively

Gene	**Gene annotation**	**log2 fold change**				
		nup62	***nup160***	***dra2-1***	**TIBA**	**NPA**
NUP98B	AT1G59660	2.64	2.22	5.55	3.35	*0.28*
RAE1	AT1G80670	1.45	1.18	2.59	1.24	*-0.03*
RAN1	AT5G44790	1.76	1.35	1.85	*-0.16*	*-0.22*
XPO1B	AT3G03110	1.87	1.36	2.96	0.79	*0.12*
RAN2, *RAN1*	AT5G20010, AT5G20020	1.03	1.17	/	0.90	*0.30*

6. References

Al-Sady B, Kikis E a, Monte E, Quail PH. 2008. Mechanistic duality of transcription factor function in phytochrome signaling. Proc Natl Acad Sci U S A. 105:2232–2237. doi:10.1073/pnas.0711675105.

Alonso JM, Stepanova AN, Leisse TJ, Kim CJ, Chen H, Shinn P, Stevenson DK, Zimmerman J, Barajas P, Cheuk R, et al. 2003. Genome-wide insertional mutagenesis of Arabidopsis thaliana. Science. 301:653–7. doi:10.1126/science.1086391.

Baluska F, Mancuso S, Trewavas T, Volkmann D. 2013. Nucleoporins Nup160 and seh1 are required for disease resistance in arabidopsis. Nucl (United States). 4:1. doi:10.4161/nucl.23781.

Blobel G. 1985. Gene gating: a hypothesis. Proc Natl Acad Sci U S A. 82:8527–9.

Bognár LK, Hall a, Adám E, Thain SC, Nagy F, Millar a J. 1999. The circadian clock controls the expression pattern of the circadian input photoreceptor, phytochrome B. Proc Natl Acad Sci USA. 96:14652–14657. doi:10.1073/pnas.96.25.14652.

Bou-Torrent J, Roig-Villanova I, Galstyan A, Martínez-García JF. 2008. PAR1 and PAR2 integrate shade and hormone transcriptional networks. Plant Signal Behav. 3:453–454. doi:10.4161/psb.3.7.5599.

Burns LT, Wente SR. 2014. From hypothesis to mechanism: uncovering nuclear pore complex links to gene expression. Mol Cell Biol. 34:2114–20. doi:10.1128/MCB.01730-13.

Van Buskirk EK, Decker P V., Chen M. 2012. Photobodies in Light Signaling. Plant Physiol. 158:52–60. doi:10.1104/pp.111.186411.

Van Buskirk EK, Reddy AK, Nagatani A, Chen M. 2014. Photobody Localization of Phytochrome B Is Tightly Correlated with Prolonged and Light-Dependent Inhibition of Hypocotyl Elongation in the Dark. Plant Physiol. 165:595–607. doi:10.1104/pp.114.236661.

Capelson M, Liang Y, Schulte R, Mair W, Wagner U, Hetzer MW. 2010. Chromatin-Bound Nuclear Pore Components Regulate Gene Expression in Higher Eukaryotes. Cell. 140:372–383. doi:10.1016/j.cell.2009.12.054.

Casolari JM, Brown CR, Drubin DA, Rando OJ, Silver PA. 2005. Developmentally induced changes in transcriptional program alter spatial organization across chromosomes. Genes Dev. 19:1188–1198. doi:10.1101/gad.1307205.

Chen M, Galvão RM, Li M, Burger B, Bugea J, Bolado J, Chory J. 2010. Arabidopsis HEMERA/pTAC12 Initiates photomorphogenesis by phytochromes. Cell. 141:1230–1240. doi:10.1016/j.cell.2010.05.007.

Chierchia L, Tussellino M, Guarino D, Carotenuto R, DeMarco N, Campanella C, Biffo S, Vaccaro MC. 2015. Cytoskeletal proteins associate with components of the ribosomal maturation and translation apparatus in Xenopus stage I oocytes. Zygote. 23:669–682. doi:10.1017/S0967199414000409.

Clough SJ, Bent AF. 1998. Floral dip: A simplified method for Agrobacterium-mediated transformation of *Arabidopsis thaliana*. Plant J. 16:735–743. doi:10.1046/j.1365-313X.1998.00343.x.

Dong C-H, Hu X, Tang W, Zheng X, Kim YS, Lee B -h., Zhu J-K. 2006. A Putative Arabidopsis Nucleoporin, AtNUP160, Is Critical for RNA Export and Required for Plant Tolerance to Cold Stress. Mol Cell Biol. 26:9533–9543. doi:10.1128/MCB.01063-06.

Ferrández-Ayela A, Alonso-Peral MM, Sánchez-García AB, Micol-Ponce R, Pérez-Pérez JM, Micol JL, Ponce MR. 2013. Arabidopsis TRANSCURVATA1 Encodes NUP58, a Component of the Nucleopore Central Channel. PLoS One. 8. doi:10.1371/journal.pone.0067661.

Fontoura BMA, Blobel G, Yaseen NR. 2000. The nucleoporin Nup98 is a site for GDP/GTP exchange on ran and termination of karyopherin β2-mediated nuclear import. J Biol Chem. 275:31289–31296. doi:10.1074/jbc.M004651200.

Gallemí M, Galstyan A, Paulišić S, Then C, Ferrández-Ayela A, Lorenzo-Orts L, Roig-Villanova I, Wang X, Micol JL, Ponce MR, et al. 2016. DRACULA2 is a dynamic nucleoporin with a role in regulating the shade avoidance syndrome in Arabidopsis. Development. 143:1623–1631. doi:10.1242/dev.130211.

Gallemí M, Molina-Contreras MJ, Paulišić S, Salla-Martret M, Sorin C, Godoy M, Franco-Zorrilla JM, Solano R, Martínez-García JF. 2017. A non-DNA-binding activity for the ATHB4 transcription factor in the control of vegetation proximity. New Phytol. doi:10.1111/nph.14727.

Gallemí Rovira M. 2013. Aproximació als mecanismes moleculars implicats en la regulació de la síndrome de fugida de l'ombra en Arabidopsis. TDX (Tesis Doctorals en Xarxa), Universitat de Barcelona.

Geldner N, Friml J, Stierhof YD, Jürgens G, Palme K. 2001. Auxin transport inhibitors block PIN1 cycling and vesicle trafficking. Nature. 413:425–428. doi:10.1038/35096571.

Gorisch SM, Wachsmuth M, Tóth KF, Lichter P, Rippe K. 2005. Histone acetylation increases chromatin accessibility. J Cell Sci. 118:5825–5834. doi:10.1242/jcs.02689.

Griffis ER. 2002. Nup98 Is a Mobile Nucleoporin with Transcription-dependent Dynamics. Mol Biol Cell. 13:1282–1297. doi:10.1091/mbc.01-11-0538.

Gross SR, Kinzy TG. 2007. Improper organization of the actin cytoskeleton affects protein synthesis at initiation. Mol Cell Biol. 27:1974–89. doi:10.1128/MCB.00832-06.

Higby KJ, Bischak MM, Campbell CA, Anderson RG, Broskin SA, Foltz LE, Koper JA, Nickle AC, Resendes KK. 2017. 5-Flurouracil disrupts nuclear export and nuclear pore permeability in a calcium dependent manner. Apoptosis. 22:393–405. doi:10.1007/s10495-016-1338-y.

Hodel AE, Hodel MR, Griffis ER, Hennig KA, Ratner GA, Xu S, Powers MA. 2002. The three-dimensional structure of the autoproteolytic, nuclear pore-targeting domain of the human nucleoporin Nup98. Mol Cell. 10:347–358. doi:10.1016/S1097-2765(02)00589-0.

Ishii K, Arib G, Lin C, Van Houwe G, Laemmli UK. 2002. Chromatin boundaries in budding yeast: the nuclear pore connection. Cell. 109:551–62.

Jacob Y, Michaels SD. 2008. Peering through the pore: The role of AtTPR in nuclear transport and development. Plant Signal Behav. 3:62–64. doi:10.4161/psb.3.1.4903.

Jacob Y, Mongkolsiriwatana C, Veley KM, Kim SY, Michaels SD. 2007. The Nuclear Pore Protein AtTPR Is Required for RNA Homeostasis, Flowering Time, and Auxin Signaling. Plant Physiol. 144:1383–1390. doi:10.1104/pp.107.100735.

Kaiserli E, Páldi K, O'Donnell L, Batalov O, Pedmale U V., Nusinow DA, Kay SA, Chory J. 2015. Integration of Light and Photoperiodic Signaling in Transcriptional Nuclear Foci. Dev Cell. 35:311–321. doi:10.1016/j.devcel.2015.10.008.

Kalverda B, Pickersgill H, Shloma V V., Fornerod M. 2010. Nucleoporins Directly Stimulate Expression of Developmental and Cell-Cycle Genes Inside the Nucleoplasm. Cell. 140:360–371. doi:10.1016/j.cell.2010.01.011.

Kleine-Vehn J, Dhonukshe P, Swarup R, Bennett M, Friml J. 2006. Subcellular Trafficking of the Arabidopsis Auxin Influx Carrier AUX1 Uses a Novel Pathway Distinct from PIN1. Plant Cell. 18:3171–3181. doi:10.1105/tpc.106.042770.

Labade AS, Karmodiya K, Sengupta K. 2016. HOXA repression is mediated by nucleoporin Nup93 assisted by its interactors Nup188 and Nup205. Epigenetics Chromatin. 9:54. doi:10.1186/s13072-016-0106-0.

Liang Y, Franks TM, Marchetto MC, Gage FH, Hetzer MW. 2013. Dynamic Association of NUP98 with the Human Genome. PLoS Genet. 9. doi:10.1371/journal.pgen.1003308.

Liashkovich I, Pasrednik D, Prystopiuk V, Rosso G, Oberleithner H, Shahin V. 2015. Clathrin inhibitor Pitstop-2 disrupts the nuclear pore complex permeability barrier. Sci Rep. 5. doi:10.1038/srep09994.

Light WH, Freaney J, Sood V, Thompson A, D'Urso A, Horvath CM, Brickner JH. 2013. A Conserved Role for Human Nup98 in Altering Chromatin Structure and Promoting Epigenetic Transcriptional Memory. PLoS Biol. 11. doi:10.1371/journal.pbio.1001524.

Lu Q, Tang X, Tian G, Wang F, Liu K, Nguyen V, Kohalmi SE, Keller WA, Tsang EWT, Harada JJ, et al. 2010. Arabidopsis homolog of the yeast TREX-2 mRNA export complex: Components and anchoring nucleoporin. Plant J. 61:259–270. doi:10.1111/j.1365-313X.2009.04048.x.

MacGregor DR, Gould P, Foreman J, Griffiths J, Bird S, Page R, Stewart K, Steel G, Young J, Paszkiewicz K, et al. 2013. HIGH EXPRESSION OF OSMOTICALLY RESPONSIVE GENES1 Is Required for Circadian Periodicity through the Promotion of Nucleo-Cytoplasmic mRNA Export in Arabidopsis. Plant Cell. 25:4391–4404. doi:10.1105/tpc.113.114959.

Martínez-García JF, Gallemí M, Molina-Contreras MJ, Llorente B, Bevilaqua MRR, Quail PH. 2014. The shade avoidance syndrome in Arabidopsis: The antagonistic role of phytochrome A and B differentiates vegetation proximity and canopy shade. Huq E, editor. PLoS One. 9:e109275. doi:10.1371/journal.pone.0109275.

Martínez-García JF, Huq E, Quail PH. 2000. Direct targeting of light signals to a promoter element-bound transcription factor. Science (80-). 288:859–863. doi:10.1126/science.288.5467.859.

Murashige T, Skoog F. 1962. A revised medium for rapid growth and bioassays with tobacco tissue cultures. Physiol Plant. 15:473–497. doi:DOI: 10.1111/j.1399-3054.1962.tb08052.x.

Ortiz Alcaide M. 2017. Interrelación entre la respuesta a sombra y la síntesis de carotenoides en Arabidopsis thaliana. Universitat de Barcelona.

Parry G. 2014. Components of the Arabidopsis nuclear pore complex play multiple diverse roles in control of plant growth. J Exp Bot. 65:6057–6067. doi:10.1093/jxb/eru346.

Parry G, Ward S, Cernac A, Dharmasiri S, Estelle M. 2006. The Arabidopsis SUPPRESSOR OF AUXIN RESISTANCE proteins are nucleoporins with an important role in hormone signaling and development. Plant Cell. 18:1590–1603. doi:10.1105/tpc.106.041566.

Paulišić S, Molina-Contreras MJ, Roig-Villanova I, Martínez-García JF. 2017. Approaches to study light effects on brassinosteroid sensitivity.

Powers MA, Forbes DJ, Dahlberg JE, Lund E. 1997. The vertebrate GLFG nucleoporin, Nup98, is an essential component of multiple RNA export pathways. J Cell Biol. 136:241–250. doi:10.1083/jcb.136.2.241.

Radu A, Moore MS, Blobel G. 1995. The peptide repeat domain of nucleoporin Nup98 functions as a docking site in transport across the nuclear pore complex. Cell. 81:215–222. doi:10.1016/0092-8674(95)90331-3.

Rahman A, Bannigan A, Sulaman W, Pechter P, Blancaflor EB, Baskin TI. 2007. Auxin, actin and growth of the Arabidopsis thaliana primary root. Plant J. 50:514–528. doi:10.1111/j.1365-313X.2007.03068.x.

Roig-Villanova I, Bou-Torrent J, Galstyan A, Carretero-Paulet L, Portolés S, Rodríguez-Concepción M, Martínez-García JF. 2007. Interaction of shade avoidance and auxin responses: a role for two novel atypical bHLH proteins. EMBO J. 26:4756–67. doi:10.1038/sj.emboj.7601890.

Schmidt HB roder, Görlich D. 2015. Nup98 FG domains from diverse species spontaneously phase-separate into particles with nuclear pore-like permselectivity. Elife. 4:1–30. doi:10.7554/eLife.04251.

Stapulionis R, Kolli S, Deutscher MP. 1997. Efficient mammalian protein synthesis requires an intact F-actin system. J Biol Chem. 272:24980–6. doi:10.1074/JBC.272.40.24980.

Struski S, Lagarde S, Bories P, Puiseux C, Prade N, Cuccuini W, Pages MP, Bidet A, Gervais C, Lafage-Pochitaloff M, et al. 2017. NUP98 is rearranged in 3.8% of pediatric AML forming a clinical and molecular homogenous group with a poor prognosis. Leukemia. 31:565–572. doi:10.1038/leu.2016.267.

Taketani T, Taki T, Nakamura H, Taniwaki M, Masuda J, Hayashi Y. 2009. NUP98-NSD3 fusion gene in radiation-associated myelodysplastic syndrome with t(8;11)(p11;p15) and expression pattern of NSD family genes. Cancer Genet Cytogenet. 190:108–112. doi:10.1016/j.cancergencyto.2008.12.008.

Tamura K, Fukao Y, Iwamoto M, Haraguchi T, Hara-Nishimura I. 2010. Identification and characterization of nuclear pore complex components in Arabidopsis thaliana. Plant Cell. 22:4084–4097. doi:10.1105/tpc.110.079947.

Tamura K, Hara-Nishimura I. 2011. Involvement of the nuclear pore complex in morphology of the plant nucleus. Nucleus. 2:168–72. doi:10.4161/nucl.2.3.16175.

Vilela B, Moreno-Cortés A, Rabissi A, Leung J, Pagès M, Lumbreras V. 2013. The Maize OST1 Kinase Homolog Phosphorylates and Regulates the Maize SNAC1-Type Transcription Factor. PLoS One. 8. doi:10.1371/journal.pone.0058105.

Wiermer M, Cheng YT, Imkampe J, Li M, Wang D, Lipka V, Li X. 2012. Putative members of the Arabidopsis Nup107-160 nuclear pore sub-complex contribute to pathogen defense. Plant J. 70:796–808. doi:10.1111/j.1365-313X.2012.04928.x.

Xu XM, Meier I. 2008. The nuclear pore comes to the fore. Trends Plant Sci. 13:20–27. doi:10.1016/j.tplants.2007.12.001.

Xu XM, Rose A, Muthuswamy S, Jeong SY, Venkatakrishnan S, Zhao Q, Meier I. 2007. NUCLEAR PORE ANCHOR, the Arabidopsis Homolog of Tpr/Mlp1/Mlp2/Megator, Is Involved in mRNA Export and SUMO Homeostasis and Affects Diverse Aspects of Plant Development. Plant Cell. 19:1537–1548. doi:10.1105/tpc.106.049239.

Yamaguchi R, Nakamura M, Mochizuki N, Kay SA, Nagatani A. 1999. Light-dependent translocation of a phytochrome B-GFP fusion protein to the nucleus in transgenic Arabidopsis. J Cell Biol. 145:437–445. doi:10.1083/jcb.145.3.437.

Zhao Q, Meier I. 2011. Identification and characterization of the arabidopsis FG-repeat nucleoporin Nup62. Plant Signal Behav. 6:330–334. doi:10.4161/psb.6.3.13402.

CHAPTER II

Chapter II is a research article planned for publication:

Shade tolerance in *Cardamine hirsuta* is maintained by HFR1

Sandi Pauličić, Christiane Then, Violeta Sanchez, Benjamin Alary, Miltos Tsiantis,
Manuel Rodríguez-Concepción, Jaime F. Martínez-García

1. Introduction

The ability of plants to perceive and adjust their development according to different environmental stimuli is of uttermost importance. This plasticity takes into account many cues such as water, nutrients, and light. Conditions in nature often involve simultaneous changes in multiple light cues leading to an interplay of various photoreceptors to adjust plant growth appropriately. In dense plant communities, close proximity of vegetation can often limit the availability of light for driving plant photosynthesis, forcing the neighbours in close proximity to adopt strategies to respond to light limitation. In general, two strategies have emerged to cope with vegetation proximity or shade: avoidance and tolerance (Valladares and Niinemets, 2008; Gommers *et al.*, 2013; Pierik and Testerink, 2014). Shade avoiders usually promote hypocotyl and stem elongation, to outgrow the neighbours and avoid light shortages, and accelerate flowering even with lower yield (Smith and Whitelam, 1997), to ensure species survival. This set of responses is collectively known as the shade avoidance syndrome (SAS). In contrast, shade-tolerant species have developed a variety of traits to adapt to low light conditions and optimize net carbon gain that usually do not involve a promotion of elongation growth (Smith, 1982; Valladares and Niinemets, 2008).

Vegetation proximity and shade can be perceived as a reduction of the red (R) to far-red light (FR) ratio (R:FR) by phytochromes. In *Arabidopsis thaliana*, low R:FR results in phytochrome inactivation, which allows PHYTOCHROME INTERACTING FACTORS (PIFs) to initiate an expression cascade of genes involved in auxin biosynthesis and signalling, and cell elongation such as *YUCCA 8* (*YUC8*), *INDOLE-3-ACETIC ACID INDUCIBLE 19* (*IAA19*), *IAA29* and *XYLOGLUCAN ENDOTRANSGLYCOSYLASE 7* (*XTR7*), as well as various transcriptional regulators, such as LONG HYPOCOTYL IN FAR-RED 1 (HFR1) (Sasidharan *et al.*, 2010; Müller-Moulé *et al.*, 2016; Yang and Li, 2017). Genetic analyses indicate that PIF7 is the key PIF regulator of the low R:FR-induced hypocotyl elongation since the *pif7* mutants are quite unresponsive to low R:FR in this response compared with the *pif4 pif5* double or *pif1 pif3 pif4 pif5* quadruple (also known as *pifq*) mutants (Lorrain *et al.*, 2008; Cole, Kay and Chory, 2011; Li *et al.*, 2012). HFR1, a member of the bHLH family of proteins and structurally related with PIFs (Fairchild, Schumaker and Quail, 2000), lacks the DNA binding ability that PIFs possess (Galstyan *et al.*, 2011; Hornitschek *et al.*, 2012). HFR1 modulates PIF activity through heterodimerization with them, as it has been described for PIF1 (Shi *et al.*, 2013), PIF3 (Fairchild, Schumaker and Quail, 2000), PIF4 and PIF5 (Hornitschek *et al.*, 2009) preventing them to bind to the DNA and affecting gene expression. In this manner HFR1 acts as a transcriptional cofactor that modulates SAS responses, e.g. it inhibits hypocotyl elongation in seedlings (Galstyan *et al.*, 2011).

What mechanistic and regulatory adjustments in shade signalling are made between species displaying divergent response to vegetation proximity has been a topic that has not received much attention until now. This question has been recently addressed performing comparative analyses between phylogenetically related species. When working with two related *Geranium* species, transcriptomic analysis led to propose that species dependent expression of three factors, *FERONIA*, *THESEUS1* and *KIDARI*, shown to activate SAS elongation responses in *A. thaliana*, might be part of the adjustments necessary to acquire a shade-avoiding or tolerant habit (Gommers *et al.*, 2017). When comparing two species belonging to the *Brassicaceae* family, the shade-avoider *A. thaliana* and the shade-tolerant *Cardamine hirsuta* (Hay *et al.*, 2014), genetic analyses resulted in the identification of the *slender in shade 1* (*sis1*) mutants, that were deficient in ChphyA. These results indicated that phyA suppressed the shade-induced hypocotyl elongation in the shade avoider *C. hirsuta* (Molina-Contreras *et al.*, 2018). This mechanism is the result of a differential but stronger phyA activity in *C. hirsuta* than in *A. thaliana* in suppressing hypocotyl elongation (Molina-Contreras *et al.*, 2018). Despite the differences in approaches and results, both works indicated that shade avoidance and shade tolerance share genetic components, even though they represent opposite adaptive strategies to vegetation proximity.

With this frame of reference, we have determined the role of the negative SAS regulator *HFR1* (Sessa *et al.*, 2005; Hornitschek *et al.*, 2009) in the control of shade tolerance in *C. hirsuta*. Genetic analyses indicated that ChHFR1 has a role in suppressing the hypocotyl elongation in *C. hirsuta*. Importantly, HFR1 activity assays performed using *hfr1-5* lines complemented with either AtHFR1 or ChHFR1, indicate that the two HFR1 species show a differential intrinsic activity and shade stability. Together with the differences in their endogenous expression in both species, we propose that HFR1 can sustain the divergent responses to vegetation proximity between *A. thaliana* and *C. hirsuta*.

2. Results

2.1 *HFR1* is required for *C. hirsuta* shade tolerance habit

We wanted to determine first if HFR1 has a role in the shade-tolerance habit of *C. hirsuta*, i.e., whether *ChHFR1* inhibited the shade-induced hypocotyl elongation in this species. For this purpose, we generated several *C. hirsuta* RNAi-HFR1 lines. When growing under white light (W), hypocotyl length of the two selected RNAi-HFR1 lines (#01 and #21) was undistinguishable from wild type (Ch WT) (**Figure 1A, C)**. By contrast, under three different low R:FR conditions applied (that simulated either vegetation proximity or canopy shade), the hypocotyl elongation of RNAi-HFR1 seedlings was significantly promoted compared to Ch WT, that was quite unresponsive (**Figure 1A, C**). As expected, *ChHFR1* expression was attenuated in W-grown seedlings of the two RNAi-HFR1 lines compared to the wild type (**Figure S1A**), suggesting they were plants with reduced HFR1 function. We also obtained two mutant lines of *ChHFR1* using CRISPR-Cas9 (named *chfr1-1* and *chfr1-2*) that showed a non-significant decrease of *ChHFR1* expression in W-grown seedlings (**Figure S1B**). These mutants had a single nucleotide insertion in their sequence leading to a premature stop codon (**Figure S1C**) and, likely to a loss of function. As in the RNAi-HFR1 lines, hypocotyl length of the two mutants was undistinguishable from Ch WT under W and elongated strongly in response to low R:FR conditions (**Figure 1B, D)**, showing a *sis* phenotype. Together, these results suggested that HFR1 represses shade-induced hypocotyl elongation in *C. hirsuta*.

Prolonged exposure to shade also results in a drop in the levels of photosynthetic pigments chlorophylls and carotenoids in *A. thaliana* and *C. hirsuta* seedlings (Bou-Torrent *et al.*, 2015; Molina-Contreras *et al.*, 2018). To compare the effect of HFR1 in this shade-induced response, the *A. thaliana hfr1-5* mutant was incorporated in our analyses. In *A. thaliana* seedlings, removal of HFR1 function resulted in a further shade-induced drop in the levels of these pigments (**Figure S2A**). These results indicate that HFR1 promotes the accumulation of these pigments in this species. By contrast, the reduction of HFR1 in the two analyzed *C. hirsuta* RNAi-HFR1 lines does not appear to be enough to further reduce the levels of total chlorophylls and carotenoids after prolonged exposure to shade (**Figure S2B**).

Simulated shade induces a rapid increase in the expression of various direct target genes of PIFs, including *HFR1* itself, *PIF3-LIKE 1* (*PIL1*), *YUC8* and *XTR7* in both wild-type *A. thaliana* (Ciolfi *et al.*, 2013; Hersch *et al.*, 2014) and *C. hirsuta* seedlings (Molina-Contreras *et al.*, 2018) (**Figure 1E, F**).

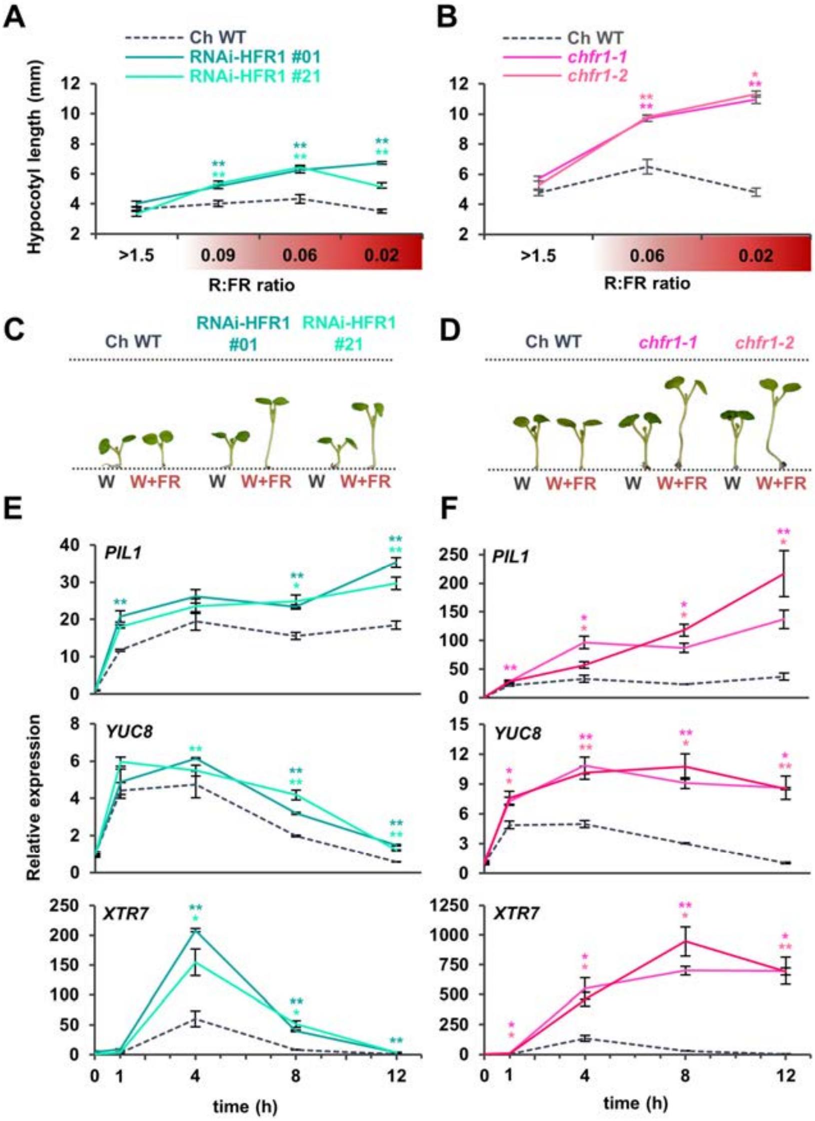

Figure 1. Hypocotyls of C. hirsuta seedlings with reduced levels of ChHFR1 strongly elongate in response to simulated shade. Hypocotyl length of C. hirsuta wild type (Ch WT), (A) RNAi-ChHFR1 transgenic and (B) chfr1 mutant seedlings grown under different R:FR. Seedlings were grown for 7 days in continuous W (R:FR>1.5) or for 3 days in W then transferred to W supplemented with increasing amounts of FR (W+FR) for 4 more days, producing moderate (0.09), low (0.05-0.06) and very low (0.02) R:FR. Aspect of representative 7-day old Ch WT, (C) RNAi-HFR1 and (D) chfr1-1 seedlings grown in W or W+FR (very low R:FR). Effect of W+FR exposure on the expression of PIL1, YUC8 and XTR7 genes in seedlings of Ch WT, (E) RNAi-HFR1 and (F) chfr1 mutant lines. Expression was analyzed in 7-day old W-grown seedlings transferred to W+FR (R:FR = 0.02) for 0, 1, 4, 8 and 12 h. Transcript abundance is normalized to EF1α levels. Values are the means ± SE of three independent biological replicates relative to Ch WT value at 0 h. Asterisks mark significant differences (Student t-test: ** p-value <0.01; * p-value <0.05) relative to Ch WT value at the same time point.

The analyses of transcript levels of these three shade marker genes in RNAi-HFR1 and *chfr1* mutant lines showed that the shade-induced expression of *PIL1*, *YUC8* and *XTR7* was significantly higher in RNAi-HFR1 and *chfr1* mutant lines compared to the Ch WT (**Figure 1E, F**), indicating that ChHFR1 has a role in repressing the expression of these genes in shade in *C. hirsuta*. These results are in agreement with the previous information from *A. thaliana* seedlings (Hornitschek *et al.*, 2009). This molecular phenotype, as well as the shade-induced hypocotyl elongation, was stronger in *chfr1* than in RNAi-HFR1 lines, suggesting that the RNAi-HFR1 lines are knock-down while *chfr1* lines are likely knock-out mutants.

2.2 Expression of *HFR1* gene is constitutively higher in *C. hirsuta* compared to *A. thaliana*

The observed suppression of the hypocotyl elongation response of *C. hirsuta* seedlings to shade might be a consequence of higher ChHFR1 activity that could be achieved by differences in either *HFR1* expression levels between the two species or in HFR1 intrinsic activities. Using shared primer pairs for *HFR1* and for the housekeeping gene *EF1α* we were able to directly compare the transcript levels of *HFR1* in *A. thaliana* and *C. hirsuta* wild-type seedlings (**Figure S3**), as previously done to compare *PHYA* expression (Molina-Contreras *et al.*, 2018). Transcript levels of *ChHFR1* in *C. hirsuta* seedlings are higher during the whole period analyzed (from day 3 until day 7) compared to those of *AtHFR1* in either W or W+FR (**Figure 2**). More importantly, although *HFR1* expression was strongly induced by W+FR in both species, transcript levels of *HFR1* were maintained significantly higher in *C. hirsuta* than in *A. thaliana* seedlings (**Figure 2**). These results suggested that HFR1 might be imposing a stronger suppression on the hypocotyl elongation in the shade-tolerant *C. hirsuta* seedlings, such that could contribute to the overall shade tolerance habit.

This observation suggested that the native promoters of *AtHFR1* (*pAtHFR1*) and *ChHFR1* (*pChHFR1*) could influence the response to shade through the control of *HFR1* expression. The 2 kbp region of both promoters contains PIF-binding sites (corresponding to CACGTG sequence, named G-box): *pAtHFR1* has 2 (Hornitschek *et al.*, 2009) and *pChHFR1* 3 G-boxes in the corresponding fragment (**Figure S4A**). Lines expressing the *GUS* reporter gene under the control of *pAtHFR1* (pAtHFR1:GUS) or *pChHFR1* (pChHFR1:GUS) were generated and a representative one for each type is shown. A lower activity was detected for the *C. hirsuta* promoter, as well as a slight different spatial activity: pAtHFR1:GUS lines display activity in cotyledons and roots of seedlings grown in W, whereas pChHFR1:GUS lines had almost no activity (**Figure S4B**).

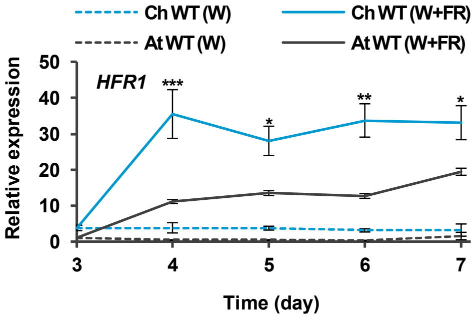

Figure 2. Levels of HFR1 transcript are higher in C. hirsuta than A. thaliana seedlings. Wild-type seedlings of C. hirsuta Ox (Ch WT) and A. thaliana Col-0 (At WT) were grown for 3 days in W then either kept under the same conditions or transferred to W+FR (R:FR = 0.02) for the indicated times. Plant material was harvested every 24 h. Transcript abundance of ChHFR1 and AtHFR1 was normalized to ChEF1α and AtEF1α. Expression values are the means ± SE of three independent biological replicates relative to the data of At WT grown in continuous W at day 3. Asterisks mark significant differences (2-way ANOVA: * p-value <0.05, ** p-value <0.01, *** p-value <0.001) between Ch WT and At WT when grown under W+FR.

Nonetheless, GUS activity was induced with short (2-4 h) W+FR treatments in hypocotyls when driven by either of the two *HFR1* promoters (**Figure S4B**), which suggests that hypocotyls are the main place of action for HFR1 in response to simulated shade for both species. Lower activity of *pChHFR1* obtained with GUS staining contrasts with the higher expression of ChHFR1 than At*HFR1* in their native species context (**Figure 2**). This suggests that the differences in promoter behaviour could be due to (1) the lack of *trans*-acting factors in *A. thaliana* that are necessary for promoting the *ChHFR1* expression in *C. hirsuta*, or (2) differences in promoter DNA *cis*-acting elements in the 2 kbp cloned region, making *pChHFR1* less expressed.

2.3 ChHFR1 has higher biological activity than AtHFR1

The role of HFR1 in maintaining the shade tolerance habit of *C. hirsuta* could be also explained by a higher intrinsic activity of ChHFR1 compared to its *A. thaliana* orthologue AtHFR1. To test this possibility, we transformed *hfr1-5* plants of *A. thaliana* with two *AtHFR1* or *ChHFR1* derivative constructs. We employed the 2 kb *pAtHFR1* to drive the expression of *ChHFR1* (*hfr1*$^{pAt:ChHFR1}$ lines) or *AtHFR1* (*hfr1*$^{pAt:AtHFR1}$ lines), both fused to the 3x Hemagglutinin (HA) tag (3xHA). For each construct, several independent transgenic lines (4-6) were selected. Homozygous plants were analyzed for hypocotyl length in W and W+FR, and transgenic *HFR1* transcript abundance. In these lines, HFR1 biological activity was estimated as a function of the hypocotyl elongation in response to shade [calculated as the difference in hypocotyl length of seedlings grown under W+FR (HL_{W+FR}) and W (HL_W), HL_{W+FR}-HL_W]. We assumed that the potential to suppress the hypocotyl elongation in shade below that of *hfr1-5* seedlings would depend on the transcript level of *HFR1* and/or its protein levels. From correlations between HFR1 biological activity (HL$_{W+FR}$-HL$_{W}$) and transcript levels of *HFR1* in shade conditions, two different equations were obtained: one for *hfr1*$^{pAt:ChHFR1}$ lines and another for *hfr1*$^{pAt:AtHFR1}$ lines. Based on the calculated R^2, a strong correlation was observed for both line types, *hfr1*$^{pAt:ChHFR1}$ (R^2 = 0.96) and *hfr1*$^{pAt:AtHFR1}$ (R^2 = 0.63) (**Figure 3**), which indicated that the level of complementation correlated with the expression levels of the transgenic *HFR1* in both cases. More importantly, the slope of both regression lines (**Figure 3**) diverged, indicating intrinsic differences in the biological activities of ChHFR1 and AtHFR1. In relation to these differences, *hfr1*$^{pAt:ChHFR1}$ lines with similar levels of *HFR1* expression had shorter hypocotyls in shade compared to *hfr1*$^{pAt:AtHFR1}$ lines, suggesting a stronger biological activity for ChHFR1 than AtHFR1. Lines that had *pChHFR1* driving the expression of *ChHFR1* (*hfr1*$^{pCh:ChHFR1}$ lines) or *AtHFR1* (*hfr1*$^{pCh:AtHFR1}$ lines), were poorly complemented but retained a positive correlation between HFR1 biological activity and *HFR1* transcript level (**Figure S5A**). These correlations, although weaker, were consistent with ChHFR1 having a stronger biological activity than AtHFR1.

Figure 3. **The activity of ChFR1 is higher than that of AtHFR1 in A. thaliana seedlings.** Seedlings of hfr1$^{pAt:AtHFR1}$ and hfr1$^{pAt:ChHFR1}$ lines were grown for 7 days in continuous W or 2 days in W then transferred for 5 days to W+FR (R:FR = 0.02). The mean hypocotyl length in W (HL$_{W}$) and W+FR (HL$_{W+FR}$) for these lines was used to calculate HL$_{W+FR}$-HL$_{W}$, that was plotted against their corresponding HFR1 relative expression in seedlings grown under W+FR. Data corresponding to untransformed hfr1-5 seedlings are indicated with asterisks. Relative expression of ChHFR1 and AtHFR1 was normalized to UBQ10. Expression values are the means ± SE of three independent biological replicates relative to the data of 7 days old wild-type A. thaliana Col-0 (At WT) grown in continuous W, taken as 1 (not shown). The regression equations and R^2 values are shown at the lower part of the graph.

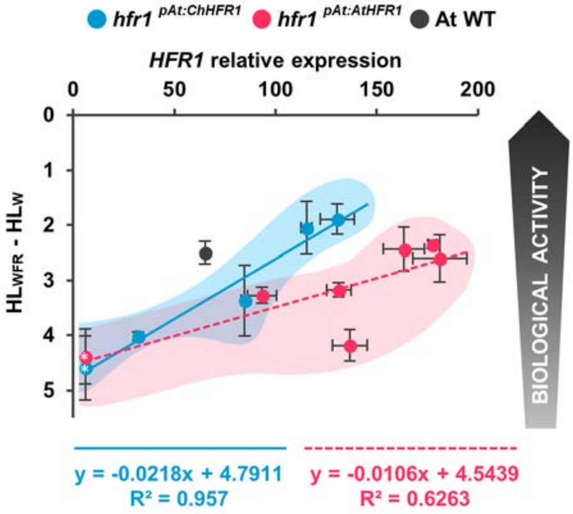

To further examine HFR1 action in *hfr1*$^{pAt:ChHFR1}$ and *hfr1*$^{pAt:AtHFR1}$ lines, we assessed the expression levels of *XTR7*, *YUC8* and *IAA29* in very low R:FR conditions, all being direct targets of PIFs. Compared to *hfr1-5* mutant, all lines which were expressing *HFR1* also had repressed levels of these three genes (**Figure S5B**), suggesting that the mechanism of ChHFR1 action in *A. thaliana* is comparable to AtHFR1, i.e., that ChHFR1 inhibits PIF action.

2.4 Stability of HFR1 determines its activity in shade

It is known that in etiolated seedlings exposure to W promotes stabilization and accumulation of AtHFR1 (Duek *et al.*, 2004; Yang, Lin, Sullivan, *et al.*, 2005), and in light-grown seedlings, high intensities of W also increase AtHFR1 abundance (Yang, Lin, Sullivan, *et al.*, 2005). Predicted AtHFR1 and ChHFR1 primary structure is similar, with a major difference in the N-terminal part of ChHFR1 which contains an additional 30 amino acids compared to AtHFR1 (**Figure 4A**). Yet, it is not known whether the structural differences relate to the observed differences in biological activities between ChHFR1 and AtHFR1. For this reason, we wanted to determine if these differences are reflected in changes in protein abundance or stability in shade.

To test if ChHFR1 behaves similarly in response to high W, we first examined ChHFR1 protein accumulation in response to different light conditions (**Figure S6A**). For this purpose, we used seedlings of *hfr*$^{35S:ChHFR1}$ lines, which express *ChHFR1* under the 35S promoter. Seedlings of *hfr*$^{35S:ChHFR1}$ grown in low W conditions (~20 µmol m^{-2} s^{-1}) accumulate low but detectable levels of ChHFR1; transfer of these seedlings from low to high W (~100 µmol m^{-2} s^{-1}) results in a 10-fold increase in ChHFR1 levels (**Figure S6B, C**). Since *ChHFR1* is under the constitutive 35S promoter, these results suggest that ChHFR1 accumulation is induced by high W intensity, as it has been described for AtHFR1. This prompted us to pretreat seedlings with high W intensity in all our subsequent experiments.

To compare the behaviour of ChHFR1 and AtHFR1 proteins, we exposed the obtained *hfr1*$^{pAt:ChHFR1}$ and *hfr1*$^{pAt:AtHFR1}$ lines (in which *HFR1* are under the regulation of *A. thaliana HFR1* promoter) to W+FR (**Figure 4B**). In all lines except one, this setting resulted in the accumulation and detection of HFR1-3xHA proteins. Moreover, all four *hfr1*$^{pAt:ChHFR1}$ lines tested displayed higher levels of HFR1 in relation to its transcript levels compared to *hfr1*$^{pAt:AtHFR1}$ lines (**Figure 4C**), suggesting a difference in the intrinsic properties of the two proteins.

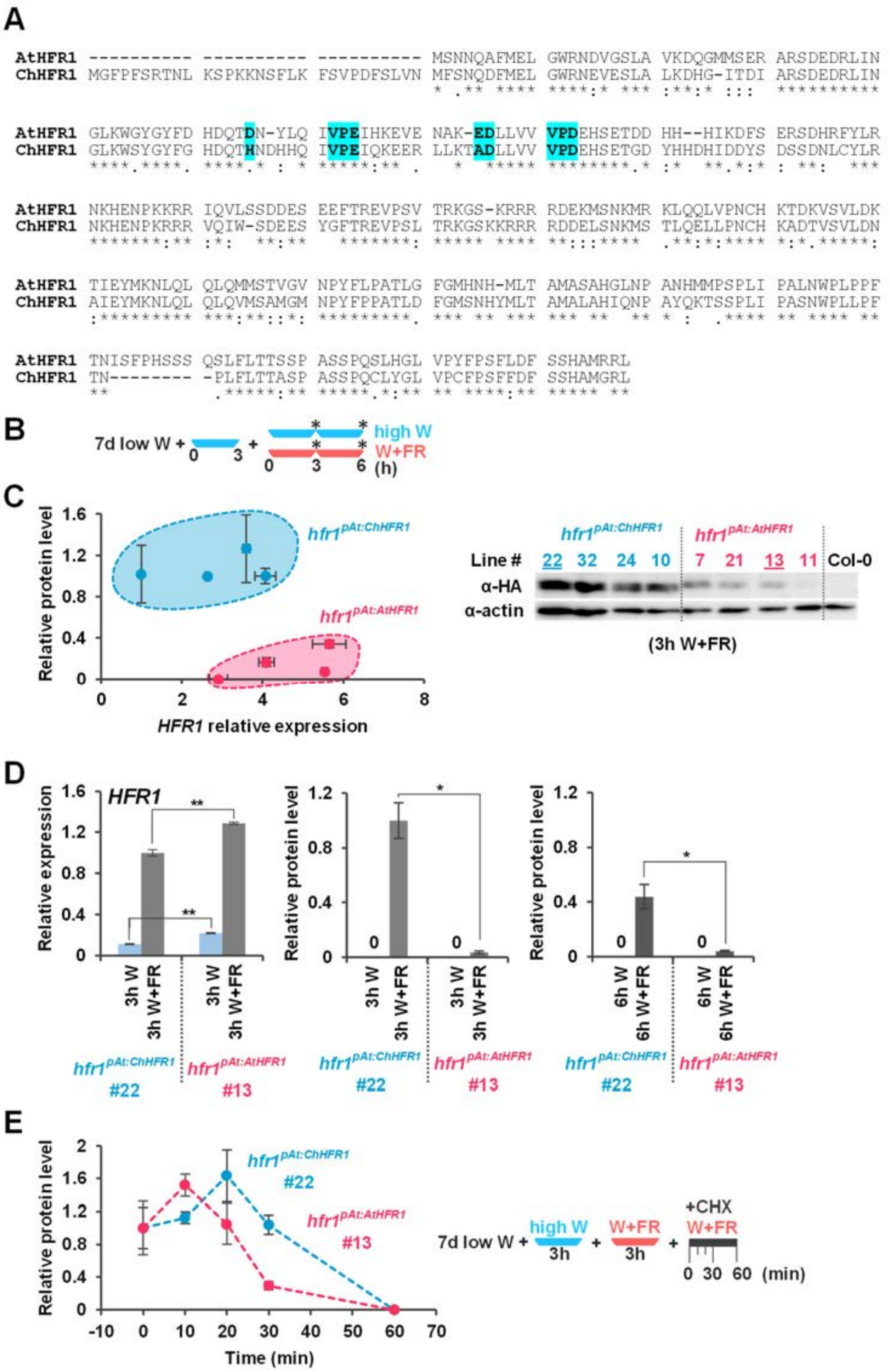

```
AtHFR1 ---------- ---------- ---------- MSNNQAFMEL GWRNDVGSLA VKDQGMMSER ARSDEDRLIN
ChHFR1 MGFPFSRTNL KSPKKNSFLK FSVPDFSLVN MFSNQDFMEL GWRNEVESLA LKDHG-ITDI ARSDEDRLIN
                                    * .** **** ****:* *** :**:* :::  **********

AtHFR1 GLKWGYGYFD HDQTDN-YLQ IVPEIHKEVE NAK-EDLLVV VPDEHSETDD HH--HIKDFS ERSDHRFYLR
ChHFR1 GLKWSYGYFG HDQTHNDHHQ IVPEIQKEER LLKTADLLVV VPDEHSETGD YHHDHIDDYS DSSDNLCYLR
       ****.****. ****.* : * *****:** .   *  ***** ********.* :*  **.*:* : **:  ***

AtHFR1 NKHENPKKRR IQVLSSDDES EEFTREVPSV TRKGS-KRRR RDEKMSNKMR KLQQLVPNCH KTDKVSVLDK
ChHFR1 NKHENPKRRR VQIW-SDEES YGFTREVPSL TRKGSKKRRR RDDELSNKMS TLQELLPNCH KADTVSVLDN
       *******:** :*:  **:**   *******: ***** **** **:::****  .**:*:**** *:*.*****:

AtHFR1 TIEYMKNLQL QLQMMSTVGV NPYFLPATLG FGMHNH-MLT AMASAHGLNP ANHMMPSPLI PALNWPLPPF
ChHFR1 AIEYMKNLQL QLQVMSAMGM NPYFPPATLD FGMSNHYMLT AMALAHIQNP AYQKTSSPLI PASNWPLLPF
       :********* ***:**::*: *********. *** ** *** *** **  ** * :  .**** ** **** **

AtHFR1 TNISFPHSSS QSLFLTTSSP ASSPQSLHGL VPYFPSFLDF SSHAMRRL
ChHFR1 TN-------- -PLFLTTASP ASSPQCLYGL VPCFPSFFDF SSHAMGRL
       **          .*****:** *****.*:** ** ****:** ***** **
```

A
B
7d low W +
0
3
+
0
3
6
(h)
*
*
high W
W+FR
C
1.6
1.2
0.8
0.4
0
0
2
4
6
8
Relative protein level
HFR1 relative expression
hfr1pAt:ChHFR1
hfr1pAt:AtHFR1
Line #
22
32
24
10
7
21
13
11
Col-0
α-HA
α-actin
(3h W+FR)
D
HFR1
Relative expression
Relative protein level
1.6
1.2
0.8
0.4
0
**
**
*
*
0
3h W
3h W+FR
6h W
6h W+FR
hfr1pAt:ChHFR1 #22
hfr1pAt:AtHFR1 #13
E
Relative protein level
2
1.6
1.2
0.8
0.4
0
-10
0
10
20
30
40
50
60
70
Time (min)
hfr1pAt:ChHFR1 #22
hfr1pAt:AtHFR1 #13
7d low W +
high W
3h
+
W+FR
3h
+
+CHX
W+FR
0
30
60
(min)

Figure 4. ChHFR1 and AtHFR1 proteins show different stability in shade. (A) Alignment of AtHFR1 and ChHFR1 protein sequences. Putative COP1 interacting motifs, defined in AtHFR1, are indicated in blue. **(B)** Cartoon summarizing growth conditions and treatments applied. Seedlings were grown for 7 days in continuous low W (~20 μmol m^{-2} s^{-1}) after which they were incubated for 3 h in high W (~100 μmol m^{-2} s^{-1}) and then either kept at high W or transferred to W+FR for 3 or 6 h. **(C)** Relative HFR1 protein levels in hfr1$^{At:ChHFR1}$ and hfr1$^{At:AtHFR1}$ lines were plotted against HFR1 relative expression (left). Relative HFR1-3xHA protein levels, normalized to actin protein levels, are the means ± SE of three independent biological replicates relative to hfr1$^{At:ChHFR1}$ line #22, that is taken as 1. Expression levels of HFR1, normalized to UBQ10, are the means ± SE of three independent biological replicates relative to data of hfr1$^{At:ChHFR1}$ line #22, taken as 1. Samples were collected from seedlings grown for 2 d in W and then transferred to W+FR for 5 additional days. Representative immunoblots detecting ChHFR1 and AtHFR1 from hfr1$^{At:ChHFR1}$ and hfr1$^{At:AtHFR1}$ seedlings separated on a 10% SDS-PAGE are shown (right); α-HA was used to detect ChHFR1 and AtHFR1, and α-actin was used as a loading control. **(D)** Expression and protein levels of HFR1 and HFR1-3xHA in hfr1$^{At:ChHFR1}$ line #22 and hfr1$^{At:AtHFR1}$ line #13, grown for 3 or 6 h in W or W+FR, as indicated in **B**. Relative HFR1 transcript levels, normalized to UBQ10 are the means ± SE of three independent biological replicates relative to hfr1$^{At:ChHFR1}$ line #22 grown for 3 h under W+FR. Relative protein levels, normalized to actin, are the means ± SE of three independent biological replicates relative to hfr1$^{At:ChHFR1}$ line #22. Samples were collected at data points marked with asterisks in **B**. **(E)** Degradation of ChHFR1 (hfr1$^{At:ChHFR1}$ line #22) and AtHFR1 (hfr1$^{At:AtHFR1}$ line #13) in seedlings treated with cycloheximide under W+FR during the indicated time, as summarized in the right part of the section. Relative protein levels, normalized to actin, are the means ± SE of three independent biological replicates relative to data point 0, taken as 1 for each line.

Next, a more in-depth analysis was done focusing on a single line of *hfr1*$^{pAt:ChHFR1}$ (line #22) and *hfr1*$^{pAt:AtHFR1}$ (line #13), both showing detectable levels of proteins under W+FR and similar *HFR1* expression levels in W and W+FR (**Figure 4D**). We observed that (1) ChHFR1 or AtHFR1 proteins were not detected in W conditions, and (2) ChHFR1 was significantly more abundant than AtHFR1 after 3 and 6 h of W+FR exposure. We reasoned that such behaviour indicated a differential regulation of AtHFR1 and ChHFR1 protein levels.

An increased ChHFR1 abundance might be the result of increased protein stability due to differences (1) in interaction with COP1/SPA E3 ubiquitin ligase and/or (2) in degradation kinetics by 26S proteasome. We addressed the potential differences in degradation kinetics by treating *hfr1*$^{pAt:ChHFR1}$ and *hfr1*$^{pAt:AtHFR1}$ seedlings with the protein synthesis inhibitor cycloheximide (CHX); HFR1 protein accumulation was previously induced in shade (**Figure 4E**). CHX treatment resulted first in a mild increase in protein accumulation and later in a decrease. After 1 h of CHX treatment, ChHFR1 and AtHFR1 protein levels became undetectable (**Figure 4E**). However, protein quantification showed that ChHFR1 degradation was slower compared to that of AtHFR1 (**Figure 4E**), supporting that ChHFR1 was more stable than AtHFR1 in low R:FR. These observations suggested that the higher ChHFR1 stability could contribute to its specifically higher biological activity in suppressing hypocotyl elongation in response to W+FR.

2.5 HFR1 modulates the elongation response to shade through interaction with PIF7

AtHFR1 has been shown to interact with all the AtPIFQ members. Because AtPIF7 is the main AtPIF promoting hypocotyl elongation in response to shade (Li *et al.*, 2012), we aimed to address whether HFR1 also interacts with PIF7. First, we analyzed the genetic interaction between AtHFR1 and AtPIF7. To do so, we crossed *A. thaliana hfr1-5* with *pif7-1* and/or *pif7-2* mutants and analyzed the hypocotyl response of the obtained double mutants to W+FR. Absence of *HFR1* resulted in a stronger hypocotyl elongation to shade compared to Col-0 (**Figure 5A**). Hypocotyls of *pif7-1* and *pif7-2* seedlings, by contrast, show a lack of hypocotyl elongation in response to both W+FR conditions used (**Figure 5A**), supporting the main role of PIF7 action in promoting the SAS response. Double *pif7-1 hfr1-5* and *pif7-2 hfr1-5* mutant seedlings behaved mostly as *pif7* single mutants in W and low R:FR (0.06) and elongated as much as Col-0 hypocotyls in very low R:FR (0.02), although never reached the length of the *hfr1-5* single mutant hypocotyls in this later W+FR condition (**Figure 5A**). These results indicate that *pif7* is epistatic over *hfr1* at low R:FR, whereas it seems more additive under very low R:FR. In any case, this is consistent with HFR1 functioning as a suppressor of PIF7.

To further establish the HFR1-PIF7 interaction, we aimed to test if a stable but truncated form of *HFR1* (with the N-terminal deletion, 35S:ΔNt-HFR1-GFP, line #03) (Galstyan *et al.*, 2011) will impede the effects of *PIF7* overexpression (35S:PIF7-CFP, lines #1 and #2) (Leivar *et al.*, 2008). Overexpression of the truncated *HFR1* derivative strongly and specifically inhibits shade-induced hypocotyl elongation in *A. thaliana* (Galstyan *et al.*, 2011) (**Figure 5B, C**). Even though *PIF7* is considered to be a positive regulator of SAS (Li *et al.*, 2012), its overexpression might have contrasting effects: (i) either a positive effect (Li *et al.*, 2012) or (ii) a negative effect on growth, including on the shade-induced hypocotyl elongation. We took advantage of the two available 35S:PIF7-CFP transgenic lines (Leivar *et al.*, 2008) that were almost unresponsive to W+FR (**Figure 5B**) and smaller and less developed than the wild type Col-0 in W (**Figure 5C**). In W, 35S:ΔNt-HFR1-GFP 35S:PIF7-CFP double transgenic seedlings (#1 and #2) did not differ in hypocotyl length and general aspect with Col-0; interestingly they did elongate clearly in low and very low R:FR (**Figure 5B, C**). The recovery of the shade-induced hypocotyl elongation and size of the seedlings took place even though *PIF7* transcript levels were not significantly different in the double transgenic seedlings than in their respective mother lines (**Figure S7**). *HFR1* transcript levels were significantly lower than in the respective 35S:ΔNt-HFR1-GFP mother line (**Figure S7**), although this transgene was not shown to affect the size and development of seedlings (Galstyan *et al.*, 2011). Therefore, the inhibitory effect of *PIF7-CFP* overexpression seemed counteracted by the overexpression of the truncated *HFR1*, further supporting the genetic interaction between HFR1 and PIF7 (**Figure 5B**).

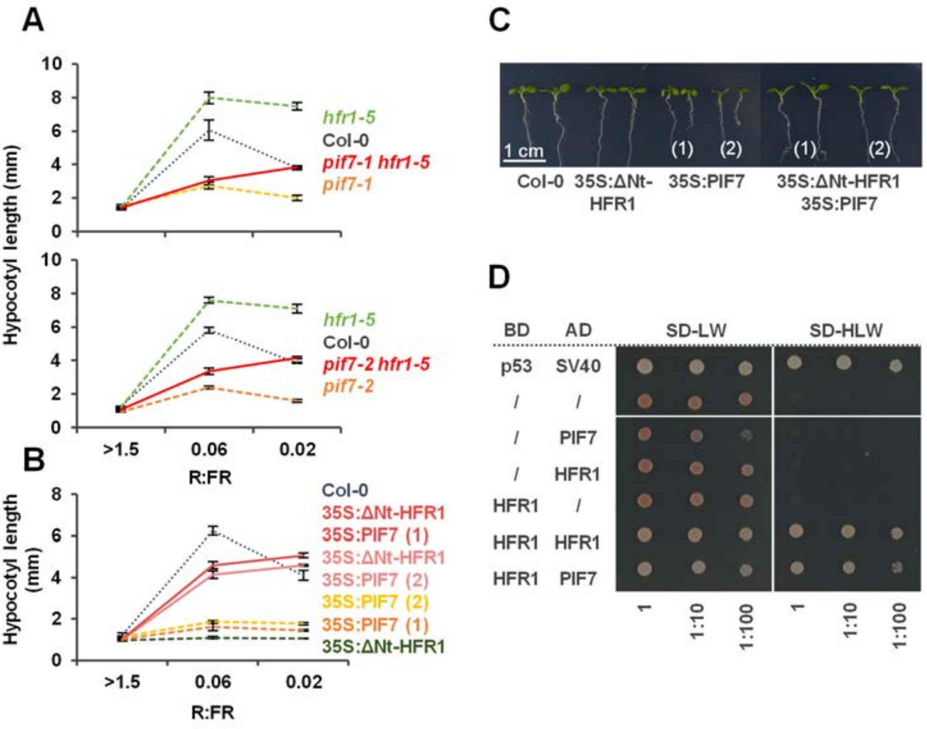

Figure 5. AtHFR1 interacts with AtPIF7. Hypocotyl length of A. thaliana Col-0, **(A)** pif7-1, hfr1-5, pif7-1 hfr1-5 (top graph), pif7-2, hfr1-5 and pif7-2 hfr1-5 (bottom graph) mutants, and **(B)** transgenic 35S:ΔNt-HFR1–GFP (35S:ΔNt-HFR1), two lines of 35S:PIF7-CFP (35S:PIF7 #1 and #2), and 35S:ΔNt-HFR1–GFP 35S:PIF7-CFP double transgenic (35S:ΔNt-HFR1 x 35S:PIF7 #1 and #2) seedlings grown under different R:FR conditions. Seedlings were grown in W (R:FR > 1.5) for 7 days or for 2 days in W and then transferred to two W+FR treatments (R:FR = 0.06 or 0.02) for 5 additional days. Values of hypocotyl length are the means ± SE of three independent biological replicates (at least 10 seedlings per replica). **(C)** Aspect of representative 7-day-old W-grown seedlings shown in **B**. **(D)** Y2H growth assay showing the interaction between AtHFR1 and AtPIF7. The BD- and the AD- derivative constructs used in the assay are shown on the left side of the panel. SD-LW or SD-HLW refer to the selective medium (plated as drops in dilutions of 1, 1:10 and 1:100) indicative of transformed cells or interaction between the hybrid proteins, respectively. Truncated forms of murine p53 (BD-fused) and SV40 large T-antigen (AD-fused), known to interact, were used as a positive control. Empty vectors (/) were used as negative controls.

The dimerization ability of bHLH protein family members relies on their HLH domain. Previously confirmed interactions between HFR1 and PIF1, PIF3, PIF4 and PIF5 (Fairchild, Schumaker and Quail, 2000; Hornitschek *et al.*, 2009; Shi *et al.*, 2013) suggested that AtHFR1 would physically and directly interact with AtPIF7 as well. To test this possibility, we performed a yeast two-hybrid (Y2H) assay. The observed HFR1 homodimerization indicated that its HLH domain is functional in this assay (**Figure 5D**). In the same assay, HFR1 was shown to interact with PIF7 (**Figure 5D**). Altogether, the Y2H and genetic analyses support that HFR1 and PIF7 physically interact, and this interaction is important for the regulation of hypocotyl elongation in simulated shade.

2.6 Different PIF regulated processes are affected by high HFR1 activity in *C. hirsuta*

Because HFR1 is supposed to act mainly by heterodimerizing and inhibiting the activity of various PIFs (Fairchild, Schumaker and Quail, 2000; Hornitschek *et al.*, 2009; Shi *et al.*, 2013), we expected that a high HFR1 activity would also affect other PIF regulated processes in *C. hirsuta*. In *A. thaliana*, the increased potency of HFR1 at warmer temperatures was previously shown to provide an important restraint on PIF4 action that drives elongation growth (Foreman *et al.*, 2011). Similarly, we hypothesized that the increased potency of HFR1 in *C. hirsuta* might provide an important restraint on PIF activity and consequently, on various PIF-dependent processes, such as warm temperature-induced hypocotyl elongation (thermogenesis) (**Figure 6A**). We first used *A. thaliana* Col-0 and *pifq* mutant to assess PIF activity in our conditions. Transfer from 22ºC to 28ºC after day 2 clearly promoted hypocotyl elongation in wild-type *A. thaliana* Col-0 (At WT) seedlings (more than twice compared to those growing at 22ºC); a similar effect was observed when seedlings grew constantly at 28ºC (**Figure 6B**). By contrast, *A. thaliana pifq* (At *pifq*) mutant seedlings were almost unresponsive to 28ºC, in agreement with published information for *pif4* and *pif5* mutants (Franklin *et al.*, 2011; Nozue, Harmer and Maloof, 2011). A similar lack of response was observed in wild-type *C. hirsuta* Ox (Ch WT) (**Figure 6B**). In *A. thaliana*, *HFR1* expression is increased by warm temperature in a PIF4-dependent manner (Foreman *et al.*, 2011). We also observed that *HFR1* expression was induced by 28ºC in At WT but not in At *pifq* (**Figure S8A**). In Ch WT, *HFR1* expression was induced by 28ºC but not significantly (**Figure S8A**). More importantly, since *HFR1* expression levels were much higher in Ox than in Col-0 at 22ºC, these results suggested that the high HFR1 activity in *C. hirsuta* is efficiently repressing PIF-mediated thermogenesis. It is therefore conceivable that both *A. thaliana pifq* mutant and *C. hirsuta* wild-type seedlings would be unable to promote hypocotyl elongation at 28ºC, one due to impairment of PIF4 and PIF5 action, the other through the strong suppression of PIFs by HFR1, as suggested (**Figure 6A**).

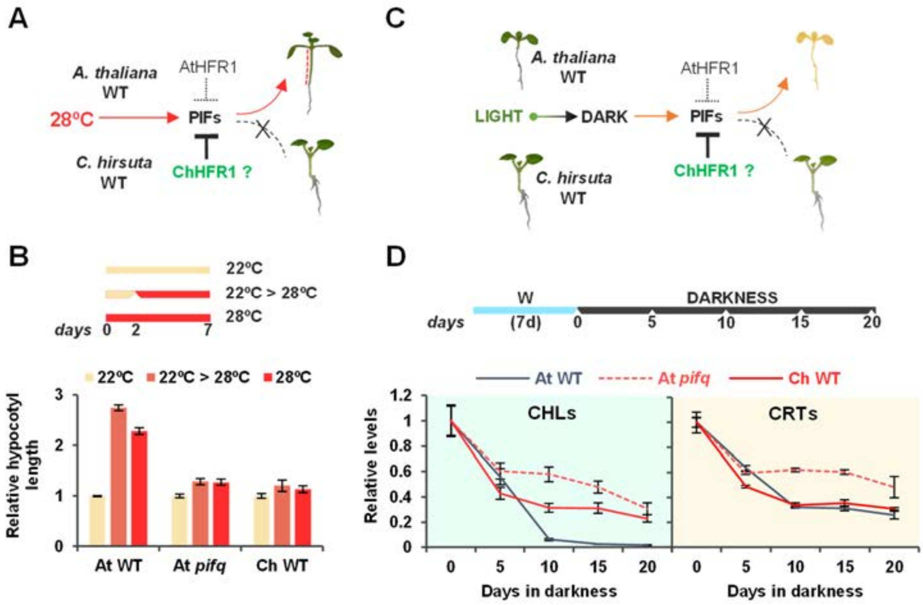

Figure 6. C. hirsuta has reduced responses to warm temperature-induced hypocotyl elongation and dark-induced senescence (DIS). (A) In wild-type A. thaliana (At WT), PIFs promote hypocotyl elongation as a response to warm temperature (28ºC). HFR1 activity is expected to inhibit this response by repressing PIFs. If ChHFR1 activity is high in wild-type C. hirsuta (Ch WT), hypocotyl elongation in this species would be attenuated at 28ºC compared to A. thaliana. (B) Hypocotyl length of A. thaliana Col-0 (At WT) and pifq mutant (At pifq), and Ch WT seedlings grown at warm temperatures. Seedlings were grown for 7 days in W at either 22ºC, 2 days at 22ºC then transferred to 28ºC for additional 5 days (22ºC > 28ºC) or for 7 days at 28ºC, as shown at the top of the panel. To compare genotypes, data are relative to the hypocotyl length of seedlings grown at 22ºC. (C) In At WT, DIS is mediated by PIF4 and PIF5 and involves a reduction of chlorophyll and carotenoid levels. HFR1 activity is expected to inhibit DIS through repression of PIF4 and PIF5. If ChHFR1 activity is high in wild-type C. hirsuta, DIS would be delayed in this species compared to A. thaliana. (D) Relative chlorophylls and carotenoids levels of At WT, At pifq and Ch WT seedlings in response to DIS. Seedlings were grown for 7 days in W and then transferred to total darkness for several days to induce senescence, as illustrated at the top of the panel. Plant material was harvested at the indicated times. For each genotype, data are relative to pigment levels at time point 0 (7 days in W).

We also studied dark-induced senescence (DIS) in *C. hirsuta*, another PIF-dependent process (**Figure 6C**). In *A. thaliana*, DIS can be induced by transferring light grown seedlings to complete darkness, a process in which PIF4 and PIF5 have major roles (Sakuraba *et al.*, 2014; Song *et al.*, 2014; Liebsch and Keech, 2016). DIS results in a degradation of photosynthetic pigments chlorophylls and carotenoids, which can be quantified as markers of senescence progression (Sakuraba *et al.*, 2014; Song *et al.*, 2014). To examine DIS, we transferred light-grown At WT, At *pifq* mutant and Ch WT seedlings to total darkness for up to 20 days. After DIS was activated, At WT seedlings became pale and eventually died (**Figure S8B**). As a way to register DIS, chlorophyll and carotenoid levels were measured in dark-treated seedlings. Carotenoid levels did not mirror the yellowing seedling phenotype (carotenoid level profiles were similar in all three genotypes, although remained higher in At *pifq*) whereas chlorophyll levels better correlated with the DIS phenotype (**Figures 6D, S8B**). After just 5 days of darkness, chlorophyll levels dropped to about 50% in all three genotypes, whereas longer dark treatments resulted in differences. *A. thaliana* WT (At WT) seedlings became visibly yellow at day 10, accompanied by a strong reduction of chlorophyll levels that dropped to less than 10% (**Figures 6D, S8B**). By contrast, chlorophyll levels in *C. hirsuta* WT (Ch WT) seedlings declined more slowly and seedlings were still green after 20 days of darkness, just like At *pifq* (**Figures 6D, S8B**). The observed delay in the DIS in *C. hirsuta* is consistent with an attenuated PIF promoting activity, suggesting that increased HFR1 activity might strongly antagonize this PIF-regulated response (**Figure 6B, D**).

3. Discussion

It is currently unknown whether the switch between shade avoidance and tolerance strategies is an easily adjustable trait in plants. The existence of closely related species with divergent strategies to shade provides a good opportunity to study the genetic and molecular basis for differential regulation of shade responses. We have focused on comparative analyses of the hypocotyl response to shade in young seedlings of two related *Brassicaceae*: *A. thaliana* and *C. hirsuta*. *A. thaliana*, a model broadly used to study the SAS hypocotyl response, is well characterized on a physiological, genetic and molecular level. By contrast, little is known about shade response of *C. hirsuta*, which was previously described as a likely shade tolerant species whose hypocotyls are unresponsive to shade (Hay *et al.*, 2014). Our comparative analyses are aimed to fill this gap.

3.1 ChHFR1 has a role in shade signalling in *C. hirsuta*

In *C. hirsuta*, the absence of HFR1 function shows a phenotype similar (but milder) to that of plants deficient in the phyA photoreceptor, known as *sis1* mutants (Molina-Contreras *et al.*, 2018), providing genetic evidence for the role of *HFR1* in restraining the *C. hirsuta* hypocotyl elongation in shade (**Figure 1A-D**). This indicates that HFR1, like phyA, is part of the mechanism that implements a shade tolerant habit in *C. hirsuta* seedlings. Both phyA and HFR1 are effectively downregulating many of shade marker genes, although there are temporal differences: the effect of phyA is observed after 4-8 hours of shade exposure (Molina-Contreras *et al.*, 2018), whereas that of HFR1 is rapidly detected after just 1 h of shade exposure (**Figure 1E, F**). These results suggest that ChHFR1 is acting independently of the phyA suppressor mechanism in *C. hirsuta*, as it was reported for *A. thaliana* (Ciolfi *et al.*, 2013; Jang, Henriques and Chua, 2013). Additionally, we have found that only AtHFR1, and not ChHFR1, regulate carotenoid and chlorophyll levels in shade (**Figure S2A-B**), a conclusion reached comparing *A. thaliana hfr1* mutants and *C. hirsuta* RNAi-HFR1 transgenic lines. However, we cannot discard that there might be a threshold level of HFR1 activity below which this factor becomes limiting for the accumulation of chlorophylls and carotenoids in shade, a level that might not be reached in the RNAi-HFR1 *C. hirsuta* plants that are likely knock-downs for ChHFR1. Thus, an excess of HFR1 activity might not be enough to impact carotenoid accumulation, which led to the contrasting conclusion that AtHFR1 does not regulate carotenoid levels (Bou-Torrent *et al.*, 2015).

3.2 ChFR1 has higher biological activity than AtHFR1

The observed role of ChHFR1 in making wild-type *C. hirsuta* seedlings unresponsive to shade is based on the strong shade phenotype of *chfr1* and RNAi-HFR1 seedlings (**Figure 1B, D, F**), which led us to hypothesize that HFR1 activity is higher in *C. hirsuta* than in *A. thaliana*. A higher HFR1 activity in *C. hirsuta* could be the result of several interdependent and non-excluding factors: (1) differential gene expression, (2) post-translational regulation affecting protein stability and degradation, and (3) intrinsic protein activity differences, e.g., affecting HFR1 interaction with PIFs or other proteins. Although *HFR1* expression was shade-induced in both species, expression levels of *HFR1* were consistently and significantly higher in *C. hirsuta* compared to *A. thaliana* in W and W+FR (**Figure 2**), suggesting that HFR1 protein levels might also be increased in *C. hirsuta* seedlings. Even though this may not be relevant in W because of the expected lower abundance of ChPIFs, a high pool of ChHFR1 ready to suppress early PIF action in shade could provide a fast and sustained repression of the elongation response.

By complementing *A. thaliana hfr1-5* plants with *ChHFR1* and *AtHFR1* (*hfr1*$^{pAt:ChHFR1}$ and *hfr1*$^{pAt:AtHFR1}$ lines), we confirmed that both ChHFR1 and AtHFR1 were functional, since they repressed shade-induced (i) excessive hypocotyl elongation and (ii) expression of several shade marker genes, as opposed to *hfr1-5* (**Figure S5**). We also found that these two proteins have intrinsic differences in their biological activities, as ChHFR1 appears to have higher biological activity than AtHFR1 per unit of expression, indicating that lower levels of ChHFR1 are more efficient in suppressing the shade-induced hypocotyl elongation (**Figure 3**). A similar approach also led to conclude that AtphyA and ChphyA photoreceptors are not fully exchangeable when regulating the shade-induced hypocotyl elongation (Molina-Contreras *et al.*, 2018). However, this approach does not inform about the molecular causes of the intrinsic functional differences between orthologous proteins.

A common aspect shared by both phyA and HFR1 is that the stability of these proteins is strongly affected by light conditions (Kircher *et al.*, 1999; Duek *et al.*, 2004; Casal, Candia and Sellaro, 2014). Whereas phyA stability is reduced by light (phyA is a photolabile phytochrome), in the case of AtHFR1, light promotes its stability (Duek *et al.*, 2004; Park *et al.*, 2008). AtHFR1 protein abundance is modified post-translationally by phosphorylation (Park *et al.*, 2008) and ubiquitination in a light-dependent manner (Jang *et al.*, 2005; Yang, Lin, Hoecker, *et al.*, 2005). Several Ser residues on the Nt domain of AtHFR1 were shown to be phosphorylated by casein kinase II (CKII) (Park *et al.*, 2008), with various degrees of effect on protein stability. In particular, phosphorylation of Ser122 had the most pronounced effect on AtHFR1 stability. In addition, phosphorylation of AtHFR1 that is promoted in light, reduces AtHFR1 degradation rate (Park *et al.*, 2008), which is consistent with the notion of light promoting the stability of AtHFR1 (Duek *et al.*, 2004). We have shown that high light intensity also induces accumulation of ChHFR1 (**Figure S6**), which has a conserved Ser (Ser154) in the same position as AtHFR1 (Ser122) (**Figure 4A**).

Our comparative analyses using complemented *hfr1-5* lines with the *AtHFR1* and *ChHFR1* transgenes under the *pAtHFR1* control indicated that (1) in W, HFR1-3xHA proteins cannot be detected, likely due to their low transcript levels, and (2) shade promotes HFR1 protein accumulation, likely as a consequence of the strong shade-induced expression (**Figure 4D**). ChHFR1 accumulates despite the fact that shade has been shown to promote AtHFR1 degradation, as observed in transgenic plants expressing AtHFR1 under the 35S promoter (Pacín *et al.*, 2016). More importantly, ChHFR1 accumulates significantly more than AtHFR1 in shade (**Figure 4C, D**).

These results indicated the existence of intrinsic differences in AtHFR1 and ChHFR1 protein accumulation. COP1 directly interacts and polyubiquitinates AtHFR1 leading to its degradation by the 26S proteasome (Jang *et al.*, 2005; Yang, Lin, Sullivan, *et al.*, 2005). Presumably, light-induced phosphorylation of AtHFR1 could reduce its interaction with the COP1 (Park *et al.*, 2008), rendering it more stable in the light to modulate photomorphogenic responses. It is not completely clear how shade relates to HFR1 phosphorylation and how this affects its COP1-mediated polyubiquitination for further degradation. The use of the protein synthesis inhibitor CHX showed a delayed pattern of ChHFR1 degradation in comparison to AtHFR1 (**Figure 4D**) indicating that ChHFR1 is more stable in shade. Therefore, it seems likely that differences in phosphorylation may contribute to the strong differences in ChHFR1 and AthHFR1 protein stability (**Figure 4D**).

The N-terminal domain (amino acids 1-131) of AtHFR1 that contains the COP1 binding site (likely amino acids 48-83) affects its stability (Jang *et al.*, 2005). Indeed, deletion of Nt part of AtHFR1 led to its stabilization in the dark and light (Duek *et al.*, 2004), resulting in a stronger biological activity (Jang *et al.*, 2005; Yang, Lin, Sullivan, *et al.*, 2005; Galstyan *et al.*, 2011), and highlights the importance of the COP1-interacting domain for light regulation of AtHFR1. Therefore, protein sequence and/or other structural differences between AtHFR1 and ChHFR1 (**Figure 4A**) could influence their differential stability and, at least in part, may account for the difference in response to vegetation proximity between *C. hirsuta* and *A. thaliana*.

3.3 High ChHFR1 activity affects several PIF regulated processes in *C. hirsuta*

AtHFR1 was previously shown to interact with several PIFs in *A. thaliana*, such as AtPIF1, AtPIF3, AtPIF4 and AtPIF5, and to sequester them forming nonfunctional heterodimers (Fairchild, Schumaker and Quail, 2000; Hornitschek *et al.*, 2009; Shi *et al.*, 2013). Our genetic and Y2H experiments extend the list of AtHFR1 interactors to AtPIF7, a major SAS promoting PIF (**Figure 5**). It seems likely that ChHFR1 maintains the same PIF-binding abilities. A higher stability of ChHFR1 over AtHFR1 in shade, suggests a stronger repression of PIF activity, i.e., an attenuated PIF activity in *C. hirsuta* that can contribute to the hypocotyls unresponsiveness to shade. The attenuation of the warm temperature-induced hypocotyl elongation and DIS in *C. hirsuta*, processes known to be PIF-regulated in *A. thaliana* (Koini *et al.*, 2009; Sakuraba *et al.*, 2014; Song *et al.*, 2014; Press, Lanctot and Queitsch, 2016; Hayes *et al.*, 2017), further support our hypothesis that in *C. hirsuta* PIF activity is attenuated compared to *A. thaliana*. Therefore, we suggest that the increased stability of ChHFR1 makes it more active and leads to a stronger repression of several PIF regulated processes in *C. hirsuta*, as shown in here.

3.4 Final remarks

Our findings propose a new model for differential regulation of shade responses in closely related species of *A. thaliana* and *C. hirsuta* (**Figure 7**). Activity of negative regulators such as HFR1 (this work) and phyA (Molina-Contreras *et al.*, 2018) appears to be increased in *C. hirsuta* to maintain unresponsiveness of hypocotyls to shade. We suggest that in *C. hirsuta* this activity is increased through higher stability of ChHFR1, coupled with upregulated expression, which could provide a more repressive state in conditions of shade. Most likely, the increased activity of HFR1 works in pair with other components, such as phyA, that was reported to have a differential regulation in *C. hirsuta* (Molina-Contreras *et al.*, 2018). Whether other shade tolerant species employ the same or different components is something we aim to explore in the future. Finally, an extensive study will be needed to decipher the exact mechanism of the HFR1-mediated shade tolerance in *C. hirsuta* seedlings and whether additional downstream steps might also contribute to this trait.

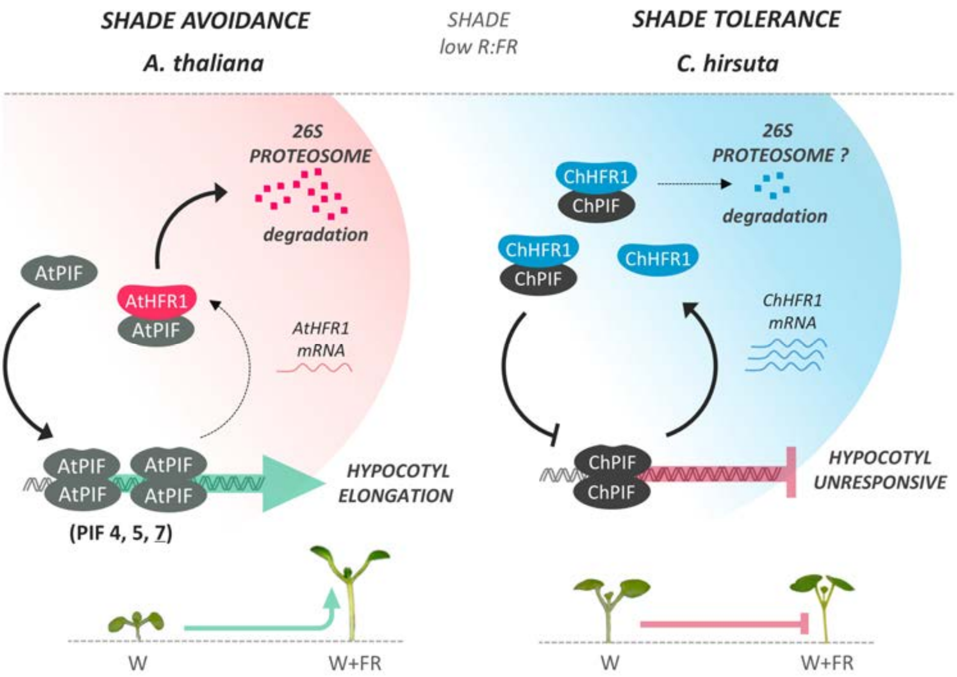
SHADE AVOIDANCE
A. thaliana
SHADE
low R:FR
SHADE TOLERANCE
C. hirsuta
26S
PROTEOSOME
degradation
AtPIF
AtHFR1
AtPIF
AtHFR1
mRNA
AtPIF
AtPIF
AtPIF
AtPIF
HYPOCOTYL
ELONGATION
(PIF 4, 5, 7)
W
W+FR
ChHFR1
ChPIF
26S
PROTEOSOME ?
degradation
ChHFR1
ChPIF
ChHFR1
ChHFR1
mRNA
ChPIF
ChPIF
HYPOCOTYL
UNRESPONSIVE
W
W+FR

Figure 7. Model for a role of HFR1 in establishing shade-avoidance or tolerance in A. thaliana and C. hirsuta. Shaded (low R:FR) conditions alter the phytochrome photoequilibrium displacing them towards inactive state, allowing PIFs to promote the expression of shade avoidance related genes, such as HFR1. HFR1 modulates this response by heterodimerizing with PIFs and inhibiting their DNA binding ability, which attenuates the hypocotyl elongation of A. thaliana seedlings. Our data support that in C. hirsuta, a higher HFR1 activity more effectively inhibits the action of PIFs than in A. thaliana, preventing hypocotyl elongation and establishing the shade tolerance habit. An increased activity of ChHFR1 is due to upregulated expression and lower ChHFR1 protein degradation rate in simulated shade conditions.

4. Materials and Methods

4.1 Plant material and growth conditions

Arabidopsis thaliana hfr1-5, *pif7-1*, *pif7-2* mutants and 35S:PIF7-CFP lines (in the Col-0 background) and *Cardamine hirsuta* (Oxford ecotype, Ox) plants have been described before (Leivar *et al.*, 2008; Hay *et al.*, 2014). *A. thaliana* and *C. hirsuta* plants were grown in the greenhouse under long-day photoperiods (16 h light and 8 h dark) to produce seeds, as described (Martínez-García *et al.*, 2014; Gallemí *et al.*, 2016, 2017). For hypocotyl assays, seeds were surface-sterilized and sown on solid growth medium (half strength Murashige and Skoog, (Murashige and Skoog, 1962)) without sucrose (0.5xGM–). For gene expression analyses, immunoblot experiments and pigment quantification, seeds were sown on a sterilized nylon membrane placed on top of the solid 0.5xGM– medium. After stratification (dark at 4ºC) of 3-6 days, plates with seeds were incubated in plant chambers at 22ºC under continuous white light (W) for at least 2 h to break dormancy and synchronize germination (Paulišić *et al.*, 2017). W was emitted from cool fluorescent tubes that provided from 20 to 100 µmol m^{-2} s^{-1} of photosynthetically active radiation (PAR) with a red (R) to far-red light (FR) ratio (R:FR) from 1.3-3.3. The different simulated shade treatments were produced by supplementing W with increasing amounts of FR (W+FR). FR was emitted from GreenPower LED module HF far-red (Philips), providing R:FR of 0.02-0.09. Light fluence rates were measured with a Spectrosense2 meter (Skye Instruments Ltd) (Martínez-García *et al.*, 2014). Temperature induced hypocotyl elongation assays were done by placing the plates with seeds under continuous W in growth chambers at 22ºC for 7 days, at 28ºC for 7 days or 2 days at 22ºC and then 5 days at 28ºC.

4.2 Measurement of hypocotyl length

Hypocotyl length was measured as described (Paulišić *et al.*, 2017). Experiments were repeated at least three times with more than 10 seedlings per genotype and/or treatment and average values are shown.

4.3 Generation of transgenic lines, mutants and crosses

A. thaliana hfr1-5 plants were transformed to express *AtHFR1* and *ChHFR1* under the promoters of 35S, pAtHFR1 (pAt) and pChHFR1 (pCh). The obtained lines were named as *hfr1*$^{35S:AtHFR1}$, *hfr1*$^{35S:ChHFR1}$, *hfr1*$^{pAt:AtHFR1}$, *hfr1*$^{pAt:ChHFR1}$, *hfr1*$^{pCh:AtHFR1}$ and *hfr1*$^{pCh:ChHFR1}$. Transgenic RNAi-HFR1 lines are in *C. hirsuta* wild-type (Ox) background. Mutant lines of *ChHFR1* (*chfr1-1* and *chfr1-2*) were generated by CRISPR-Cas9. Details of the constructs used for the generation of transgenic lines and mutants are provided as Supplementary information.

4.4 Gene expression analyses

Real-time qPCR analyses were performed using biological triplicates, as indicated (Gallemí *et al.*, 2017). Total RNA was extracted from seedlings, treated as indicated, using commercial kits (Maxwell® SimplyRNA and Maxwell® RSC Plant RNA Kits; www.promega.com). 2 µg of RNA was reverse-transcribed with Transcriptor First Strand cDNA synthesis Kit (Roche, www.roche.com). The *A. thaliana UBIQUITIN 10* (*UBQ10*) was used for normalization in *A. thaliana hfr1-5* lines expressing *AtHFR1* or *ChHFR1*. The *ELONGATION FACTOR 1α* (*EF1α*) was used for normalizing and comparing the levels of *HFR1* between *A*. *thaliana* and *C. hirsuta*. All primers sequences for qPCR analyses are provided as Supplementary information (**Table S1**).

4.5 Protein extraction and immunoblotting analyses

To detect and quantify transgenic AtHFR1 and ChHFR1, proteins were extracted from ~50 mg of 7-day old seedlings, grown as indicated. Plant material was frozen in liquid nitrogen, ground to powder and total proteins were extracted using an SDS-containing extraction buffer (1.5 µL per mg of fresh weight), as described (Gallemí et al., 2017). Protein concentration was estimated using Pierce™ BCA Protein Assay Kit (Thermo Scientific, www.thermofisher.com). Proteins (30 - 45 µg per lane) were resolved on a 10% SDS-PAGE gel, transferred to a PVDF membrane and immunoblotted with rat monoclonal anti-HA (High Affinity, clone 3F10, Roche, www.roche.com; 1:2000 dilution) and hybridized with peroxidase conjugated goat anti-rat (Polyclonal, A9037, Sigma, www.sigmaaldrich.com; 1:5000 dilution) and after membrane stripping, with rabbit polyclonal anti-actin (Agrisera, www.agrisera.com; 1:5000 dilution) then hybridized with peroxidase conjugated donkey anti-rabbit (Amersham, www.gelifesciences.com; 1:10000 dilution). Development of blots was carried out in ChemiDoc™ Touch Imaging System (Bio-Rad, www.bio-rad.com) using ECL Prime Western Blotting Detection Reagent (GE Healthcare, RPN2236). Relative protein levels of three biological replicates were quantified using Image Lab™ Software (Bio-Rad, www.bio-rad.com).

4.6 Yeast 2 Hybrid (Y2H) assays

For Y2H assays we employed a cell mating system, as described (Gallemí *et al.*, 2017). The leucine (Leu) auxotroph YM4271a yeast strain was transformed with the AD-derived constructs and the tryptophan (Trp) auxotroph pJ694α strain with the BD-derived constructs. Colonies were selected on synthetic defined medium (SD) lacking Leu (SD-L) or Trp (SD-W), grown in liquid medium and set to mate by mixing equal volumes of transformed cells. Dilutions of the mated cells were selected on SD-LW and protein interactions were tested on SD-LW medium lacking histidine (SD-HLW). Details of the yeast constructs used are provided as Supplementary information.

4.7 Photosynthetic pigments quantification

Whole seedlings were harvested, ground in liquid nitrogen, and the resulting powder was used for the quantification of chlorophylls and carotenoids spectrophotometrically or by HPLC, as described (Rodríguez-Villalón, Gas and Rodríguez-Concepción, 2009). Additional details are provided as Supplementary information.

5. Acknowledgements

We are grateful to Rosa Rodríguez for her technical support. SP received predoctoral fellowships from the *Agència d’Ajuts Universitaris i de Recerca* (AGAUR - Generalitat de Catalunya, FI program). CT received a Marie Curie IEF postdoctoral contract funded by the European Commission and a CRAG short-term fellowship. Our research is supported by grants from BBSRC (BB/H006974/1) and Max Planck Society (core grant) to MT, and from MINECO-FEDER (BIO2014-59895-P, BIO2014-59092-P, BIO2017-85316-R) and AGAUR (2014-SGR447, 2017-SGR1211 and Xarba) to JFM-G and MRC. We also acknowledge the support of the MINECO for the “Centro de Excelencia Severo Ochoa 2016-2019” award SEV-2015-0533 and by the CERCA Programme / Generalitat de Catalunya.

6. Supplementary information

6.1 Generation of RNAi-HFR1 plants of *C. hirsuta*

To generate an RNAi construct for silencing of the endogenous *ChHFR1*, a fragment of 222 bp was PCR amplified using primers CTO35 + CTO36 (**Table S2**) and cDNA of 7-day old *C. hirsuta* seedlings grown 1 h under W+FR. This partial fragment of *ChHFR1* (ptChHFR1) was cloned into pCRII-TOPO (Invitrogen, www.thermofisher.com) to generate pCT17, which was confirmed by sequencing. An *Eco*RI fragment of pCT17 was subcloned into pENTR3C vector (Invitrogen, www.thermofisher.com), to create the Gateway entry clone pCT19 (to have ptChHFR1 flanked with attL1 and attL2, attL1<ptChHFR1<attL2). Recombination of pCT19 with the destination vector pB7GWIWG2(I), which contains attR1 and attR2 sites, using Gateway LR Clonase II (Invitrogen), gave pCT33 (35S:attB1<RNAi-ChHFR1<attB2). This plasmid is a binary vector conferring resistance to the herbicide phosphinothricin (PPT) in plants and the antibiotic Spectinomycin in bacteria. *Agrobacterium tumefaciens* strain $C_{58}C_1$ (pGV2260) was transformed with pCT33 by electroporation and colonies were selected on solid YEB medium with Rifampicin (100 µg/mL), Kanamycin (25 µg/mL) and Spectinomycin (100 µg/mL). Wild type *C. hirsuta* plants (Ox) were transformed by floral dipping and transgenic seedlings were selected on 0.5xGM- medium (Murashige and Skoog, 1962; Roig-Villanova *et al.*, 2006) containing 50 µg/mL PPT. Transgene in seedlings of T1 generation was verified by PCR genotyping using specific primers. Plants homozygous for the transgene were finally used for experiments.

6.2 Isolation of *HFR1* mutants of *C. hirsuta*

To obtain loss-of-function mutants of *ChHFR1* in *C. hirsuta* (named as *chfr1*) we employed the CRISPR-Cas9 gene editing system (Morineau *et al.*, 2017). The guide RNA targeting ChHFR1 ($gRNA_{ChHFR1}$, 5’-GTT-GAA-GAC-TGC-AGA-TTT-GT-3’) was synthesized to be under the control of the *A. thaliana U6* promoter (pU6) sequence and flanked by the Gateway attB1 and attB2 recombination sites (IDT, eu.idtdna.com/site) (attB1<pU6:$gRNA_{ChHFR1}$<attB2). This sequence was recombined with the vector pDONR207 using Gateway BP Clonase II (Invitrogen) to generate the entry vector pSP101 (attL1<pU6:$gRNA_{ChHFR1}$<attL2). In a recombination reaction of pSP101 with pDE-Cas9 (Fauser, Schiml and Puchta, 2014) using Gateway LR Clonase II (Invitrogen), a binary vector pSP102 was created (attB1<pU6:$gRNA_{ChHFR1}$<attB2, Cas9). This vector, that contains the information to target ChHFR1, confers resistance to PPT in plants and Spectinomycin in bacteria. *Agrobacterium tumefaciens* strain

$C_{58}C_1$ (pGV2260) was transformed with pSP102 by electroporation and colonies were selected on solid YEB medium with antibiotics, as indicated before for pCT33. Wild type *C. hirsuta* (Ox) plants were transformed by floral dipping and resistant transgenic seedlings were selected on 0.5xGM- medium containing PPT (30 µg/mL). These T1 seedlings were PCR genotyped using primers MJO27 and MJO28 (**Table S2**) to detect the presence of the transgene. In the following T2 generation, a total of six seedlings with a *sis* phenotype from 1 independent transgenic line were selected and grown to maturity. An *HFR1* fragment of 664 bp around the $gRNA_{ChHFR1}$ target sequence was amplified by PCR from gDNA of each plant using primers CTO29 + CTO36 (**Table S2**). Sequencing of these fragments indicated the presence of mutations in *ChHFR1* gene. Descendants of these plants (T3 generation) were reselected in shade and sequenced to confirm the unambiguous presence of the mutated *chfr1* alleles. In the T4 generation, seedlings sensitive to PPT (indicating the loss of T-DNA insertion) were selected, which resulted in the isolation of the *chfr1-1* and *chfr1-2* mutant allele lines (**Figure S1**). These mutants were genotyped by PCR using primers SPO104 + SPO107 (for *chfr1-1*) and SPO106 + SPO107 (for *chfr1-2*) (**Table S2**).

6.3 Generation of *A. thaliana hfr1-5* transgenic lines expressing *AtHFR1* or *ChHFR1* under the control of different promoters

We amplified a 2 kbp fragment of *AtHFR1* promoter starting immediately before the ATG of *AtHFR1* gene using *A. thaliana* (Col-0) gDNA as a template and primers SPO26 + SPO27 (**Table S2**). This fragment was subcloned into pCRII-TOPO (Invitrogen) to generate pSP51. From the different clones analyzed, the best one was pSP51.10, with three 1 bp-deletions in the amplified region, none affecting the G-boxes, known to be necessary for PIF binding.

AtHFR1 coding sequence was amplified from pJB30 (Galstyan *et al.*, 2011) using primers RO25 + SPO30 (**Table S2**), which removed the stop codon and introduced a *Xho*I site at the N-terminal site. After subcloning this fragment into pCRII-TOPO, which gave pSP54 (*AtHFR1*), the insert was sequenced to confirm its identity. The 3xHA fragment was amplified from plasmid pEN-R2-3xHA-L3 (Karimi, Depicker and Hilson, 2007) and primers SPO31 (which added a *Sal*I site) + SPO32 (which added a *Xho*I site, **Table S2**). This fragment was subcloned into pCRII-TOPO to generate pSP55 (*3xHA*), whose insert was sequenced to confirm its identity. A *BamH*I-*Xho*I fragment of pSP54 was subcloned into pSP55 digested with *BamH*I and *Sal*I to generate pSP57 (*AtHFR1-3xHA*). A *BamH*I-*Xho*I fragment of pSP57 was subcloned into the same sites of pENTR3C vector (Invitrogen) which gave pSP59. This plasmid contained *AtHFR1-3xHA*, with an extra *Xba*I site in the C-terminus end, flanked with attL1 and attL2 sites (attL1<*AtHFR1-3xHA*^{XbaI}<attL2). *Xba*I restriction site in pSP59 was removed by filling the site with Klenow enzyme after digestion, and religation to generate pSP84 (attL1<*AtHFR1-3xHA*<attL2). Recombination of pSP84 with the binary vector pIR101 (attR1<*ccdB*<attR2) (Molina-Contreras et al., 2018) using Gateway LR Clonase II (Invitrogen) resulted in pSP88 (attB1<*AtHFR1-3xHA*<attB2). An *Xba*I fragment of pSP51 was subcloned into the same site of pSP88 which gave pPS90 (*pAtHFR1*:attB1<*AtHFR1-3xHA*<attB2). This binary vector confers resistance to Spectinomycin in bacteria and PPT in plants.

ChHFR1 CDS was amplified using *C. hirsuta* wild-type (Ox) cDNA and primers SPO28 + SPO29 (**Table S2**), which removed the stop codon and introduced a *Xho*I site. This PCR product was subcloned into pCRII-TOPO to generate pSP53 (*ChHFR1*). Selected colonies were sequenced to confirm their identity. A *BamH*I-*Xho*I fragment of pSP53 was subcloned into pSP55 digested with *BamH*I-*Sal*I to generate pSP56 (*ChHFR1-3xHA*). A *BamH*I-*Xho*I fragment of pSP56 was subcloned into the same site of pENTR3C vector (Invitrogen), which gave pSP58. This plasmid contained *ChHFR1-3xHA*, with an *Xba*I site in the C-terminus end, flanked with attL1 and attL2 sites (attL1<*ChHFR1-3xHA*^{XbaI}<attL2). *Xba*I restriction site in pSP58 was removed by filling the site with Klenow enzyme after digestion, and religation to generate pSP83 (attL1<*ChHFR1-3xHA*<attL2). Recombination of pSP83 with the binary vector pIR101 using Gateway LR Clonase II (Invitrogen) resulted in pSP87 (attB1<*ChHFR1-3xHA*<attB2). An *Xba*I fragment of pSP51 was subcloned into the same site of pSP87 which gave pPS89 (*pAtHFR1*:attB1<*ChHFR1-3xHA*<attB2). This binary vector confers resistance to Spectinomycin in bacteria and PPT in plants.

We amplified a 2 kbp fragment of *ChHFR1* promoter (*pChHFR1*) starting immediately before the predicted ATG of the *ChHFR1* gene. *C. hirsuta* (Ox) gDNA was used as a template. Cloning was done by amplifying two overlapping fragments: the first fragment, of 1282 bp, was amplified with primers SPO51 + SPO49 (**Table S2**) and the second fragment, of 1273 bp, with primers SPO48 + SPO36-b (**Table S2**). These fragments were used together as templates to amplify 2 kbp promoter of ChHFR1 with the primers SPO36-b + SPO35-b (**Table S2**) that resulted in a 2000 bp fragment flanked with *Xba*I sites. The *pChHFR1* fragment was then subcloned into pCRII-TOPO (Invitrogen) to generate pSP85. Insert was sequenced, and the best fragment contained one mutation that was not affecting any of the G-boxes found. An *Xba*I fragment of pSP85 containing *pChHFR1* was subcloned into (i) the same site of pSP87, which gave pSP92 (*pChHFR1*:attB1<*ChHFR1-3xHA*<attB2), and (ii) the same site of pSP88, which gave pSP93 (*pChHFR1*:attB1<*AtHFR1-3xHA*<attB2). These two binary vectors confer resistance to Spectinomycin in bacteria and PPT in plants.

To overexpress *ChHFR1* and *AtHFR1*, *BamH*I-*Xho*I fragments of pSP57 and pSP58 were subcloned into the *BamH*I-*Sal*I digested pCAMBIA1300 based pCS14 (Sorin *et al.*, 2009) to generate pSP81 (*35S:ChHFR1*) and pSP82 (*35S:AtHFR1*), respectively. These two binary vectors confer resistance to kanamycin in bacteria and hygromycin in plants.

A. thaliana hfr1-5 plants were transformed with pSP81, pSP82, pSP89, pSP90, pSP92 and pSP93, as previously described. Transgenic seedlings were selected on 0.5xGM- medium with PPT (15 µg/mL) or hygromycin (30 µg/mL), verified by PCR genotyping using specific primers. Homozygous transgenic plants with 1 T-DNA insertion were finally used for experiments.

6.4 Generation of constructs for the Yeast 2 Hybrid (Y2H) assays

AtPIF7 CDS was amplified using *A. thaliana* (Col-0) cDNA and primers JO414 + JO415 (**Table S2**), which removed the STOP codon and introduced a *Xho*I site. This PCR product was subcloned into pCRII-TOPO to generate pRA1 (*AtPIF7*). The insert was sequenced to confirm its identity. A *Xho*I fragment of pRA1 was subcloned into pSP55 digested with *Sal*I to generate pRA2 (*AtPIF7-3xHA*). An *Eco*RI fragment of pRA2 was subcloned into the same site of pENTR3C entry vector (Invitrogen) which gave pRA3 (attL1<*AtPIF7-3xHA*<attL2). This PIF7-3xHA had a stop codon immediately before the ATG, which prevented from cloning it in frame with the yeast derived proteins. Therefore, the *PIF7-3xHA* gene was PCR amplified using pRA3 as a DNA template and primers BAO4 + BAO5 (**Table S2**) to add attB1 and attB2 sequences (attB1<*AtPIF7-3xHA*<attB2). This fragment was recombined with pDONR207 using Gateway BP Clonase II (Invitrogen) to obtain pBA7 (attL1<*AtPIF7-3xHA*<attL2). The insert was sequenced to confirm its identity. In a recombination reaction of pBA7 and pGBKT7-GW (Chini *et al.*, 2009) which contained the Gal4 DNA-binding domain (BD, attR1<ccdB<attL2; it confers Trp auxtrophy), and pBA7 and pGADT7-GW (Chini *et al.*, 2009) which contained the Gal4 activation domain (AD, attR1<ccdB<attL2; it confers Leu auxtrophy), using Gateway LR Clonase II (Invitrogen), pBA10 (BD-attB1<*AtPIF7-3xHA*<attB2) and pBA11 (AD-attB1<*AtPIF7-3xHA*<attB2) were obtained. These plasmids allowed expressing the fusion BD-PIF7-3xHA or AD-PIF7-3xHA proteins under the *ADH1* promoter in yeast, respectively.

6.5 GUS lines

Transgenic lines expressing GUS were based on a modified pIR101 plasmid which contains the reporter *GUS* gene in a promoterless context (attB1<*GUS*<attB2). *Xba*I fragments of pSP51 and of pSP85 were subcloned into the same site of pJD5 to give

pSP86 (pAtHFR1:attB1<*GUS*<attB2) and pSP91 (pChHFR1:attB1<*GUS*<attB2). These two binary vectors confer resistance to Spectinomycin in bacteria and PPT in plants. Col-0 plants were transformed with these constructs as described previously.

6.6 GUS staining

Histochemical GUS assays were done as described (Roig-Villanova, 2006), incubating seedlings at 37ºC without ferricyanide/ferrocyanide.

6.7 Photosynthetic pigments quantification

In **Figure S2**, levels of total chlorophylls and carotenoids in shade experiments were quantified by HPLC as described (Rodríguez-Villalón, Gas and Rodríguez-Concepción, 2009) from 7-day-old seedlings grown in either W or W+FR.

For senescence experiments (**Figure 6D**), total chlorophylls and carotenoids were quantified from light grown seedlings incubated in the darkness for the indicated amount of days to induce senescence. Extracts were prepared according to (Lichtenthaler, 1987) with 100% acetone and measured spectrophotometrically at 470, 644.8 and 661.6 nm. Pigment contents were calculated as described in (Lichtenthaler and Buschmann, 2005).

6.8 Tables:

Table S1. Primers used for gene expression analyses. Primers BO40 and BO41 (Sorin *et al.*, 2009) have been described before.

Gene	Primer name	Sequence (5’ – 3’)
ChEF1α	CTO9	GGCCGATTGTGCTGTCCTTA
	CTO10	TCACGGGTCTGACCATCCTTA
ChHFR1	CTO13	CGGCGTCGTGTCCAGATC
	CTO14	TGAACCTTTTCGCGTCAGTG
ChPIL1	CTO17	GAAGACCCCAAAACAACGGTT
	CTO18	CCCTCATCGTACTCGGTCTCA
ChYUC8	CTO51	TTACGCCGGGAAAAAAGTTCT
	CTO52	GCGAAATGGTTGGCTAGGTC
ChXTR7	CTO69	TGGTGTTCCTTTCCCAAAAAA
	CTO70	CCACCTCTCGTAGCCCAATC
EF1α	SPO102	ATGATTACTGGTACCTCCCAGGC
	SPO103	CTCACGGGTCTGACCATCCT
HFR1	SPO88	GTTGTCCCTGATGAACATTCTG
	SPO89	GGTTCTCATGTTTGTTTCTCA

Table S2. Primers used for cloning and genotyping. Primer RO25 (Roig-Villanova *et al.*, 2007) has been described before.

Gene	Primer name	Sequence (5’ – 3’)
ChHFR1 WT	SPO104	CTGTTGAAGACTGCAGATTTG
	SPO107	CCTAAGGCAAGATTCTTTGAA
chfr1-1	SPO105	CTGTTGAAGACTGCAGATTA
chfr1-2	SPO106	CTGTTGAAGACTGCAGATTTT
attB1	MJO27	GGGGACAAGTTTGTACAAAAAAGCAGGCT
attB2	MJO28	GGGGACCACTTTGTACAAGAAAGCTGGGT
pAtHFR1	SPO26	GCTCTAGAGTAAAGATAACGTTCT
	SPO27	GCTCTAGAGTTAGTTAAAGAGATA
pChHFR1	SPO35-b	GGTCTAGAAAGGAGAAGAATAAGAAGGTATTTTAG
	SPO36-b	GGTCTAGAAAGTTTATGATATATGGATGCG
	SPO48	GAGATTTCTGGATAACAACAAC
	SPO49	ACAGACGCTTAAGAAATCTTAG
	SPO51	CTTAATCATCGATCAACCATC
ChHFR1	SPO28	CCATGGGTTTTCCATTTTCTCG
	SPO29	GGCTCGAGGAGTCTTCCCATCGCA

ChHFR1	CTO29	ATGATCATCATCAAATTGTTC
AtHFR1	SPO30	GGCTCGAGTAGTCTTCTCATCGCA
3xHA	SPO31	CCGTCGACGGTGGAGGCGGTTCAG
	SPO32	GGCTCGAGTCAAGCGTAATCTGGA
RNAi-ChHFR1	CTO35	CAAACACATAATGATCATCATC
	CTO36	ATCACTCCAGATCTGGACACGA
AtPIF7	JO414	TAACACATGTCGAATTATGGAG
	JO415	GGCTCGAGATCTCTTTTCTCATGATTC
AtPIF7 + attB1	BAO4	GGGGACAAGTTTGTACAAAAAAGCAGGCTACATGTCGAATTATGGAGTTAAAG
AtPIF7 + attB2	BAO5	GGGGACCACTTTGTACAAGAAAGCTGGGTGTCAAGCGTAATCTGGAACGTC

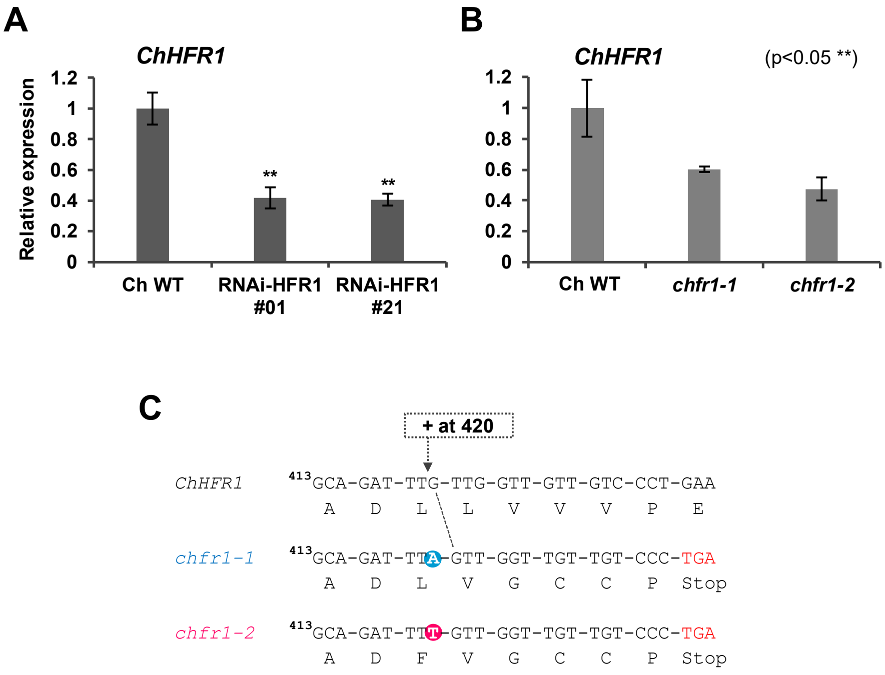

Figure S1. Molecular characterization of RNAi-HFR1 and chfr1 mutants in C. hirsuta. Relative expression levels of ChHFR1 gene, normalized to EF1α in Ch WT, (A) two RNAi-HFR1 lines (#01 and #21) and (B) the two chfr1 mutants of C. hirsuta. Seedlings were grown for 7 days in W. Expression values are the mean ± SE of three independent biological replicates relative to wild type (Ch WT). (C) The two identified chfr1-1 and chfr1-2 mutants have an insertion of one nucleotide at the position 420 of the ChHFR1 ORF (from the start codon ATG), which leads to a frame shift and a premature stop codon.

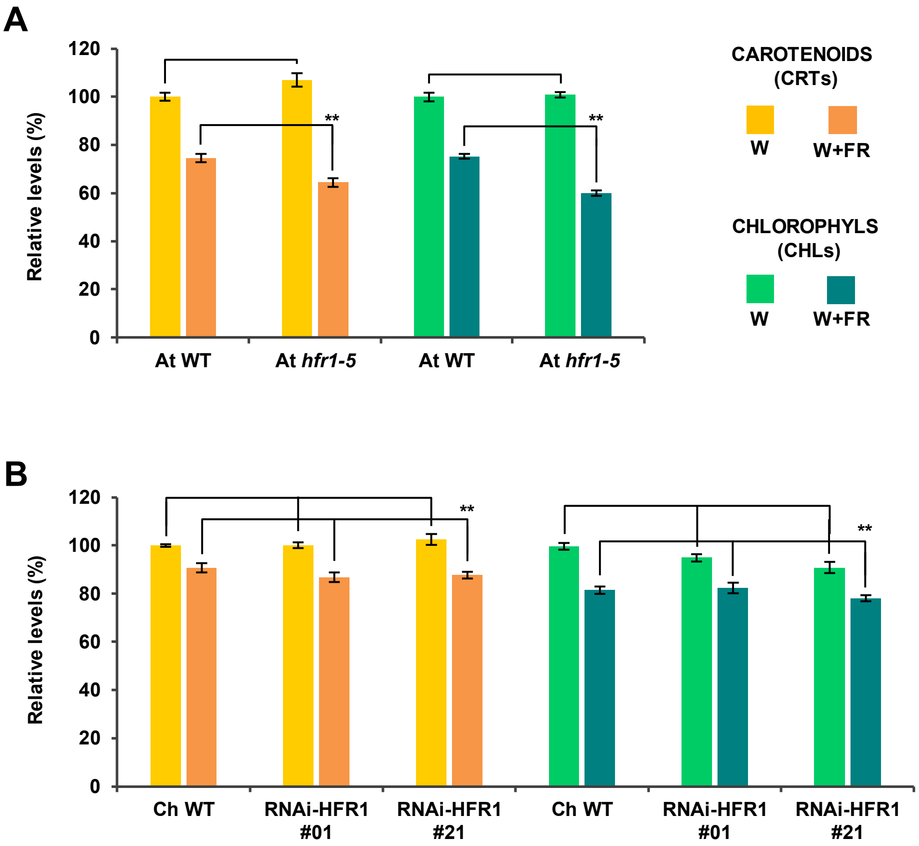

Figure S2. Carotenoid and chlorophyll levels in C. hirsuta RNAi-HFR1 and A. thaliana hfr1 mutant lines. Relative carotenoid and chlorophyll levels in (A) A. thaliana wild type Col-0 (At WT) and hfr1-5 mutant (At hfr1-5) seedlings and (B) C. hirsuta wild type Ox (Ch WT) and RNAi-HFR1 seedlings grown under W or W+FR. Seedlings were grown as indicated in Figure 1A, B. Total chlorophylls and carotenoids were extracted and analyzed by HPLC and expressed as a percentage of the levels quantified in At WT (A) or Ch WT (B) grown in W, respectively. Pigment levels are the mean ± SE of five independent biological replicates. Asterisks mark significant differences (Student t-test: ** p-value <0.01; * p-value <0.05) relative to At WT or Ch WT value at 7d W, respectively.

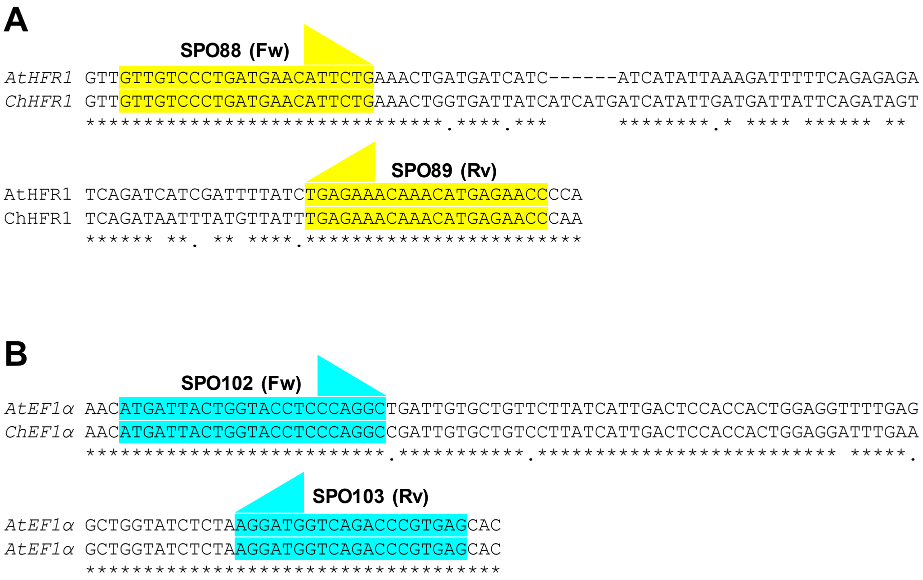

```
AtHFR1 GTTGTTGTCCCTGATGAACATTCTGAAACTGATGATCATC------ATCATATTAAAGATTTTTCAGAGAGA
ChHFR1 GTTGTTGTCCCTGATGAACATTCTGAAACTGGTGATTATCATCATGATCATATTGATGATTATTCAGATAGT
       *******************************.****.***      ********.* **** ****** **

AtHFR1 TCAGATCATCGATTTTATCTGAGAAACAAACATGAGAACCCCA
ChHFR1 TCAGATAATTTATGTTATTTGAGAAACAAACATGAGAACCCAA
       ****** **. ** ****.************************
```

```
AtEF1α AACATGATTACTGGTACCTCCCAGGCTGATTGTGCTGTTCTTATCATTGACTCCACCACTGGAGGTTTTGAG
ChEF1α AACATGATTACTGGTACCTCCCAGGCCGATTGTGCTGTCCTTATCATTGACTCCACCACTGGAGGATTTGAA
       **************************.***********.************************* *****.

AtEF1α GCTGGTATCTCTAAGGATGGTCAGACCCGTGAGCAC
AtEF1α GCTGGTATCTCTAAGGATGGTCAGACCCGTGAGCAC
       ************************************
```

Figure S3. Alignments of (A) HFR1 and (B) EF1α partial DNA sequences in A. thaliana and C. hirsuta. Location of shared primers and amplicons used for comparison of expression levels by RT-qPCR between species is shown.

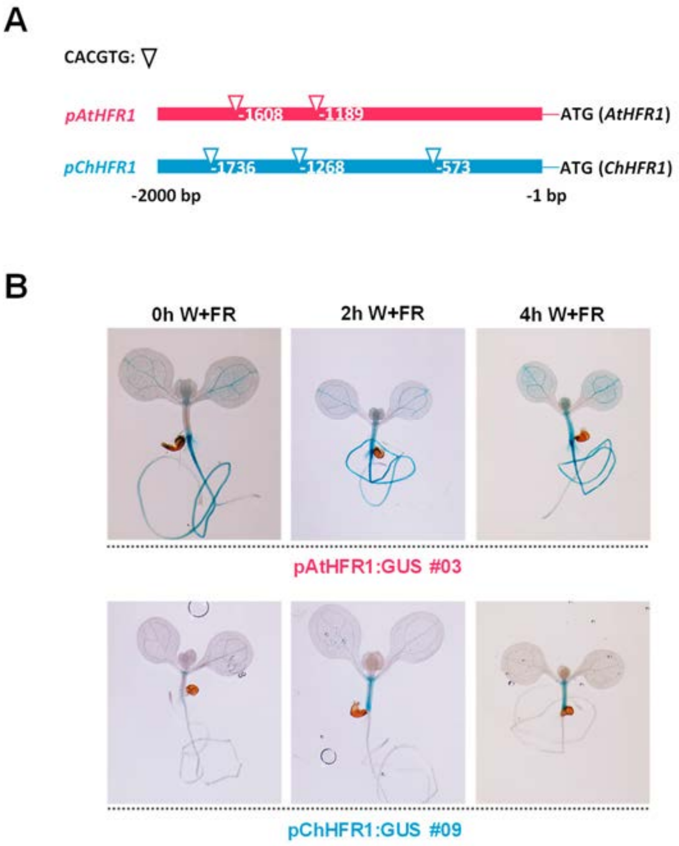
A
CACGTG: ▽
pAtHFR1
-1608
-1189
ATG (AtHFR1)
pChHFR1
-1736
-1268
-573
ATG (ChHFR1)
-2000 bp
-1 bp
B
0h W+FR
2h W+FR
4h W+FR
pAtHFR1:GUS #03
pChHFR1:GUS #09

Figure S4. ChHFR1 promoter has lower biological activity than AtHFR1 promoter in A. thaliana. (A) Cartoon of HFR1 promoters from A. thaliana (pAtHFR1) and C. hirsuta (pChHFR1). These promoters cover 2000 bp from the beginning of the ORF of the two HFR1 genes. G-boxes (CACGTG) are represented with arrows and their positions are indicated. **(B)** GUS staining of representative A. thaliana seedlings expressing GUS under the pAtHFR1 (line #03) or pChHFR1 (line #09). Seven-day-old W-grown seedlings were treated with W+FR for the indicated amount of time.

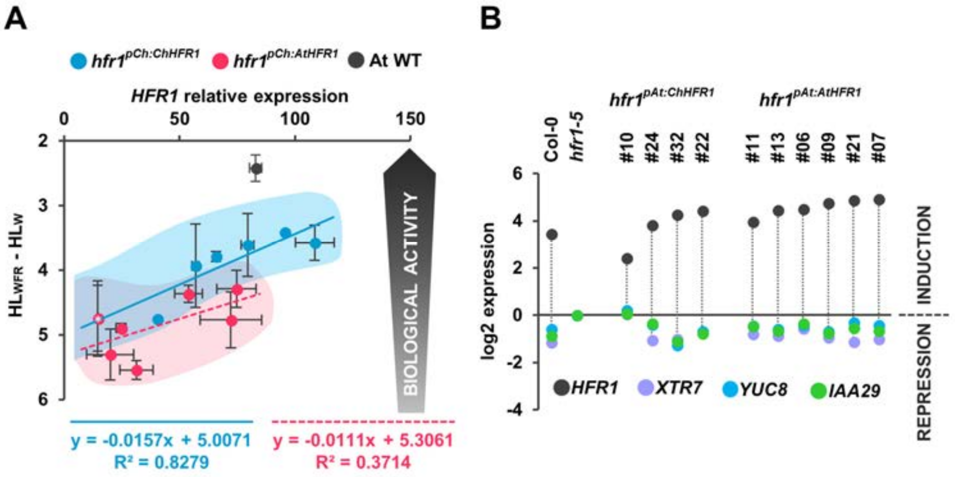

Figure S5. Scatter plot analysis of ChHFR1 and AthHFR1 biological activities. **(A)** Seedlings of hfr1$^{pCh:AtHFR1}$ and hfr1$^{pCh:ChHFR1}$ were grown as indicated in Figure 3. The mean hypocotyl length under W (HL$_{W}$) and W+FR (HL$_{W+FR}$) for these specific lines was used to calculate HL$_{W+FR}$-HL$_{W}$, that was plotted against their corresponding HFR1 relative expression in seedlings grown under W+FR. Data corresponding to untransformed hfr1-5 seedlings are indicated with asterisks. Relative expression of ChHFR1 and AtHFR1 genes, normalized to UBQ10, was analyzed in seedlings grown for 2 days in W then transferred for 5 days to W+FR (R:FR=0.02). The regression equations and R^{2} values are shown at the lower part of the graph. **(B)** Log2 expression levels of HFR1, XTR7, YUC8 and IAA29 genes, normalized to UBQ10 in hfr1$^{pAt:AtHFR1}$ and hfr1$^{pAt:ChHFR1}$ lines. Seedlings were grown as in Figure 3. Expression values are the mean ± SE of three independent biological replicates relative to A. thaliana hfr1-5 (which is represented as 0 value).

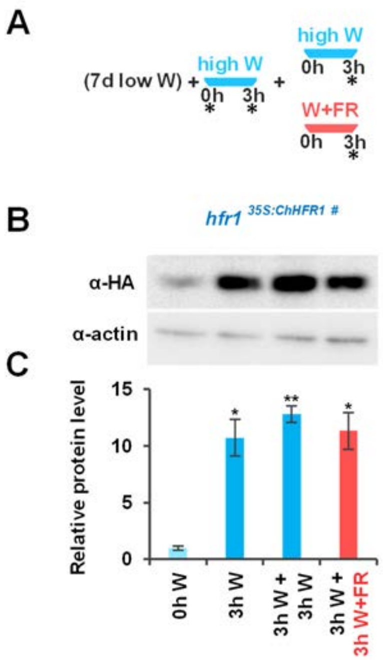

Figure S6. ChHFR1 protein levels accumulate in high W. **(A)** Cartoon representing the light treatments given to seedlings to estimate relative HFR1-3xHA levels. Seedlings grown for 7 d in low W (~20 µmol m^{-2} s^{-1}, R:FR≈6.4) were first moved to high W (~100 µmol m^{-2} s^{-1}, R:FR≈3.9) for 3h and then either transferred to high W (control) or high W+FR (R:FR≈0.06) for 3h. Samples from hfr1$^{35S:ChHFR1}$ seedlings (line #16) were collected at the time points indicated with asterisks. **(B)** Representative immunoblot of ChHFR1-3xHA protein of hfr1$^{35S:ChHFR1}$ seedlings grown as indicated in **A**. **(C)** Relative HFR1-3xHA protein levels of hfr1$^{35S:ChHFR1}$ seedlings grown as indicated in **A**. Relative protein levels are the mean ± SE of three independent biological replicates relative to the data point of 0h in high W (0h W). Asterisks mark significant differences in protein levels (Student t-test: ** p-value <0.01; * p-value <0.05) relative to the 0h W value.

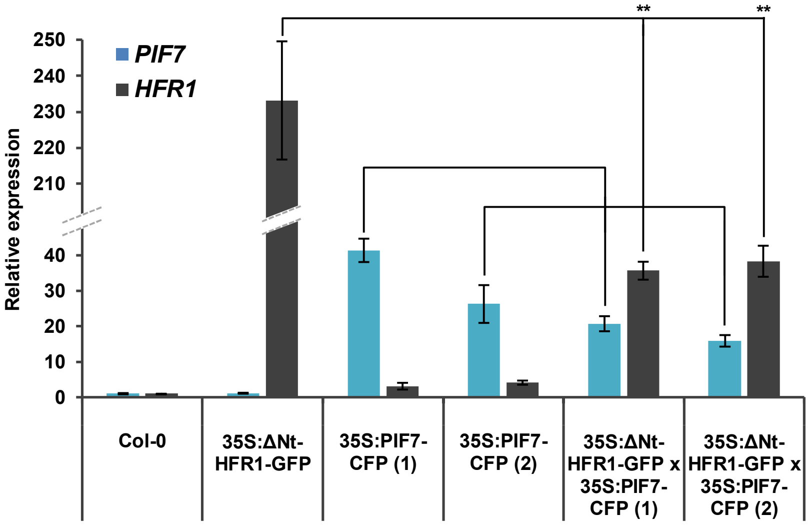

Figure S7. Relative expression levels of AtHFR1 and AtPIF7 genes in transgenic lines overexpressing ΔNt-HFR1-GFP and/or PIF7-CFP. Relative expression, normalized to UBQ10, was estimated in seedlings grown for 7 days in W. Expression values are the mean ± SE of three independent biological replicates relative to A. thaliana wild type (Col-0). Black asterisks mark significant differences (Student t-test: ** p-value <0.01; * p-value <0.05) relative to 35S:ΔNt-HFR1-GFP value.

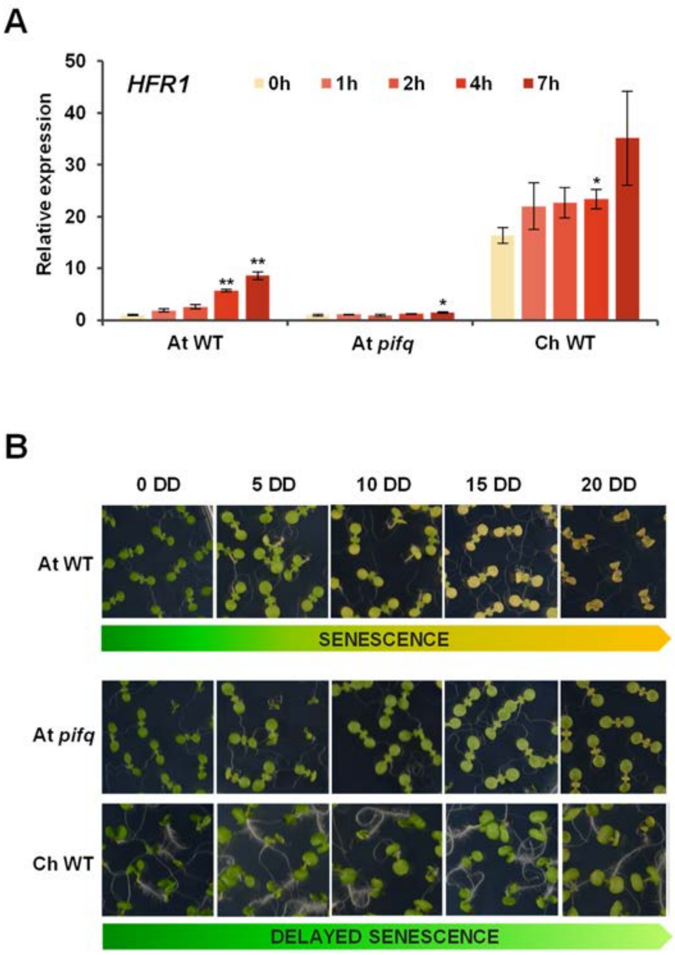

Figure S8. Comparison of PIF-modulated responses in A. thaliana and C. hirsuta seedlings. (A) Effect of warm temperature on HFR1 expression in seedlings of A. thaliana wild-type Col-0 (At WT) and pifq mutant (At pifq), and in C. hirsuta wild-type Ox (Ch WT). Expression levels of HFR1 gene were normalized to EF1α. Seedlings were grown for 7 days in W at 22ºC and then they were transferred to 28ºC for the indicated amount of time (0-7 h). Expression values are the mean ± SE of three independent biological replicates relative to At WT at 0h. Asterisks mark significant differences (Student t-test: ** p-value <0.01; * p-value <0.05) relative to 0h value for each genotype. **(B)** Aspect of At WT, At pifq and Ch WT seedlings grown for 7 days in W and then transferred to darkness for the indicated amount of time (0-20 days) to induce DIS. DD, days in the dark.

7. References

Bou-Torrent J, Toledo-Ortiz GG, Ortiz-Alcaide M, Cifuentes-Esquivel N, Halliday KJ, Martinez-García JF, Rodríguez-Concepción M. 2015. Regulation of carotenoid biosynthesis by shade relies on specific subsets of antagonistic transcription factors and co-factors. Plant Physiol. 168:00552.2015. doi:10.1104/pp.15.00552.

Casal JJ, Candia AN, Sellaro R. 2014. Light perception and signalling by phytochrome A. J Exp Bot. 65:2835–2845. doi:10.1093/jxb/ert379.

Chini A, Fonseca S, Chico JM, Fernández-Calvo P, Solano R. 2009. The ZIM domain mediates homo- and heteromeric interactions between Arabidopsis JAZ proteins. Plant J. 59:77–87. doi:10.1111/j.1365-313X.2009.03852.x.

Ciolfi A, Sessa G, Sassi M, Possenti M, Salvucci S, Carabelli M, Morelli G, Ruberti I. 2013. Dynamics of the shade-avoidance response in Arabidopsis. Plant Physiol. 163:331–53. doi:10.1104/pp.113.221549.

Cole B, Kay SA, Chory J. 2011. Automated analysis of hypocotyl growth dynamics during shade avoidance in Arabidopsis. Plant J. 65:991–1000. doi:10.1111/j.1365-313X.2010.04476.x.

Duek PD, Elmer M V., Van Oosten VR, Fankhauser C. 2004. The Degradation of HFR1, a Putative bHLH Class Transcription Factor Involved in Light Signaling, Is Regulated by Phosphorylation and Requires COP1. Curr Biol. 14:2296–2301. doi:10.1016/j.cub.2004.12.026.

Fairchild CD, Schumaker MA, Quail PH. 2000. HFR1 encodes an atypical bHLH protein that acts in phytochrome A signal transduction. Genes Dev. 14:2377–2391. doi:10.1101/gad.828000.

Fauser F, Schiml S, Puchta H. 2014. Both CRISPR/Cas-based nucleases and nickases can be used efficiently for genome engineering in Arabidopsis thaliana. Plant J. doi:10.1111/tpj.12554.

Foreman J, Johansson H, Hornitschek P, Josse E-M, Fankhauser C, Halliday KJ. 2011. Light receptor action is critical for maintaining plant biomass at warm ambient temperatures. Plant J. 65:441–52. doi:10.1111/j.1365-313X.2010.04434.x.

Franklin KA, Lee SH, Patel D, Kumar SV, Spartz AK, Gu C, Ye S, Yu P, Breen G, Cohen JD, et al. 2011. Phytochrome-interacting factor 4 (PIF4) regulates auxin biosynthesis at high temperature. Proc Natl Acad Sci U S A. 108:20231–5. doi:10.1073/pnas.1110682108.

Gallemí M, Galstyan A, Paulišić S, Then C, Ferrández-Ayela A, Lorenzo-Orts L, Roig-Villanova I, Wang X, Micol JL, Ponce MR, et al. 2016. DRACULA2 is a dynamic nucleoporin with a role in regulating the shade avoidance syndrome in Arabidopsis. Development. 143:1623–1631. doi:10.1242/dev.130211.

Gallemí M, Molina-Contreras MJ, Paulišić S, Salla-Martret M, Sorin C, Godoy M, Franco-Zorrilla JM, Solano R, Martínez-García JF. 2017. A non-DNA-binding activity for the ATHB4 transcription factor in the control of vegetation proximity. New Phytol. doi:10.1111/nph.14727.

Galstyan A, Cifuentes-Esquivel N, Bou-Torrent J, Martinez-Garcia JF. 2011. The shade avoidance syndrome in Arabidopsis: A fundamental role for atypical basic helix-loop-helix proteins as transcriptional cofactors. Plant J. 66:258–267. doi:10.1111/j.1365-313X.2011.04485.x.

Gommers CMM, Keuskamp DH, Buti S, van Veen H, Koevoets IT, Reinen E, Voesenek LACJ, Pierik R. 2017. Molecular Profiles of Contrasting Shade Response Strategies in Wild Plants: Differential Control of Immunity and Shoot Elongation. Plant Cell. 29:331–344. doi:10.1105/tpc.16.00790.

Gommers CMM, Visser EJW, Onge KRS, Voesenek LACJ, Pierik R. 2013. Shade tolerance: When growing tall is not an option. Trends Plant Sci. 18:65–71. doi:10.1016/j.tplants.2012.09.008.

Hay AS, Pieper B, Cooke E, Mandáková T, Cartolano M, Tattersall AD, Ioio RD, McGowan SJ, Barkoulas M, Galinha C, et al. 2014. Cardamine hirsuta: A versatile genetic system for comparative studies. Plant J. 78:1–15. doi:10.1111/tpj.12447.

Hayes S, Sharma A, Fraser DP, Trevisan M, Cragg-Barber CK, Tavridou E, Fankhauser C, Jenkins GI, Franklin KA. 2017. UV-B Perceived by the UVR8 Photoreceptor Inhibits Plant Thermomorphogenesis. Curr Biol. 27:120–127. doi:10.1016/j.cub.2016.11.004.

Hersch M, Lorrain S, de Wit M, Trevisan M, Ljung K, Bergmann S, Fankhauser C. 2014. Light intensity modulates the regulatory network of the shade avoidance response in Arabidopsis. Proc Natl Acad Sci U S A. 111:2–7. doi:10.1073/pnas.1320355111.

Hornitschek P, Kohnen M V., Lorrain S, Rougemont J, Ljung K, López-Vidriero I, Franco-Zorrilla JM, Solano R, Trevisan M, Pradervand S, et al. 2012. Phytochrome interacting factors 4 and 5 control seedling growth in changing light conditions by directly controlling auxin signaling. Plant J. 71:699–711. doi:10.1111/j.1365-313X.2012.05033.x.

Hornitschek P, Lorrain S, Zoete V, Michielin O, Fankhauser C. 2009. Inhibition of the shade avoidance response by formation of non-DNA binding bHLH heterodimers. EMBO J. 28:3893–3902. doi:10.1038/emboj.2009.306.

Jang IC, Henriques R, Chua NH. 2013. Three transcription factors, HFR1, LAF1 and HY5, regulate largely independent signaling pathways downstream of phytochrome a.

Plant Cell Physiol. 54:907–916. doi:10.1093/pcp/pct042.

Jang IC, Yang JY, Seo HS, Chua NH. 2005. HFR1 is targeted by COP1 E3 ligase for post-translational proteolysis during phytochrome A signaling. Genes Dev. 19:593–602. doi:10.1101/gad.1247205.

Karimi M, Depicker A, Hilson P. 2007. Recombinational cloning with plant gateway vectors. Plant Physiol. 145:1144–54. doi:10.1104/pp.107.106989.

Kircher S, Kozma-Bognar L, Kim L, Adam E, Harter K, Schafer E, Nagy F. 1999. Light quality-dependent nuclear import of the plant photoreceptors phytochrome A and B. Plant Cell. 11:1445–1456. doi:10.1105/tpc.11.8.1445.

Koini MA, Alvey L, Allen T, Tilley CA, Harberd NP, Whitelam GC, Franklin KA. 2009. High Temperature-Mediated Adaptations in Plant Architecture Require the bHLH Transcription Factor PIF4. Curr Biol. 19:408–413. doi:10.1016/j.cub.2009.01.046.

Leivar P, Monte E, Al-Sady B, Carle C, Storer A, Alonso JM, Ecker JR, Quail PH. 2008. The Arabidopsis Phytochrome-Interacting Factor PIF7, Together with PIF3 and PIF4, Regulates Responses to Prolonged Red Light by Modulating phyB Levels. Plant Cell Online. 20:337–352. doi:10.1105/tpc.107.052142.

Li L, Ljung K, Breton G, Schmitz RJ, Pruneda-Paz J, Cowing-Zitron C, Cole BJ, Ivans LJ, Pedmale U V., Jung H-SHS, et al. 2012. Linking photoreceptor excitation to changes in plant architecture. Genes Dev. 26:785–790. doi:10.1101/gad.187849.112.

Lichtenthaler HK. 1987. Chlorophylls and Carotenoids: Pigments of Photosynthetic Biomembranes. Methods Enzymol. 148:350–382. doi:10.1016/0076-6879(87)48036-1.

Lichtenthaler HK, Buschmann C. 2005. Chlorophylls and Carotenoids: Measurement And Characterization by UV-VIS Spectroscopy. In: Handbook of Food Analytical Chemistry. Vol. 2–2. p. 171–178.

Liebsch D, Keech O. 2016. Dark-induced leaf senescence: new insights into a complex light-dependent regulatory pathway. New Phytol. 212:563–570. doi:10.1111/nph.14217.

Lorrain S, Allen T, Duek PD, Whitelam GC, Fankhauser C. 2008. Phytochrome-mediated inhibition of shade avoidance involves degradation of growth-promoting bHLH transcription factors. Plant J. 53:312–323. doi:10.1111/j.1365-313X.2007.03341.x.

Martínez-García JF, Gallemí M, Molina-Contreras MJ, Llorente B, Bevilaqua MRR, Quail PH. 2014. The shade avoidance syndrome in Arabidopsis: The antagonistic role of phytochrome A and B differentiates vegetation proximity and canopy shade. Huq E, editor. PLoS One. 9:e109275. doi:10.1371/journal.pone.0109275.

Molina-Contreras MJ, Then C, Paulišić S, Pastor-Andreu P, Roig-Villanova I, Jenkins H, Hallab A, Gan X, Tsiantis M, Rodriguez-Concepcion M, Martínez-García JF. 2018. Photoreceptor activity contributes to contrasting response habits to vegetation proximity in seedlings. Submitted to Nat Commun.

Morineau C, Bellec Y, Tellier F, Gissot L, Kelemen Z, Nogué F, Faure JD. 2017. Selective gene dosage by CRISPR-Cas9 genome editing in hexaploid Camelina sativa. Plant Biotechnol J. 15:729–739. doi:10.1111/pbi.12671.

Müller-Moulé P, Nozue K, Pytlak ML, Palmer CM, Covington MF, Wallace AD, Harmer SL, Maloof JN. 2016. YUCCA auxin biosynthetic genes are required for Arabidopsis shade avoidance. PeerJ. 4:e2574. doi:10.7717/peerj.2574.

Murashige T, Skoog F. 1962. A revised medium for rapid growth and bioassays with tobacco tissue cultures. Physiol Plant. 15:473–497. doi:DOI: 10.1111/j.1399-3054.1962.tb08052.x.

Nozue K, Harmer SL, Maloof JN. 2011. Genomic analysis of circadian clock-, light-, and growth-correlated genes reveals PHYTOCHROME-INTERACTING FACTOR5 as a modulator of auxin signaling in Arabidopsis. Plant Physiol. 156:357–72. doi:10.1104/pp.111.172684.

Pacín M, Semmoloni M, Legris M, Finlayson SA, Casal JJ. 2016. Convergence of CONSTITUTIVE PHOTOMORPHOGENESIS 1 and PHYTOCHROME INTERACTING FACTOR signalling during shade avoidance. New Phytol. 211:967–979. doi:10.1111/nph.13965.

Park HJ, Ding L, Dai M, Lin R, Wang H. 2008. Multisite phosphorylation of Arabidopsis HFR1 by casein kinase II and a plausible role in regulating its degradation rate. J Biol Chem. 283:23264–23273. doi:10.1074/jbc.M801720200.

Paulišić S, Molina-Contreras MJ, Roig-Villanova I, Martínez-García JF. 2017. Approaches to study light effects on brassinosteroid sensitivity.

Pierik R, Testerink C. 2014. The art of being flexible: how to escape from shade, salt, and drought. Plant Physiol. 166:5–22. doi:10.1104/pp.114.239160.

Press MO, Lanctot A, Queitsch C. 2016. PIF4 and ELF3 act independently in Arabidopsis thaliana thermoresponsive flowering. PLoS One. 11:14–16. doi:10.1371/journal.pone.0161791.

Rodríguez-Villalón A, Gas E, Rodríguez-Concepción M. 2009. Phytoene synthase activity controls the biosynthesis of carotenoids and the supply of their metabolic precursors in dark-grown Arabidopsis seedlings. Plant J. 60:424–435. doi:10.1111/j.1365-313X.2009.03966.x.

Roig-Villanova I, Bou-Torrent J, Galstyan A, Carretero-Paulet L, Portolés S, Rodríguez-Concepción M, Martínez-García JF. 2007. Interaction of shade avoidance and auxin responses: a role for two novel atypical bHLH proteins. EMBO J. 26:4756–67. doi:10.1038/sj.emboj.7601890.

Roig-Villanova I, Bou J, Sorin C, Devlin PF, Martínez-García JF. 2006. Identification of Primary Target Genes of Phytochrome Signaling. Early transcriptional control during shade avoidance responses in Arabidopsis. Plant Physiol. 141:85–96. doi:10.1104/pp.105.076331.photointerconvertible.

Sakuraba Y, Jeong J, Kang M-Y, Kim J, Paek N-C, Choi G. 2014. Phytochrome-interacting transcription factors PIF4 and PIF5 induce leaf senescence in Arabidopsis. Nat Commun. 5:4636. doi:10.1038/ncomms5636.

Sasidharan R, Chinnappa CC, Staal M, Elzenga JTM, Yokoyama R, Nishitani K, Voesenek LACJ, Pierik R. 2010. Light Quality-Mediated Petiole Elongation in Arabidopsis during Shade Avoidance Involves Cell Wall Modification by Xyloglucan Endotransglucosylase/Hydrolases. Plant Physiol. 154:978–990. doi:10.1104/pp.110.162057.

Sessa G, Carabelli M, Sassi M, Ciolfi A, Possenti M, Mittempergher F, Becker J, Morelli G, Ruberti I. 2005. A dynamic balance between gene activation and repression regulates the shade avoidance response in Arabidopsis. Genes Dev. 19:2811–5. doi:10.1101/gad.364005.

Shi H, Zhong S, Mo X, Liu N, Nezames CD, Deng XW. 2013. HFR1 Sequesters PIF1 to Govern the Transcriptional Network Underlying Light-Initiated Seed Germination in Arabidopsis. Plant Cell. 25:3770–3784. doi:10.1105/tpc.113.117424.

Smith H. 1982. Light Quality, Photoperception, and Plant Strategy. Annu Rev Plant Physiol. 33:481–518. doi:10.1146/annurev.pp.33.060182.002405.

Smith H, Whitelam GC. 1997. The shade avoidance syndrome: multiple responses mediated by multiple phytochromes. Plant, Cell Environ. 20:840–844. doi:10.1046/j.1365-3040.1997.d01-104.x.

Song Y, Yang C, Gao S, Zhang W, Li L, Kuai B. 2014. Age-Triggered and Dark-Induced Leaf Senescence Require the bHLH Transcription Factors PIF3, 4, and 5. Mol Plant. 7:1776–1787. doi:10.1093/mp/ssu109.

Sorin C, Salla-Martret M, Bou-Torrent J, Roig-Villanova I, Martínez-García JF. 2009. ATHB4, a regulator of shade avoidance, modulates hormone response in Arabidopsis seedlings. Plant J. 59:266–277. doi:10.1111/j.1365-313X.2009.03866.x.

Valladares F, Niinemets Ü. 2008. Shade tolerance, a key plant feature of complex nature and consequences. Annu Rev Ecol Evol Syst. 39:237–257. doi:10.1146/annurev.ecolsys.39.110707.173506.

Yang C, Li L. 2017. Hormonal Regulation in Shade Avoidance. Front Plant Sci. 8:1527.

doi:10.3389/fpls.2017.01527.

Yang J, Lin R, Hoecker U, Liu B, Xu L, Wang H. 2005. Repression of light signaling by Arabidopsis SPA1 involves post-translational regulation of HFR1 protein accumulation. Plant J. 43:131–141. doi:10.1111/j.1365-313X.2005.02433.x.

Yang J, Lin R, Sullivan J, Hoecker U, Liu B, Xu L, Deng XW, Wang H. 2005. Light regulates COP1-mediated degradation of HFR1, a transcription factor essential for light signaling in Arabidopsis. Plant Cell. 17:804–21. doi:10.1105/tpc.104.030205.

GENERAL DISCUSSION

General discussion

Although SAS regulation has been thoroughly analyzed and described in *A. thaliana*, new components implicated in this process are still being discovered. One of them is DRA2, which we investigated. NPC and particular NUPs, such as DRA2, seem to function as important components of various cellular processes, including shade signalling. It is not surprising that the NPC would be implicated in shade signalling, because of its crucial role in transport of important molecules such as protein and RNA between the cytoplasm and the nucleus. Besides the importance of NPC for the nuclear import of newly synthesised nuclear proteins, many light signalling components are also transported in a light-dependent manner between these two compartments, such as the phyA and phyB photoreceptors (Kircher *et al.*, 1999; Chen, Schwab and Chory, 2003; Hiltbrunner *et al.*, 2005; Genoud *et al.*, 2008). The impairment in phytochrome import or export when the balance of Pr and Pfr forms changes because of the specific light conditions, would clearly have direct implications on its downstream regulatory network, such as the ability to interact with the PIF signalling hub. Other proteins were shown to be regulated in this manner as well, including COP1, an essential part of E3 ubiquitin ligase that regulates protein degradation inside the nucleus, which is slowly exported from the nucleus in the light (Lu *et al.*, 2015) and whose nuclear abundance is also shade promoted (Pacín *et al.*, 2016). Moreover, auxin signalling and mRNA export, also shown to be altered by the impaired NPC in general (Parry, 2014), could have direct consequences on SAS responses. Altogether, our results could fit well with the gene gating hypothesis and in addition, bring two new concepts to shade signalling: NPC transport-dependent and –independent regulation. We suggest that NPC or some specific dynamic NUPs, such as DRA2, would regulate gene expression on a transport-independent manner, in combination with transcription factors, chromatin modifiers and/or components of the basic transcriptional machinery. This does not exclude the possibility of direct NPC-bound regulation of gene expression. Finally, NPC could also control and facilitate mRNA export (gating) outside of the nucleus on a transport-dependent manner and indirectly affect protein biosynthesis.

The knowledge of components and mechanisms regulating *A. thaliana* response to vegetation proximity, including the NPC and DRA2 mediated regulation of this response, is also crucial to better understand the alternative responses to vegetation proximity of other plants. Indeed, comparative genetic analyses between *C. hirsuta* and *A. thaliana* showed that orthologous shade-signalling components from these two related species can have a differential function in their native context to modulate divergent responses. The differential regulation and functional modification of genetically related components as a mechanism to achieve an opposite response to shade, demonstrates the extent of evolutionary plasticity in plants. HFR1 and phyA are two of the so far known components that functionally contribute to completely suppress the shade-induced hypocotyl elongation response in *C. hirsuta*, in contrast to *A. thaliana*. It seems reasonable to assume that this is not only a consequence of higher biological activity of HFR1, but most likely a part of several evolutionary adaptive modifications of the shade signalling pathway. To fully understand the basis of the differential activity of orthologous components, as well as having a better map of the involved regulators will be key to translate this knowledge to crops.

Altogether, DRA2 and HFR1 both affect shade-induced *PAR* gene expression, and while we assume that in *C. hirsuta* this is a consequence of HFR1 inhibition of PIFs, as described in *A. thaliana* (Hornitschek *et al.*, 2009; Leivar and Monte, 2014; Xu *et al.*, 2017), the connection of DRA2 with PIF-regulated *PAR* genes is not clear and remains to be answered. In addition, it would be interesting to explore the mutual connection of HFR1 and phyA in *C. hirsuta* and broaden the view on shade tolerance mechanism in this species, including studying if shade tolerance trait is maintained in all developmental stages.

CONCLUSIONS

Conclusions

1. RNAi-DRA2 plants confirmed that the nucleoporin-encoding *DRA2* has a regulatory role in shade signalling.
2. *dra2-1* and other NUP-deficient mutants share pleiotropic phenotypes as the result of a general perturbation of transport-dependent activities of the NPC.
3. DRA2 behaves as a mobile dynamic nucleoporin, since it is located in the cytoplasm, nucleoplasm and NPC; moreover, its Ct-region is responsible for nuclear localization.
4. DRA2 regulates shade-induced expression of specific *PAR* genes (*HFR1*, *PIL1* and *IAA19*), possibly in a transport-independent way, without direct association with their genomic regulatory regions.

5. The hypocotyl phenotype of RNAi-HFR1 lines and *chfr1* mutants indicate that HFR1 in *C. hirsuta* (ChHFR1) has a role in maintaining hypocotyls unresponsive to shade.
6. ChHFR1 has higher biological activity than AtHFR1 as a result of its specifically higher stability in shade.
7. Higher expression levels of *ChHFR1* compared to *AtHFR1* in their native species, together with higher protein stability, probably contribute to hypocotyl shade tolerance of *C. hirsuta*.
8. Comparative genetic analyses of *A. thaliana* and *C. hirsuta* suggest that differential activity of related orthologous components can result in divergent shade responses.

GENERAL REFERENCES

General references

Ahmad M, Lin C, Cashmore AR. 1995. Mutations throughout an Arabidopsis blue-light photoreceptor impair blue-light-responsive anthocyanin accumulation and inhibition of hypocotyl elongation. Plant J. 8:653–8.

Bae G, Choi G. 2008. Decoding of light signals by plant phytochromes and their interacting proteins. Annu Rev Plant Biol. 59:281–311. doi:10.1146/annurev.arplant.59.032607.092859.

Ballaré CL. 1999. Keeping up with the neighbours: phytochrome sensing and other signalling mechanisms. Trends Plant Sci. 4:201. doi:10.1016/S1360-1385(99)01408-9.

Ballare CL, Sanchez RA, Scopel AL, Casal JJ, Ghersa CM. 1987. Early detection of neighbour plants by phytochrome perception of spectral changes in reflected sunlight. Plant, Cell Environ. 10:551–557. doi:10.1111/1365-3040.ep11604091.

Barkoulas M, Hay A, Kougioumoutzi E, Tsiantis M. 2008. A developmental framework for dissected leaf formation in the Arabidopsis relative Cardamine hirsuta. Nat Genet. 40:1136–1141. doi:10.1038/ng.189.

Beilstein MA, Al-Shehbaz IA, Mathews S, Kellogg EA. 2008. Brassicaceae phylogeny inferred from phytochrome A and ndhF sequence data: tribes and trichomes revisited. Am J Bot. 95:1307–1327. doi:10.3732/ajb.0800065.

Blein T, Pulido A, Vialette-Guiraud A, Nikovics K, Morin H, Hay A, Johansen IE, Tsiantis M, Laufs P. 2008. A Conserved Molecular Framework for Compound Leaf Development . Science (80-). 322:1835–1839. doi:10.1126/science.1166168.

Boeglin M, Fuglsang AT, Luu D-T, Sentenac H, Gaillard I, Chérel I. 2016. Reduced expression of AtNUP62 nucleoporin gene affects auxin response in Arabidopsis. BMC Plant Biol. 16:2. doi:10.1186/s12870-015-0695-y.

Bonan GB, Shugart HH. 1989. Environmental Factors and Ecological Processes in Boreal Forests. Annu Rev Ecol Syst. 20:1–28. doi:10.1146/annurev.es.20.110189.000245.

Bonser SP, Geber MA. 2005. Growth form evolution and shifting habitat specialization in annual plants. J Evol Biol. 18:1009–1018. doi:10.1111/j.1420-9101.2005.00904.x.

Botto JF, Smith H. 2002. Differential genetic variation in adaptive strategies to a common environmental signal in Arabidopsis accessions: phytochrome-mediated shade avoidance. Plant Cell Environ. 25:53–63. doi:10.1046/j.0016-8025.2001.00812.x.

Bou-Torrent J, Galstyan A, Gallemí M, Cifuentes-Esquivel N, Molina-Contreras MJ, Salla-Martret M, Jikumaru Y, Yamaguchi S, Kamiya Y, Martínez-García JF. 2014. Plant proximity perception dynamically modulates hormone levels and sensitivity in Arabidopsis. J Exp Bot. 65:2937–2947. doi:10.1093/jxb/eru083.

Bou-Torrent J, Roig-Villanova I, Galstyan A, Martínez-García JF. 2008. PAR1 and PAR2 integrate shade and hormone transcriptional networks. Plant Signal Behav. 3:453–454. doi:10.4161/psb.3.7.5599.

Brickner DG, Ahmed S, Meldi L, Thompson A, Light W, Young M, Hickman TL, Chu F, Fabre E, Brickner JH. 2012. Transcription Factor Binding to a DNA Zip Code Controls Interchromosomal Clustering at the Nuclear Periphery. Dev Cell. 22:1234–1246. doi:10.1016/j.devcel.2012.03.012.

Brickner JH, Walter P. 2004. Gene recruitment of the activated INO1 locus to the nuclear membrane. PLoS Biol. 2. doi:10.1371/journal.pbio.0020342.

Brohawn SG, Partridge JR, Whittle JRR, Schwartz TU. 2009. The Nuclear Pore Complex Has Entered the Atomic Age. Structure. 17:1156–1168. doi:10.1016/j.str.2009.07.014.

Burgie ES, Vierstra RD. 2014. Phytochromes: An Atomic Perspective on Photoactivation and Signaling. Plant Cell Online. 26:4568–4583. doi:10.1105/tpc.114.131623.

Van Buskirk EK, Decker P V., Chen M. 2012. Photobodies in Light Signaling. Plant Physiol. 158:52–60. doi:10.1104/pp.111.186411.

Casal JJ. 2013. Photoreceptor Signaling Networks in Plant Responses to Shade. Annu Rev Plant Biol. 64:403–427. doi:10.1146/annurev-arplant-050312-120221.

Casolari JM, Brown CR, Komili S, West J, Hieronymus H, Silver PA. 2004. Genome-wide localization of the nuclear transport machinery couples transcriptional status and nuclear organization. Cell. 117:427–439. doi:10.1016/S0092-8674(04)00448-9.

Chen E, Swartz TE, Bogomolni RA, Kliger DS. 2007. A LOV story: The signaling state of the phot1 LOV2 photocycle involves chromophore-triggered protein structure relaxation, as probed by far-UV time-resolved optical rotatory dispersion spectroscopy. Biochemistry. 46:4619–4624. doi:10.1021/bi602544n.

Chen M, Chory J. 2011. Phytochrome signaling mechanisms and the control of plant development. Trends Cell Biol. 21:664–671. doi:10.1016/j.tcb.2011.07.002.

Chen M, Chory J, Fankhauser C. 2004. Light signal transduction in higher plants. Annu Rev Genet. 38:87–117. doi:10.1146/annurev.genet.38.072902.092259.

Chen M, Schwab R, Chory J. 2003. Characterization of the requirements for localization of phytochrome B to nuclear bodies. Proc Natl Acad Sci U S A.

100:14493–14498. doi:10.1073/pnas.1935989100.

Cheng C-Y, Krishnakumar V, Chan A, Schobel S, Town CD. 2016 Apr 5. Araport11: a complete reannotation of the Arabidopsis thaliana reference genome. bioRxiv.:047308. doi:10.1101/047308.

Christie JM, Blackwood L, Petersen J, Sullivan S. 2015. Plant flavoprotein photoreceptors. Plant Cell Physiol. 56:401–413. doi:10.1093/pcp/pcu196.

Christie JM, Reymond P, Powell GK, Bernasconi P, Raibekas AA, Liscum E, Briggs WR. 1998. Arabidopsis NPH1: a flavoprotein with the properties of a photoreceptor for phototropism. Science. 282:1698–701.

Cifuentes-Esquivel N, Bou-Torrent J, Galstyan A, Gallemí M, Sessa G, Salla Martret M, Roig-Villanova I, Ruberti I, Martínez-García JF. 2013. The bHLH proteins BEE and BIM positively modulate the shade avoidance syndrome in Arabidopsis seedlings. Plant J. 75:989–1002. doi:10.1111/tpj.12264.

Couvreur TLP, Franzke A, Al-Shehbaz IA, Bakker FT, Koch MA, Mummenhoff K. 2010. Molecular phylogenetics, temporal diversification, and principles of evolution in the mustard family (Brassicaceae). Mol Biol Evol. 27:55–71. doi:10.1093/molbev/msp202.

Cronshaw JM, Krutchinsky AN, Zhang W, Chait BT, Matunis MJ. 2002. Proteomic analysis of the mammalian nuclear pore complex. J Cell Biol. 158:915–927. doi:10.1083/jcb.200206106.

Demarsy E, Fankhauser C. 2009. Higher plants use LOV to perceive blue light. Curr Opin Plant Biol. 12:69–74. doi:10.1016/j.pbi.2008.09.002.

Devlin PF, Patel SR, Whitelam GC. 1998. Phytochrome E influences internode elongation and flowering time in Arabidopsis. Plant Cell. 10:1479–87.

Devlin PF, Robson PR, Patel SR, Goosey L, Sharrock RA, Whitelam GC. 1999. Phytochrome D acts in the shade-avoidance syndrome in Arabidopsis by controlling elongation growth and flowering time. Plant Physiol. 119:909–15.

Devlin PF, Yanovsky MJ, Kay SA. 2003. A genomic analysis of the shade avoidance response in Arabidopsis. Plant Physiol. 133:1617–29. doi:10.1104/pp.103.034397.

Djakovic-Petrovic T, Wit M De, Voesenek LACJCJ, Pierik R. 2007. DELLA protein function in growth responses to canopy signals. Plant J. 51:117–126. doi:10.1111/j.1365-313X.2007.03122.x.

Dong C-H, Hu X, Tang W, Zheng X, Kim YS, Lee B -h., Zhu J-K. 2006. A Putative Arabidopsis Nucleoporin, AtNUP160, Is Critical for RNA Export and Required for Plant Tolerance to Cold Stress. Mol Cell Biol. 26:9533–9543. doi:10.1128/MCB.01063-06.

Eichenberg K, Bäurle I, Paulo N, Sharrock RA, Rüdiger W, Schäfer E. 2000. Arabidopsis phytochromes C and E have different spectral characteristics from those of phytochromes A and B. FEBS Lett. 470:107–12.

Fairchild CD, Schumaker MA, Quail PH. 2000. HFR1 encodes an atypical bHLH protein that acts in phytochrome A signal transduction. Genes Dev. 14:2377–2391. doi:10.1101/gad.828000.

Favory JJ, Stec A, Gruber H, Rizzini L, Oravecz A, Funk M, Albert A, Cloix C, Jenkins GI, Oakeley EJ, et al. 2009. Interaction of COP1 and UVR8 regulates UV-B-induced photomorphogenesis and stress acclimation in Arabidopsis. EMBO J. 28:591–601. doi:10.1038/emboj.2009.4.

Fehér B, Kozma-Bognár L, Kevei É, Hajdu A, Binkert M, Davis SJ, Schäfer E, Ulm R, Nagy F. 2011. Functional interaction of the circadian clock and UV RESISTANCE LOCUS 8-controlled UV-B signaling pathways in Arabidopsis thaliana. Plant J. 67:37–48. doi:10.1111/j.1365-313X.2011.04573.x.

Feng C-M, Qiu Y, Van Buskirk EK, Yang EJ, Chen M. 2014. Light-regulated gene repositioning in Arabidopsis. Nat Commun. 5:3027. doi:10.1038/ncomms4027.

Feng S, Martinez C, Gusmaroli G, Wang Y, Zhou J, Wang F, Chen L, Yu L, Iglesias-Pedraz JM, Kircher S, et al. 2008. Coordinated regulation of Arabidopsis thaliana development by light and gibberellins. Nature. 451:475–479. doi:10.1038/nature06448.

Ferrández-Ayela A, Alonso-Peral MM, Sánchez-García AB, Micol-Ponce R, Pérez-Pérez JM, Micol JL, Ponce MR. 2013. Arabidopsis TRANSCURVATA1 Encodes NUP58, a Component of the Nucleopore Central Channel. PLoS One. 8. doi:10.1371/journal.pone.0067661.

Fierro AC, Leroux O, De Coninck B, Cammue BPA, Marchal K, Prinsen E, Van Der Straeten D, Vandenbussche F. 2015. Ultraviolet-B radiation stimulates downward leaf curling in Arabidopsis thaliana. Plant Physiol Biochem. 93:9–17. doi:10.1016/j.plaphy.2014.12.012.

Fiorucci A-S, Fankhauser C. 2017. Plant Strategies for Enhancing Access to Sunlight. Curr Biol. 27:R931–R940. doi:10.1016/j.cub.2017.05.085.

Franklin KA. 2008. Shade avoidance. New Phytol. 179:930–944. doi:10.1111/j.1469-8137.2008.02507.x.

Franklin KA, Quail PH. 2010. Phytochrome functions in Arabidopsis development. J Exp Bot. 61:11–24. doi:10.1093/jxb/erp304.

Franklin KA, Whitelam GC. 2005. Phytochromes and Shade-avoidance Responses in Plants. Ann Bot. 96:169–175. doi:10.1093/aob/mci165.

Franklin KA, Whitelam GC. 2007. Light-quality regulation of freezing tolerance in Arabidopsis thaliana. Nat Genet. 39:1410–1413. doi:10.1038/ng.2007.3.

Frey S, Görlich D. 2009. FG/FxFG as well as GLFG repeats form a selective permeability barrier with self-healing properties. EMBO J. 28:2554–2567. doi:10.1038/emboj.2009.199.

Gallemí M, Galstyan A, Paulišić S, Then C, Ferrández-Ayela A, Lorenzo-Orts L, Roig-Villanova I, Wang X, Micol JL, Ponce MR, et al. 2016. DRACULA2 is a dynamic nucleoporin with a role in regulating the shade avoidance syndrome in Arabidopsis. Development. 143:1623–1631. doi:10.1242/dev.130211.

Galstyan A, Bou-Torrent J, Roig-Villanova I, Martínez-García JF. 2012. A dual mechanism controls nuclear localization in the atypical basic-helix-loop-helix protein PAR1 of Arabidopsis thaliana. Mol Plant. 5:669–677. doi:10.1093/mp/sss006.

Galstyan A, Cifuentes-Esquivel N, Bou-Torrent J, Martinez-Garcia JF. 2011. The shade avoidance syndrome in Arabidopsis: A fundamental role for atypical basic helix-loop-helix proteins as transcriptional cofactors. Plant J. 66:258–267. doi:10.1111/j.1365-313X.2011.04485.x.

Galvão VC, Fankhauser C. 2015. Sensing the light environment in plants: Photoreceptors and early signaling steps. Curr Opin Neurobiol. 34:46–53. doi:10.1016/j.conb.2015.01.013.

Gan X, Hay A, Kwantes M, Haberer G, Hallab A, Ioio R Dello, Hofhuis H, Pieper B, Cartolano M, Neumann U, et al. 2016. The Cardamine hirsuta genome offers insight into the evolution of morphological diversity. Nat Plants. 2. doi:10.1038/nplants.2016.167.

Gangappa SN, Botto JF. 2016. The Multifaceted Roles of HY5 in Plant Growth and Development. Mol Plant. 9:1353–1365. doi:10.1016/j.molp.2016.07.002.

Gangappa SN, Holm M, Botto JF. 2013. Molecular interactions of BBX24 and BBX25 with HYH, HY5 HOMOLOG, to modulate Arabidopsis seedling development. Plant Signal Behav. 8:e25208. doi:10.4161/psb.25208.

Gasiorowski JZ, Dean DA. 2003. Mechanisms of nuclear transport and interventions. Adv Drug Deliv Rev. 55:703–716. doi:10.1016/S0169-409X(03)00048-6.

Genoud T, Schweizer F, Tscheuschler A, Debrieux D, Casal JJ, Schäfer E, Hiltbrunner A, Fankhauser C. 2008. FHY1 mediates nuclear import of the light-activated phytochrome A photoreceptor. PLoS Genet. 4. doi:10.1371/journal.pgen.1000143.

Givnish TJ. 1988. Adaptation to Sun and Shade: A Whole-plant Perspective. Aust J Plant Physiol. 15:63–92.

Gonzalez-Grandio E, Poza-Carrion C, Sorzano COS, Cubas P. 2013. BRANCHED1 Promotes Axillary Bud Dormancy in Response to Shade in Arabidopsis. Plant Cell. 25:834–850. doi:10.1105/tpc.112.108480.

Graves HS, Zon R, Graves HS. 1911. Light in relation to tree growth /. Washington, D.C. : U.S. Dept. of Agriculture, Forest Service,.

Grime PJ. 2007. Plant strategy theories: a comment on Craine (2005). J Ecol. 95:227–230. doi:10.1111/j.1365-2745.2006.01163.x.

Güttinger S, Laurell E, Kutay U. 2009. Orchestrating nuclear envelope disassembly and reassembly during mitosis. Nat Rev Mol Cell Biol. 10:178–191. doi:10.1038/nrm2641.

Halliday KJ, Koornneef M, Whitelam GC. 1994. Phytochrome B and at Least One Other Phytochrome Mediate the Accelerated Flowering Response of Arabidopsis thaliana L. to Low Red/Far-Red Ratio. Plant Physiol. 104:1311–1315.

Hao Y, Oh E, Choi G, Liang Z, Wang Z-Y. 2012. Interactions between HLH and bHLH Factors Modulate Light-Regulated Plant Development. Mol Plant. 5:688–697. doi:10.1093/mp/sss011.

Hay A, Tsiantis M. 2006. The genetic basis for differences in leaf form between Arabidopsis thaliana and its wild relative Cardamine hirsuta. Nat Genet. 38:942–947. doi:10.1038/ng1835.

Hay AS, Pieper B, Cooke E, Mandáková T, Cartolano M, Tattersall AD, Ioio RD, McGowan SJ, Barkoulas M, Galinha C, et al. 2014. Cardamine hirsuta: A versatile genetic system for comparative studies. Plant J. 78:1–15. doi:10.1111/tpj.12447.

Hayes S, Sharma A, Fraser DP, Trevisan M, Cragg-Barber CK, Tavridou E, Fankhauser C, Jenkins GI, Franklin KA. 2017. UV-B Perceived by the UVR8 Photoreceptor Inhibits Plant Thermomorphogenesis. Curr Biol. 27:120–127. doi:10.1016/j.cub.2016.11.004.

Henry HAL, Aarssen LW. 1997. On the Relationship between Shade Tolerance and Shade Avoidance Strategies in Woodland. Oikos. 80:575–582. doi:10.2307/3546632.

Hiltbrunner A, Tscheuschler A, Viczián A, Kunkel T, Kircher S, Schäfer E. 2006. FHY1 and FHL act together to mediate nuclear accumulation of the phytochrome A photoreceptor. Plant Cell Physiol. 47:1023–1034. doi:10.1093/pcp/pcj087.

Hiltbrunner A, Viczi??n A, Bury E, Tscheuschler A, Kircher S, T??th R, Honsberger A, Nagy F, Fankhauser C, Sch??fer E. 2005. Nuclear accumulation of the phytochrome A photoreceptor requires FHY1. Curr Biol. 15:2125–2130. doi:10.1016/j.cub.2005.10.042.

Hisamatsu T, King RW, Helliwell CA, Koshioka M. 2005. The Involvement of Gibberellin 20-Oxidase Genes in Phytochrome-Regulated Petiole Elongation of Arabidopsis. Plant Physiol. 138:1106–1116. doi:10.1104/pp.104.059055.

Hofhuis H, Hay A. 2017. Explosive seed dispersal. New Phytol. 216:339–342. doi:10.1111/nph.14541.

Hofhuis H, Moulton D, Lessinnes T, Routier-Kierzkowska AL, Bomphrey RJJ, Mosca G, Reinhardt H, Sarchet P, Gan X, Tsiantis M, et al. 2016. Morphomechanical Innovation Drives Explosive Seed Dispersal. Cell. doi:10.1016/j.cell.2016.05.002.

Hornitschek P, Kohnen M V., Lorrain S, Rougemont J, Ljung K, López-Vidriero I, Franco-Zorrilla JM, Solano R, Trevisan M, Pradervand S, et al. 2012. Phytochrome interacting factors 4 and 5 control seedling growth in changing light conditions by directly controlling auxin signaling. Plant J. 71:699–711. doi:10.1111/j.1365-313X.2012.05033.x.

Hornitschek P, Lorrain S, Zoete V, Michielin O, Fankhauser C. 2009. Inhibition of the shade avoidance response by formation of non-DNA binding bHLH heterodimers. EMBO J. 28:3893–3902. doi:10.1038/emboj.2009.306.

Huang X, Yang P, Ouyang X, Chen L, Deng XW. 2014. Photoactivated UVR8-COP1 Module Determines Photomorphogenic UV-B Signaling Output in Arabidopsis. PLoS Genet. 10. doi:10.1371/journal.pgen.1004218.

Hughes JE, Morgan DC, Lambton PA, Black CR, Smith H. 1984. Photoperiodic time signals during twilight. Plant, Cell Environ. 7:269–277. doi:10.1111/1365-3040.ep11589464.

Ishitani M, Xiong L, Lee H, Stevenson B, Zhu JK. 1998. HOS1, a genetic locus involved in cold-responsive gene expression in arabidopsis. Plant Cell. 10:1151–61. doi:10.1105/tpc.10.7.1151.

Ito S, Song YH, Imaizumi T. 2012. LOV domain-containing F-box proteins: Light-dependent protein degradation modules in Arabidopsis. Mol Plant. 5:573–582. doi:10.1093/mp/sss013.

Jacob Y, Mongkolsiriwatana C, Veley KM, Kim SY, Michaels SD. 2007. The Nuclear Pore Protein AtTPR Is Required for RNA Homeostasis, Flowering Time, and Auxin Signaling. PLANT Physiol. 144:1383–1390. doi:10.1104/pp.107.100735.

Jenkins G. 2014. The UV-B Photoreceptor UVR8: From Structure to Physiology. Plant Cell. 26:21–37. doi:10.1105/tpc.113.119446.

Jenkins GI. 2017. Photomorphogenic responses to ultraviolet-B light. Plant Cell Environ. 40:2544–2557. doi:10.1111/pce.12934.

Jovanovic-Talisman T, Tetenbaum-Novatt J, McKenney AS, Zilman A, Peters R, Rout

MP, Chait BT. 2009. Artificial nanopores that mimic the transport selectivity of the nuclear pore complex. Nature. 457:1023–1027. doi:10.1038/nature07600.

Kami C, Lorrain S, Hornitschek P, Fankhauser C. 2010. Light-regulated plant growth and development. Curr Top Dev Biol. 91:29–66. doi:10.1016/S0070-2153(10)91002-8.

Kanneganti TD, Bai X, Tsai CW, Win J, Meulia T, Goodin M, Kamoun S, Hogenhout SA. 2007. A functional genetic assay for nuclear trafficking in plants. Plant J. 50:149–158. doi:10.1111/j.1365-313X.2007.03029.x.

Keller MM, Jaillais Y, Pedmale U V., Moreno JE, Chory J, Ballaré CL. 2011. Cryptochrome 1 and phytochrome B control shade-avoidance responses in Arabidopsis via partially independent hormonal cascades. Plant J. 67:195–207. doi:10.1111/j.1365-313X.2011.04598.x.

Keuskamp DH, Pollmann S, Voesenek LACJ, Peeters AJM, Pierik R. 2010. Auxin transport through PIN-FORMED 3 (PIN3) controls shade avoidance and fitness during competition. Proc Natl Acad Sci. 107:22740–22744. doi:10.1073/pnas.1013457108.

Keuskamp DH, Sasidharan R, Pierik R. 2010. Physiological regulation and functional significance of shade avoidance responses to neighbors. Plant Signal Behav. 5:655–662. doi:10.4161/psb.5.6.11401.

Kevei E, Schafer E, Nagy F. 2007. Light-regulated nucleo-cytoplasmic partitioning of phytochromes. J Exp Bot. 58:3113–3124. doi:10.1093/jxb/erm145.

Kim WY, Fujiwara S, Suh SS, Kim J, Kim Y, Han L, David K, Putterill J, Nam HG, Somers DE. 2007. ZEITLUPE is a circadian photoreceptor stabilized by GIGANTEA in blue light. Nature. 449:356–360. doi:10.1038/nature06132.

Kircher S, Kozma-Bognar L, Kim L, Adam E, Harter K, Schafer E, Nagy F. 1999. Light quality-dependent nuclear import of the plant photoreceptors phytochrome A and B. Plant Cell. 11:1445–1456. doi:10.1105/tpc.11.8.1445.

Kitajima K. 1994. Relative importance of photosynthetic traits and allocation patterns as correlates of seedling shade tolerance of 13 tropical trees. Oecologia. 98:419–428. doi:10.1007/BF00324232.

Kohnen M V., Schmid-Siegert E, Trevisan M, Petrolati LA, Sénéchal F, Müller-Moulé P, Maloof JN, Xenarios I, Fankhauser C, Allenbach Petrolati L, et al. 2016. Neighbor Detection Induces Organ-specific Transcriptomes, Revealing Patterns Underlying Hypocotyl-specific Growth. Plant Cell. 28:1–53. doi:10.1105/tpc.16.00463.

Kreslavski VD, Los DA, Schmitt F-J, Zharmukhamedov SK, Kuznetsov V V., Allakhverdiev SI. 2018. The impact of the phytochromes on photosynthetic processes. Biochim Biophys Acta - Bioenerg. 1859:400–408.

doi:10.1016/J.BBABIO.2018.03.003.

Lazaro A, Valverde F, Pineiro M, Jarillo JA. 2012. The Arabidopsis E3 Ubiquitin Ligase HOS1 Negatively Regulates CONSTANS Abundance in the Photoperiodic Control of Flowering. Plant Cell. 24:982–999. doi:10.1105/tpc.110.081885.

Lee JH, Kim JJ, Kim SH, Cho HJ, Kim J, Ahn JH. 2012. The E3 ubiquitin ligase HOS1 regulates low ambient temperature-responsive flowering in arabidopsis thaliana. Plant Cell Physiol. 53:1802–1814. doi:10.1093/pcp/pcs123.

Legris M, Klose C, Burgie ES, Rojas CCR, Neme M, Hiltbrunner A, Wigge PA, Schäfer E, Vierstra RD, Casal JJ. 2016. Phytochrome B integrates light and temperature signals in Arabidopsis. Science (80-). 354:897–900. doi:10.1126/science.aaf5656.

Leivar P, Monte E. 2014. PIFs: Systems Integrators in Plant Development. Plant Cell. 26:56–78. doi:10.1105/tpc.113.120857.

Leivar P, Monte E, Oka Y, Liu T, Carle C, Castillon A, Huq E, Quail PH. 2008. Multiple Phytochrome-Interacting bHLH Transcription Factors Repress Premature Seedling Photomorphogenesis in Darkness. Curr Biol. 18:1815–1823. doi:10.1016/j.cub.2008.10.058.

Leivar P, Quail PH. 2011. PIFs: Pivotal components in a cellular signaling hub. Trends Plant Sci. 16:19–28. doi:10.1016/j.tplants.2010.08.003.

Leone M, Keller MM, Cerrudo I, Ballaré CL. 2014. To grow or defend? Low red : far-red ratios reduce jasmonate sensitivity in Arabidopsis seedlings by promoting DELLA degradation and increasing JAZ10 stability. New Phytol. 204:355–367. doi:10.1111/nph.12971.

Leyser O. 2018. Auxin Signaling. Plant Physiol. 176:465–479. doi:10.1104/pp.17.00765.

Li J, Li G, Wang H, Wang Deng X. 2011. Phytochrome signaling mechanisms. Arab B. 9:e0148. doi:10.1199/tab.0148.

Li L, Ljung K, Breton G, Schmitz RJ, Pruneda-Paz J, Cowing-Zitron C, Cole BJ, Ivans LJ, Pedmale U V., Jung H-SHS, et al. 2012. Linking photoreceptor excitation to changes in plant architecture. Genes Dev. 26:785–790. doi:10.1101/gad.187849.112.

Lian HLH-L, He SBS-B, Zhang Y-CYC, Zhu D-MDM, Zhang J-YJY, Jia KPK-P, Sun S-XSX, Li L, Yang HQH-Q. 2011. Blue-light-dependent interaction of cryptochrome 1 with SPA1 defines a dynamic signaling mechanism. Genes Dev. 25:1023–1028. doi:10.1101/gad.2025111.

Lihova J, Marhold K, Kudoh H, Koch MA. 2006. Worldwide phylogeny and biogeography of Cardamine flexuosa (Brassicaceae) and its relatives. Am J Bot. 93:1206–1221. doi:10.3732/ajb.93.8.1206.

Lin C, Shalitin D. 2003. Cryptochrome structure and signal transduction. Annu Rev Plant Biol. 54:469–496. doi:10.1146/annurev.arplant.54.110901.160901.

Lincoln C. 1990. Growth and Development of the axr1 Mutants of Arabidopsis. Plant Cell. 2:1071–1080. doi:10.1105/tpc.2.11.1071.

Liu H, Wang Q, Liu Y, Zhao X, Imaizumi T, Somers DE, Tobin EM, Lin C. 2013. Arabidopsis CRY2 and ZTL mediate blue-light regulation of the transcription factor CIB1 by distinct mechanisms. Proc Natl Acad Sci U S A. 110:17582–7. doi:10.1073/pnas.1308987110.

Liu H, Yu X, Li K, Klejnot J, Yang H, Lisiero D, Lin C. 2008. Photoexcited CRY2 interacts with CIB1 to regulate transcription and floral initiation in Arabidopsis. Science (80-). 322:1535–1539. doi:10.1126/science.1163927.

Lorrain S, Allen T, Duek PD, Whitelam GC, Fankhauser C. 2008. Phytochrome-mediated inhibition of shade avoidance involves degradation of growth-promoting bHLH transcription factors. Plant J. 53:312–323. doi:10.1111/j.1365-313X.2007.03341.x.

Lu Q, Tang X, Tian G, Wang F, Liu K, Nguyen V, Kohalmi SE, Keller WA, Tsang EWT, Harada JJ, et al. 2010. Arabidopsis homolog of the yeast TREX-2 mRNA export complex: Components and anchoring nucleoporin. Plant J. 61:259–270. doi:10.1111/j.1365-313X.2009.04048.x.

Lu X-DD, Zhou C-MM, Xu P-BB, Luo Q, Lian H-LL, Yang H-QQ. 2015. Red-light-dependent interaction of phyB with SPA1 promotes COP1-SPA1 dissociation and photomorphogenic development in arabidopsis. Mol Plant. 8:467–478. doi:10.1016/j.molp.2014.11.025.

de Lucas M, Davière J-M, Rodríguez-Falcón M, Pontin M, Iglesias-Pedraz JM, Lorrain S, Fankhauser C, Blázquez MA, Titarenko E, Prat S. 2008. A molecular framework for light and gibberellin control of cell elongation. Nature. 451:480–484. doi:10.1038/nature06520.

Ma D, Li X, Guo Y, Chu J, Fang S, Yan C, Noel JP, Liu H. 2016. Cryptochrome 1 interacts with PIF4 to regulate high temperature-mediated hypocotyl elongation in response to blue light. Proc Natl Acad Sci U S A. 113. doi:10.1073/pnas.1511437113.

MacGregor DR, Gould P, Foreman J, Griffiths J, Bird S, Page R, Stewart K, Steel G, Young J, Paszkiewicz K, et al. 2013. HIGH EXPRESSION OF OSMOTICALLY RESPONSIVE GENES1 Is Required for Circadian Periodicity through the Promotion of Nucleo-Cytoplasmic mRNA Export in Arabidopsis. Plant Cell. 25:4391–4404. doi:10.1105/tpc.113.114959.

Mancinelli AL. 1994. The physiology of phytochrome action. In: Photomorphogenesis in Plants. Dordrecht: Springer Netherlands. p. 211–269.

Marelli M, Dilworth DJ, Wozniak RW, Aitchison JD. 2001. The dynamics of karyopherin-mediated nuclear transport. Biochem Cell Biol. 79:603–12. doi:10.1139/bcb-79-5-603.

Martínez-García JF, Gallemí M, Molina-Contreras MJ, Llorente B, Bevilaqua MRR, Quail PH. 2014. The shade avoidance syndrome in Arabidopsis: The antagonistic role of phytochrome A and B differentiates vegetation proximity and canopy shade. Huq E, editor. PLoS One. 9:e109275. doi:10.1371/journal.pone.0109275.

Martínez-García JF, Galstyan A, Salla-Martret M, Cifuentes-Esquivel N, Gallemí M, Bou-Torrent J. 2010. Regulatory Components of Shade Avoidance Syndrome.

Martinez-Garcia JF, Santes CM, Garcia-Martinez JL. 2000. The end-of-day far-red irradiation increases gibberellin A1 content in cowpea (Vigna sinensis) epicotyls by reducing its inactivation. Physiol Plant. 108:426–434. doi:10.1034/j.1399-3054.2000.t01-1-100413.x.

Mazza CA, Ballaré CL. 2015. Photoreceptors UVR8 and phytochrome B cooperate to optimize plant growth and defense in patchy canopies.

Mei Q, Dvornyk V. 2015. No TitleEvolutionary History of the Photolyase/Cryptochrome Superfamily in Eukaryotes. Foulkes NS, editor. PLoS One. 10:e0135940. doi:10.1371/journal.pone.0135940.

Meier I, Brkljacic J. 2009. Adding pieces to the puzzling plant nuclear envelope. Curr Opin Plant Biol. 12:752–759. doi:10.1016/j.pbi.2009.09.016.

Menon BB, Sarma NJ, Pasula S, Deminoff SJ, Willis KA, Barbara KE, Andrews B, Santangelo GM. 2005. Reverse recruitment: the Nup84 nuclear pore subcomplex mediates Rap1/Gcr1/Gcr2 transcriptional activation. Proc Natl Acad Sci U S A. 102:5749–54. doi:10.1073/pnas.0501768102.

Merkle T. 2011. Nucleo-cytoplasmic transport of proteins and RNA in plants. Plant Cell Rep. 30:153–176. doi:10.1007/s00299-010-0928-3.

Millenaar FF, Van Zanten M, Cox MCH, Pierik R, Voesenek LACJ, Peeters AJM. 2009. Differential petiole growth in Arabidopsis thaliana: photocontrol and hormonal regulation. New Phytol. 184:141–152. doi:10.1111/j.1469-8137.2009.02921.x.

Morales LO, Brosche M, Vainonen J, Jenkins GI, Wargent JJ, Sipari N, Strid A, Lindfors A V., Tegelberg R, Aphalo PJ. 2013. Multiple Roles for UV RESISTANCE LOCUS8 in Regulating Gene Expression and Metabolite Accumulation in Arabidopsis under Solar Ultraviolet Radiation. Plant Physiol. 161:744–759. doi:10.1104/pp.112.211375.

Müller-Moulé P, Nozue K, Pytlak ML, Palmer CM, Covington MF, Wallace AD, Harmer

SL, Maloof JN. 2016. YUCCA auxin biosynthetic genes are required for Arabidopsis shade avoidance. PeerJ. 4:e2574. doi:10.7717/peerj.2574.

Nagatani A. 2004. Light-regulated nuclear localization of phytochromes. Curr Opin Plant Biol. 7:708–711. doi:10.1016/j.pbi.2004.09.010.

Nawkar GM, Kang CH, Maibam P, Park JH, Jung YJ, Chae HB, Chi YH, Jung IJ, Kim WY, Yun D-J, et al. 2017. HY5, a positive regulator of light signaling, negatively controls the unfolded protein response in Arabidopsis. Proc Natl Acad Sci U S A. 114:2084–2089. doi:10.1073/pnas.1609844114.

Ni M, Tepperman JM, Quail PH. 1998. PIF3, a phytochrome-interacting factor necessary for normal photoinduced signal transduction, is a novel basic helix-loop-helix protein. Cell. 95:657–67.

Niinemets U, Kull O, Tenhunen JD. 1998. An analysis of light effects on foliar morphology, physiology, and light interception in temperate deciduous woody species of contrasting shade tolerance. Tree Physiol. 18:681–696. doi:10.1093/treephys/18.10.681.

Niinemets U, Tenhunen JD. 1997. A model separating leaf structural and physiological effects on carbon gain along light gradients for the shade-tolerant species Acer saccharum. Plant, Cell Environ. 20:845–866. doi:10.1046/j.1365-3040.1997.d01-133.x.

Pacín M, Semmoloni M, Legris M, Finlayson SA, Casal JJ. 2016. Convergence of CONSTITUTIVE PHOTOMORPHOGENESIS 1 and PHYTOCHROME INTERACTING FACTOR signalling during shade avoidance. New Phytol. 211:967–979. doi:10.1111/nph.13965.

Parry G. 2014. Components of the Arabidopsis nuclear pore complex play multiple diverse roles in control of plant growth. J Exp Bot. 65:6057–6067. doi:10.1093/jxb/eru346.

Parry G, Ward S, Cernac A, Dharmasiri S, Estelle M. 2006. The Arabidopsis SUPPRESSOR OF AUXIN RESISTANCE proteins are nucleoporins with an important role in hormone signaling and development. Plant Cell. 18:1590–1603. doi:10.1105/tpc.106.041566.

Patel SS, Belmont BJ, Sante JM, Rexach MF. 2007. Natively Unfolded Nucleoporins Gate Protein Diffusion across the Nuclear Pore Complex. Cell. 129:83–96. doi:10.1016/j.cell.2007.01.044.

Patricia G, Kircher S, Adam E, Bury E, Kozma-Bognar L, Sch??fer E, Nagy F. 2000. Photocontrol of subcellular partitioning of phytochrome-B:GFP fusion protein in tobacco seedlings. Plant J. 22:135–145. doi:10.1046/j.1365-313X.2000.00730.x.

Pedmale U V., Huang SSC, Zander M, Cole BJ, Hetzel J, Ljung K, Reis PAB, Sridevi P, Nito K, Nery JR, et al. 2016. Cryptochromes Interact Directly with PIFs to Control Plant Growth in Limiting Blue Light. Cell. 164:233–245. doi:10.1016/j.cell.2015.12.018.

Pierik R, Testerink C. 2014. The art of being flexible: how to escape from shade, salt, and drought. Plant Physiol. 166:5–22. doi:10.1104/pp.114.239160.

del Pozo JC, Dharmasiri S, Hellmann H, Walker L, Gray WM, Estelle M. 2002. AXR1-ECR1-dependent conjugation of RUB1 to the Arabidopsis Cullin AtCUL1 is required for auxin response. Plant Cell. 14:421–433. doi:10.1105/tpc.010282.

Rabut G, Lenart P, Ellenberg J. 2004. Dynamics of nuclear pore complex organization through the cell cycle. Curr Opin Cell Biol. 16:314–321. doi:10.1016/j.ceb.2004.04.001\nS0955067404000523 [pii].

Raices M, D'Angelo MA. 2012. Nuclear pore complex composition: A new regulator of tissue-specific and developmental functions. Nat Rev Mol Cell Biol. 13:687–699. doi:10.1038/nrm3461.

Raices M, D'Angelo MA. 2017. Nuclear pore complexes and regulation of gene expression. Curr Opin Cell Biol. 46:26–32. doi:10.1016/j.ceb.2016.12.006.

Randise-Hinchliff C, Brickner JH. 2016. Transcription factors dynamically control the spatial organization of the yeast genome. Nucleus. 7:0. doi:10.1080/19491034.2016.1212797.

Randise-Hinchliff C, Coukos R, Sood V, Sumner MC, Zdraljevic S, Sholl LM, Brickner DG, Ahmed S, Watchmaker L, Brickner JH. 2016. Strategies to regulate transcription factor-mediated gene positioning and interchromosomal clustering at the nuclear periphery. J Cell Biol. 212:633–646. doi:10.1083/jcb.201508068.

Rich TCG. 1991. Crucifers of Great Britain and Ireland. Botanical Society of the British Isles.

Rizzini L, Favory J-JJJ, Cloix C, Faggionato D, O'Hara A, Kaiserli E, Baumeister R, Schafer E, Nagy F, Jenkins GI, et al. 2011. Perception of UV-B by the arabidopsis UVR8 protein. Science (80-). 332:103–106. doi:10.1126/science.1200660.

Robles LM, Deslauriers SD, Alvarez AA, Larsen PB. 2012. A loss-of-function mutation in the nucleoporin AtNUP160 indicates that normal auxin signalling is required for a proper ethylene response in Arabidopsis. J Exp Bot. 63:2231–2241. doi:10.1093/jxb/err424.

Robson PRH, Whitelam CC, Smith H. 1993. Selected Components of the Shade-Avoidance Syndrome Are Displayed in a Normal Manner in Mutants of Arabidopsis thaliana and Brassica rapa Deficient in Phytochrome B. Plant Physiol. 102:1179–1184.

Rockwell NC, Lagarias JC. 2006. The Structure of Phytochrome: A Picture Is Worth a Thousand Spectra. Plant Cell. 18:4–14. doi:10.1105/tpc.105.038513.

Rockwell NC, Su Y-S, Lagarias JC. 2006. Phytochrome Structure and Signaling Mechanisms. Annu Rev Plant Biol. 57:837–858. doi:10.1146/annurev.arplant.56.032604.144208.

Roig-Villanova I, Bou-Torrent J, Galstyan A, Carretero-Paulet L, Portolés S, Rodríguez-Concepción M, Martínez-García JF. 2007. Interaction of shade avoidance and auxin responses: a role for two novel atypical bHLH proteins. EMBO J. 26:4756–67. doi:10.1038/sj.emboj.7601890.

Roig-Villanova I, Bou J, Sorin C, Devlin PF, Martínez-García JF. 2006. Identification of Primary Target Genes of Phytochrome Signaling . ... Plant Physiol. 141:85–96. doi:10.1104/pp.105.076331.photointerconvertible.

Roig-Villanova I, Martínez-García JF. 2016. Plant Responses to Vegetation Proximity: A Whole Life Avoiding Shade. Front Plant Sci. 7:1–10. doi:10.3389/fpls.2016.00236.

Rose JKC, Braam J, Fry SC, Nishitani K. 2002. The XTH family of enzymes involved in xyloglucan endotransglucosylation and endohydrolysis: current perspectives and a new unifying nomenclature. Plant Cell Physiol. 43:1421–35.

Rout MP, Aitchison JD, Suprapto A, Hjertaas K, Zhao Y, Chait BT. 2000. The yeast nuclear pore complex: Composition, architecture, transport mechanism. J Cell Biol. 148:635–651. doi:10.1083/jcb.148.4.635.

Rout MP, Wente SR. 1994. Pores for thought: nuclear pore complex proteins. Trends Cell Biol. 4:357–365. doi:http://dx.doi.org/10.1016/0962-8924(94)90085-X.

Sakai T, Kagawa T, Kasahara M, Swartz TE, Christie JM, Briggs WR, Wada M, Okada K. 2001. Arabidopsis nph1 and npl1: Blue light receptors that mediate both phototropism and chloroplast relocation. Proc Natl Acad Sci. 98:6969–6974. doi:10.1073/pnas.101137598.

Salter MG, Franklin KA, Whitelam GC. 2003. Gating of the rapid shade-avoidance response by the circadian clock in plants. Nature. 426:680–683. doi:10.1038/nature02174.

Sánchez-Lamas M, Lorenzo CD, Cerdán PD. 2016. Bottom-up Assembly of the Phytochrome Network. PLoS Genet. 12:e1006413. doi:10.1371/journal.pgen.1006413.

Sasidharan R, Voesenek LA, Pierik R. 2011. Cell Wall Modifying Proteins Mediate Plant Acclimatization to Biotic and Abiotic Stresses. CRC Crit Rev Plant Sci. 30:548–562. doi:10.1080/07352689.2011.615706.

Schmid M, Arib G, Laemmli C, Nishikawa J, Durussel T, Laemmli UK. 2006. Nup-PI: The nucleopore-promoter interaction of genes in yeast. Mol Cell. 21:379–391. doi:10.1016/j.molcel.2005.12.012.

Schwechheimer C. 2008. Understanding gibberellic acid signaling—are we there yet? Curr Opin Plant Biol. 11:9–15. doi:10.1016/j.pbi.2007.10.011.

Schwechheimer C, Willige BC. 2009. Shedding light on gibberellic acid signalling. Curr Opin Plant Biol. 12:57–62. doi:10.1016/j.pbi.2008.09.004.

Sellaro R, Yanovsky MJ, Casal JJ. 2011. Repression of shade-avoidance reactions by sunfleck induction of HY5 expression in Arabidopsis. Plant J. 68:919–928. doi:10.1111/j.1365-313X.2011.04745.x.

Seo HS, Watanabe E, Tokutomi S, Nagatani A, Chua N-H. 2004. Photoreceptor ubiquitination by COP1 E3 ligase desensitizes phytochrome A signaling. Genes Dev. 18:617–22. doi:10.1101/gad.1187804.

Seo PJ, Jung JH, Park MJ, Lee K, Park CM. 2013. Controlled turnover of CONSTANS protein by the HOS1 E3 ligase regulates floral transition at low temperatures. Plant Signal Behav. 8. doi:10.4161/psb.23780.

Sessa G, Carabelli M, Sassi M, Ciolfi A, Possenti M, Mittempergher F, Becker J, Morelli G, Ruberti I. 2005. A dynamic balance between gene activation and repression regulates the shade avoidance response in Arabidopsis. Genes Dev. 19:2811–5. doi:10.1101/gad.364005.

Sheerin DJ, Hiltbrunner A. 2017. Molecular mechanisms and ecological function of far-red light signalling. Plant Cell Environ.:1–21. doi:10.1111/pce.12915.

Shinomura T, Nagatani A, Hanzawa H, Kubota M, Watanabe M, Furuya M. 1996. Action spectra for phytochrome A- and B-specific photoinduction of seed germination in Arabidopsis thaliana. Proc Natl Acad Sci U S A. 93:8129–33.

Shugart HH, West DC. 1980. Forest Succession Models. Bioscience. 30174254127:308–313.

Smith H. 1982. Light Quality, Photoperception, and Plant Strategy. Annu Rev Plant Physiol. 33:481–518. doi:10.1146/annurev.pp.33.060182.002405.

Smith H. 1994. Sensing the light environment: the functions of the phytochrome family. In: Photomorphogenesis in Plants. Dordrecht: Springer Netherlands. p. 377–416.

Smith H, Whitelam GC. 1997. The shade avoidance syndrome: multiple responses mediated by multiple phytochromes. Plant, Cell Environ. 20:840–844. doi:10.1046/j.1365-3040.1997.d01-104.x.

Smith TF, Gaitatzes C, Saxena K, Neer EJ. 1999. The WD repeat: A common architecture for diverse functions. Trends Biochem Sci. 24:181–185. doi:10.1016/S0968-0004(99)01384-5.

Song YH, Estrada DA, Johnson RS, Kim SK, Lee SY, MacCoss MJ, Imaizumi T. 2014. Distinct roles of FKF1, GIGANTEA, and ZEITLUPE proteins in the regulation of CONSTANS stability in Arabidopsis photoperiodic flowering. Proc Natl Acad Sci. 111:17672–17677. doi:10.1073/pnas.1415375111.

Sorin C, Salla-Martret M, Bou-Torrent J, Roig-Villanova I, Martínez-García JF. 2009. ATHB4, a regulator of shade avoidance, modulates hormone response in Arabidopsis seedlings. Plant J. 59:266–277. doi:10.1111/j.1365-313X.2009.03866.x.

Suetsugu N, Wada M. 2013. Evolution of three LOV blue light receptor families in green plants and photosynthetic stramenopiles: Phototropin, ZTL/FKF1/LKP2 and aureochrome. Plant Cell Physiol. 54:8–23. doi:10.1093/pcp/pcs165.

Taddei A, Van Houwe G, Hediger F, Kalck V, Cubizolles F, Schober H, Gasser SM. 2006. Nuclear pore association confers optimal expression levels for an inducible yeast gene. Nature. 441:774–778. doi:10.1038/nature04845.

Tamura K, Fukao Y, Iwamoto M, Haraguchi T, Hara-Nishimura I. 2010. Identification and characterization of nuclear pore complex components in Arabidopsis thaliana. Plant Cell. 22:4084–4097. doi:10.1105/tpc.110.079947.

Tamura K, Hara-Nishimura I. 2014. Functional insights of nucleocytoplasmic transport in plants. Front Plant Sci. 5:118. doi:10.3389/fpls.2014.00118.

Tao Y, Ferrer JL, Ljung K, Pojer F, Hong F, Long JA, Li L, Moreno JE, Bowman ME, Ivans LJ, et al. 2008. Rapid Synthesis of Auxin via a New Tryptophan-Dependent Pathway Is Required for Shade Avoidance in Plants. Cell. 133:164–176. doi:10.1016/j.cell.2008.01.049.

Texari L, Dieppois G, Vinciguerra P, Contreras M, Groner A, Letourneau A, Stutz F. 2013. The Nuclear Pore Regulates GAL1 Gene Transcription by Controlling the Localization of the SUMO Protease Ulp1. Mol Cell. 51:807–818. doi:10.1016/j.molcel.2013.08.047.

The Arabidopsis Genome Initiative. 2000. Analysis of the genome sequence of the flowering plant Arabidopsis thaliana. Nature. 408:796–815. doi:10.1038/35048692.

Turkington R, Klein E, Chanway CP. 1993. Interactive Effects of Nutrients and Disturbance: An Experimental Test of Plant Strategy Theory. Ecology. 74:863–878. doi:10.2307/1940812.

Valladares F, Laanisto L, Niinemets Ü, Zavala MA. 2016. Shedding light on shade: ecological perspectives of understorey plant life. Plant Ecol Divers. 9:1–15.

doi:10.1080/17550874.2016.1210262.

Valladares F, Niinemets Ü. 2008. Shade tolerance, a key plant feature of complex nature and consequences. Annu Rev Ecol Evol Syst. 39:237–257. doi:10.1146/annurev.ecolsys.39.110707.173506.

Vandenbussche F, Pierik R, Millenaar FF, Voesenek LA, Van Der Straeten D. 2005. Reaching out of the shade. Curr Opin Plant Biol. 8:462–468. doi:10.1016/j.pbi.2005.07.007.

Vaughn KC, Bowling AJ, Ruel KJ. 2011. The mechanism for explosive seed dispersal in Cardamine hirsuta (Brassicaceae). Am J Bot. 98:1276–85. doi:10.3732/ajb.1000374.

Vlad D, Kierzkowski D, Rast MI, Vuolo F, Dello Ioio R, Galinha C, Gan X, Hajheidari M, Hay A, Smith RS, et al. 2014. Leaf shape evolution through duplication, regulatory diversification, and loss of a homeobox gene. Science. 343:780–3. doi:10.1126/science.1248384.

Xu X, Kathare PK, Pham VN, Bu Q, Nguyen A, Huq E. 2017. Reciprocal proteasome-mediated degradation of PIFs and HFR1 underlying photomorphogenic development in Arabidopsis. Development. 144:dev.146936. doi:10.1242/dev.146936.

Xu XM, Rose A, Muthuswamy S, Jeong SY, Venkatakrishnan S, Zhao Q, Meier I. 2007. NUCLEAR PORE ANCHOR, the Arabidopsis Homolog of Tpr/Mlp1/Mlp2/Megator, Is Involved in mRNA Export and SUMO Homeostasis and Affects Diverse Aspects of Plant Development. Plant Cell. 19:1537–1548. doi:10.1105/tpc.106.049239.

Yamaguchi R, Nakamura M, Mochizuki N, Kay SA, Nagatani A. 1999. Light-dependent translocation of a phytochrome B-GFP fusion protein to the nucleus in transgenic Arabidopsis. J Cell Biol. 145:437–445. doi:10.1083/jcb.145.3.437.

Yang J, Lin R, Sullivan J, Hoecker U, Liu B, Xu L, Deng XW, Wang H. 2005. Light regulates COP1-mediated degradation of HFR1, a transcription factor essential for light signaling in Arabidopsis. Plant Cell. 17:804–21. doi:10.1105/tpc.104.030205.

Yang X, Montano S, Ren Z. 2015. How Does Photoreceptor UVR8 Perceive a UV-B Signal. In: Photochemistry and Photobiology. Vol. 91. p. 993–1003.

Yang Z, Liu B, Su J, Liao J, Lin C, Oka Y. 2017. Cryptochromes Orchestrate Transcription Regulation of Diverse Blue Light Responses in Plants. Photochem Photobiol. 93:112–127. doi:10.1111/php.12663.

Zhang Y, Mayba O, Pfeiffer A, Shi H, Tepperman JM, Speed TP, Quail PH. 2013. A quartet of PIF bHLH factors provides a transcriptionally centered signaling hub that regulates seedling morphogenesis through differential expression-patterning of shared target genes in Arabidopsis. PLoS Genet. 9:e1003244.

doi:10.1371/journal.pgen.1003244.

Zhao Q, Meier I. 2011. Identification and characterization of the arabidopsis FG-repeat nucleoporin Nup62. Plant Signal Behav. 6:330–334. doi:10.4161/psb.6.3.13402.

Zhao Y. 2012. Auxin Biosynthesis: A Simple Two-Step Pathway Converts Tryptophan to Indole-3-Acetic Acid in Plants. Mol Plant. 5:334–338. doi:10.1093/mp/ssr104.

Zhou P, Song M, Yang Q, Su L, Hou P, Guo L, Zheng X, Xi Y, Meng F, Xiao Y, et al. 2014. Both PHYTOCHROME RAPIDLY REGULATED1 (PAR1) and PAR2 Promote Seedling Photomorphogenesis in Multiple Light Signaling Pathways. Plant Physiol. 164:841–852. doi:10.1104/pp.113.227231.

Zuo Z, Liu H, Liu B, Liu X, Lin C. 2011. Blue light-dependent interaction of CRY2 with SPA1 regulates COP1 activity and floral initiation in arabidopsis. Curr Biol. 21:841–847. doi:10.1016/j.cub.2011.03.048.